RICE UNIVERSITY

Integration of Sight, Hearing and Touch in Human Cerebral Cortex

by

Nafi Yaşar

A THESIS SUBMITTED IN PARTIAL FULFILLMENT OF THE REQUIREMENTS FOR THE DEGREE

Doctor of Philosophy

APPROVED, THESIS COMMITTEE:

Michael S. Beauchamp, Assistant Professor, Director Department of Neurobiology and Anatomy University of Texas Health Science Center at Houston

Tomasz Tkaczyk, Assistant Professor, Chair Department of Bioengineering Rice University

Robert M. Raphael, Associate Professor Department of Bioengineering Rice University

Tatiana T. Schnur, Assistant Professor

HOUSTON, TEXAS APRIL 2009

Rice University

Department of Psychology

Abstract

Integration of Sight, Hearing and Touch in Human Cerebral Cortex

by

Nafi Yaşar

While each individual sensory modality provides us with information about a specific aspect about our environment, our senses must be integrated for us to interact with the environment in a meaningful way. My thesis describes studies of the interactions between somatosensation, vision and audition using functional Magnetic Resonance Imaging (fMRI) of normal human subjects as the primary method. In order to study somatosensation with fMRI we first built an MRI-compatible tactile-stimulation apparatus. This apparatus was then used for four separate studies. In the first study, we investigated tactile responses in lateral occipital lobe, a brain region traditionally considered "visual" cortex. We found that visual area MST, but not visual area MT, responded to tactile stimulation. In the second study we investigated a possible homologue to a macaque multisensory area that integrates visual, auditory and tactile information, called the Superior Temporal Polysensory area (STP). We found responses to tactile stimuli co-localized with auditory and visual responses in posterior superior temporal sulcus. This is likely to be a human homologue to macaque STP. In the third study, we used Multi Voxel Pattern Analysis (MVPA) to demonstrate that this homologue of macaque STP (along with traditional "somatosensory" areas) can predict the location of tactile stimulation from fMRI data. In the fourth study we used

psychophysical techniques to analyze the effects of auditory stimuli on tactile perception. We found that auditory stimuli can influence detection, frequency perception, and the perception of the spatial location of vibrotactile stimuli.

Two additional projects are also briefly described. The results of an effort to develop an MRI compatible Transcranial Magnetic Stimulation (TMS) device are included. Also a project I worked on during my summer internship in which I debugged a system capable of both stimulating and recording from cortical tissue at the same time is also discussed.

Table of Contents

Abstract	. ii
Table of Contents	iv
Preface	. v
Chapter 1: Providing Computer Controlled Tactile Stimulation in an MRI Environment	. 1
Chapter 2: Human MST But Not MT Responds to Tactile Stimulation	17
Chapter 3: Touch, Sound and Vision in Human Superior Temporal Sulcus	42
Chapter 4: Distributed Representation of Single Touches in Somatosensory and Visual Cortex . 6	68
Chapter 5: Sound Enhances Touch Perception	88
Chapter 6: Providing Transcranial Magnetic Stimulation (TMS) in an MRI Environment 13	12
Chapter 7: Industrial Internship: Simultaneous Intracranial or Intracortical Recording and	
Stimulation	27
Summary	46
References 14	49

Preface

Nearly every minute of our waking lives is dedicated to interpreting and interacting with our surrounding environment. Individually our senses give us information about specific aspects of our environment; our sense of vision inform us of the intensities and frequencies of light that is being reflected off surrounding objects, our senses of touch and hearing alert us to displacements or vibrations in the matter around us caused by movement, and our senses of smell and taste give us information about the chemical composition of what we inhale or imbibe. Individually each sense provides a very limited view of our surrounding, however by incorporating all of our senses together we are provided with a robust model of our immediate environment, allowing us to engage in complex interactions.

Primary cortical areas have been identified for all five senses; however where and how the senses are integrated largely remains a mystery. In the traditional model of the brain all cortical areas communicate in a feed-forward manner, with lower cortical areas passing information to higher areas, and all areas ultimately terminating in an undiscovered cortical area where they are integrated to form the human mind.

More recent research suggests that the brain operates in a more parallel fashion, with cortical areas having many lateral connections and higher cortical areas frequently passing information back to lower areas. This "parallel processing" is especially evident in sensory cortex, where many cortical areas previously thought to be dedicated to a single sensory modality have been shown to activate to two or more different modalities (Ghazanfar and Schroeder 2006; Grefkes, et al. 2001), and projections

between cortical areas of differing modalities have been mapped. Therefore if the mechanics of multisensory integration can be elucidated it will have a great impact on our understanding of the brain as a whole.

Since more than half of the cortex is devoted to primary and associative sensory areas it is highly desirable to be able to monitor activity in the entire cerebrum while investigating multimodal interactions. Additionally, since our research is focused on human cortex, invasive techniques that require direct access to the brain or injection of radionucliotides or contrasting agents are either impractical or impossible with ethical and legal constraints. For this reason we used BOLD fMRI as our principle tool since it is safe and noninvasive, and allows us to monitor activity of the entire brain with the level of resolution that is necessary to resolve different functional brain areas.

For those unfamiliar with the technology, BOLD fMRI (Blood-Oxygenation Level Dependant functional Magnetic Resonant Imaging) relies on the hemodynamic response, a biological response to neural activity observed over a hundred years ago (Roy and Sherrington 1890). When a signal is passed from one neuron to another, the postsynaptic cell releases nitric oxide (NO) into the synaptic cleft. The NO diffuses into the surrounding tissue and causes the smooth muscle in any blood vessels it encounters to relax, increasing blood flow to that area. The greater the number of neurons activated, or the greater the degree of individual activation, the greater the amount of NO release and the greater the hemodynamic response. Therefore measuring the hemodynamic response provides a strong correlate to the level of neural activity.

In 1936 Pauling and Coryell discovered that hemoglobin is paramagnetic by itself, but loses its magnetic moment when bound to oxygen (Pauling and Coryell 1936). Many years later Ogawa would realize that since an MRI signal depends on magnetic alignment of protons, deoxygenated hemoglobin's paramagnetic qualities would interfere with the MRI signal where it was abundant (Ogawa and Lee 1990). He realized it would therefore be possible to use MRI to measure the hemodynamic response by taking a series of MRI images and looking for voxels to become brighter as fresh blood rushed in and displaced oxygen-poor blood (Ogawa, et al. 1990). His theory has been confirmed by a large amount of data showing a positive correlation between the amplitude of somatosensory evoked potentials and fMRI BOLD signal (Arthurs, et al. 2000; Backes, et al. 2000; Heeger and Ress 2002; Ogawa, et al. 1998)

During an fMRI experiment, the subject is first given an anatomical scan providing a single 3D image at very high resolution. The subject is then provided stimulus, or asked to perform a task, or both depending on the experiment. During this time the subject is continuously scanned forming a series of low-resolution 3D images. The amount of time between each image is called the repetition time (TR), and is limited by how quickly a scanner can produce an image at the desired resolution (generally around 2 seconds for our purposes). These images are then overlaid on top of the anatomical image and allow activation to be measured by looking for changes in signal intensity in each voxel over time. These changes in signal intensity can then be correlated to the stimuli or tasks to determine which brain areas had increased or decreased activity in response to a stimulus or task.

Visual and auditory stimuli are relatively easy to present in an MRI environment; this combined with the fact that vision and audition are the two most widely studied senses has resulted with a wide array of commercially available devices for these purposes. Unfortunately presenting tactile stimulus in an MRI environment is considerably more challenging, so before we could study this modality using fMRI we had to design and build our own device. The design, construction, and performance of this device is described in the first chapter.

In the second chapter we investigated activation to tactile stimuli in visual area five (also known as MT for middle temporal). Previous studies have shown activation in area MT in response to tactile stimuli, however we showed that only a subdivision of MT, area MST (middle superior temporal) response to tactile stimuli while the rest of MT does not.

In chapter three we describe a human analog to an important multisensory area present in macaque monkeys called STP (superior temporal polysensory area) which lies along the fundus of the posterior superior temporal sulcus (STS). Individual neurons in this area show activation in response to visual, auditory, and tactile stimuli. Previous neuroimaging studies have shown multisensory activation to both visual and auditory stimuli, as well as activation to somatosensory stimuli; however this study is the first to show that responses to tactile stimuli are co-localized with responses to visual and auditory stimuli. This, along with similar anatomical and functional properties (discussed in the chapter) present strong evidence for identifying this area as a homologue to STP.

In chapter four we used multi-pattern voxel analysis (MVPA) to discriminate the body location of tactile stimuli. We analyzed voxels in primary and secondary somatosensory cortex, as well as regions of visual association cortex in lateral occipitotemporal lobe. Previous MVPA studies focused on decoding visual stimuli, although since visual cortex is the largest and most distributed of the early sensory cortices it remained unclear whether this technique could be applied to other modalities with smaller and less distributed representation. We were able to successfully discriminate the body location of stimulation to a degree much higher than chance, proving that this technique can be applied to somatosensory stimuli. In addition to using all areas to train a classifier, we also trained the classifier using SI, SII and visual association cortex separately. The results provided a great amount of insight as to the role of each area in somatosensory processing.

In chapter five we investigated cross-modal interactions between audition and somatosensation using psychophysical experiments. Our results indicated that auditory tones can affect the detection, perceived spatial location, and the perceived frequency of vibrotactile stimuli.

While fMRI provides a powerful method to find brain areas that increase or decrease activity in response to a stimulus, activity only demonstrates correlation and not causation (just because a brain area becomes active during a task does not necessarily mean that that brain area is necessary for the task). One technique that can prove causality is Transcranial Magnetic Stimulation (TMS), which can noninvasively and temporarily disable brain areas. One direction of the research that will build on the

studies described in chapters two through five will focus on using TMS combined with fMRI. Chapter six is devoted to converting a commercially available TMS system for use in an MRI environment.

In the final chapter I describe some of the work I did during my summer internship at Blackrock Microimplantible Systems, namely testing and debugging a system for concurrent microstimulation and recording. Concurrent microstimulation and recording is highly desirable because it allows a researcher to conduct research that would be difficult or impossible using these techniques separately, such as investigating connectivity between two cortical areas. Unfortunately performing concurrent microstimulation and recording is extremely challenging due to the obstacles that EMF, crosstalk, and parasitic capacitances pose to collecting such small signals. This chapter describes how I surmounted each of these problems.

Chapter 1: Providing Computer Controlled Tactile

Stimulation in an MRI Environment

Introduction

The somatosensory modality presents unique challenges for human functional neuroimaging studies. Unlike in the auditory and visual modalities, there are few (if any) commercially available somatosensory stimulators designed for functional magnetic resonance imaging (fMRI). While auditory and visual stimuli are routinely delivered to subjects in the MR scanner, delivering somatosensory stimulation directly to the body surface is more challenging due to the high magnetic fields near the scanner bore and the sensitivity to radio-frequency interference of MR image acquisition.

Because of the difficulty of constructing suitable devices, many somatosensory fMRI studies use manual stimulation, for instance stroking the skin of the subject with a brush (Kell, et al. 2005) or sponge (Disbrow, et al. 2000), or by pressing plastic gratings (Sathian, et al. 1997; Zhang, et al. 2005) or metal shapes (Weisser, et al. 2005) against the skin. While effective, manual stimulation methods are less precise and reproducible than automated stimulation. Direct electrical stimulation is another popular choice in somatosensory fMRI studies (Kurth, et al. 1998; Ruben, et al. 2001) although electrical stimulation has several disadvantages. Electrical stimulation activates a poorly-defined, diffuse population of afferents that are unlike those activated by everyday sensory stimuli, and electrical currents can be painful for the subject. In high-field strength MR scanners, induced currents in the electrodes could cause heating and injury to the subject.

A third general category of somatosensory fMRI studies use automated mechanical stimulation. Pneumatic systems have been used effectively (Briggs, et al. 2004; Stippich, et al. 1999), although only at low frequency of stimulation. A hydraulic system has also been described (Golaszewski, et al. 2002) with a slightly greater range of stimulation frequency, but still less than 130Hz, and with a minimum displacement of 0.5mm, unsuitable for near-threshold studies. It is also possible to use Lorentz-forces created by the scanner to generate vibration, although each device will only work at a fixed distance outside the bore of the scanner (Graham, et al. 2001). Custom-built motorized devices that are constructed of non-ferrous metal, with the motor placed well away from the scanner bore, can be used to deliver precise stimuli, such as a grating or embossed letters to a single body part, typically the finger tip (Burton, et al. 2006; Burton, et al. 2004; Ingeholm, et al. 2006).

Another popular solution is piezoelectric devices (Gizewski, et al. 2005;

Harrington, et al. 2000). Although piezoelectrics have been dismissed as having too little displacement to provide robust tactile stimulation (Briggs, et al. 2004; Graham, et al. 2001), modern devices are capable of displacements of over a millimeter and have the advantages of a wide range of possible stimulation frequencies and amplitudes (up to several mm). Most MR-compatible somatosensory stimulators (piezoelectric or otherwise) are capable of stimulating only a single body region at a time. Because the somatosensory system is organized somatotopically, there are advantages to delivering stimuli to many body parts in a single experiment. For instance, it allows a more complete delineation of the extent of somatosensory cortex and raises the possibility of

constructing a relatively complete map of the somatosensory homunculus in a single experiment. With this in mind I designed and built an automated multichannel tactile stimulator utilizing piezoelectric bending actuators that is safe to use in an MRI environment and does not interfere with MR image acquisition.

Piezoelectric Bending Actuators

The vibrotactile stimulus is delivered by piezoelectric bending actuators (Fig. 1) purchased from Piezo Systems (www.piezo.com). Piezoelectric materials deform when exposed to a voltage; either stretching and becoming longer and thinner, or contracting and becoming shorter and thicker, depending on the polarity of the voltage. The piezoelectric bending actuators used in this system consist of two stacked piezoelectric plates with wires attached in such a way that the two plates are in opposing polarity. When a voltage is applied one plate expands and the other contracts, causing the actuator to bend. If an alternating voltage is applied the actuator will bend back and forth, causing it to vibrate at the frequency of the applied signal.

Two different sizes of bending actuators were used, a larger one is capable of large displacements and strong stimulation (Fig. 1A), and a smaller thinner actuator that is small enough to be placed on a finger (Fig. 1B). Before the actuators could be used safely in an MRI environment they had to first be modified for safety and durability (Figs. 2.1.1C and D). (1) The lead wires were encased in rubber-coated fiberglass tubing to prevent burns in the event that the lead wires heat up from the rapidly switching

magnetic fields of the MR scanner. (2) The base was encased in 3/4" heat-shrink tubing which was filled with epoxy to secure the leads. (3) Female TA3F Switchcraft Q-G connectors (www.switchcraft.com) were attached for easy connection and disconnection. (4) The actuator itself was encased in 1" heat-shrink tubing to provide electrical and thermal insulation between the device and the subject.

The actuators are simple to implement; they can be attached to the hands or feet with elastic bandage wrap, or can be attached to the face or other body parts with medical tape (Fig. 2).

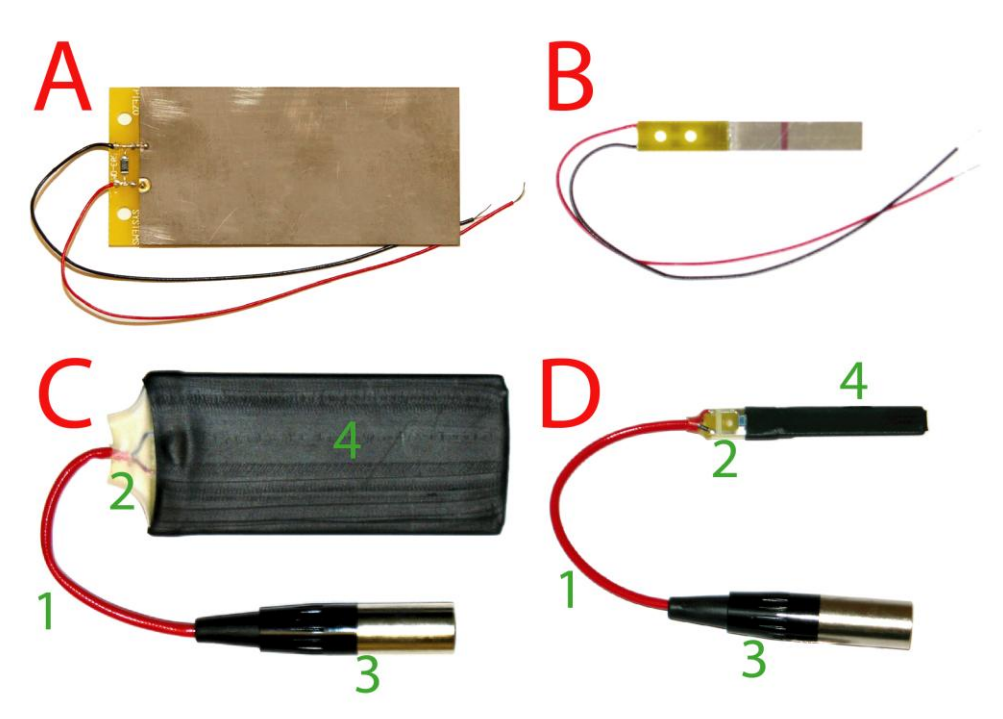


Figure 1 Piezoelectric bending actuators before and after preparation. (A) The larger unit before preparation measures 1.25 by 2.75 inches. (B) The smaller unit measures 0.25 by 1.875 inches. (C & D) The actuators are made safe and durable by 1 adding thermal insulation to the wires, 2 reinforcing the leads to the base with epoxy, 3 adding mini-XLR connectors to allow easy connection and disconnection, and 4 insulating the piezoceramic material with heat shrink tubing.



Figure 2 (Left) The piezoelectric bending actuators are attached to a subject's hands and feet using elastic bandage wrap. (Right) Six piezoelectric bending actuators are being attached to a subject's hands, feet, and face.

Performance Characteristics

The displacement of the larger piezoelectric bending actuators was measured by placing an actuator under an Olympus SZH10 research stereo microscope (www.olympusamerica.com). The microscope was focused on a thin piece of wire glued to the tip of the actuator since the actuator itself is wider than the focal length of the microscope, and a transparent scale bar 2 mm in length with 10µm intervals was placed under the wire. The wire added a negligible amount of length. A Nikon Coolpix 5000 digital camera (www.nikonusa.com) was mounted on the microscope. First an image of the scale bar was taken, and then photographs were captured of the actuator being

driven at different frequencies and amplitudes. ImageJ (rsb.info.nih.gov/ij) was used to convert the observed displacement into physical distance.

As can be seen in Figure 3b, the displacement varied considerably with frequency. However, at all frequencies measured (10Hz - 400Hz) the piezo bending actuator's displacement was greater than 0.1mm if given sufficient voltage. The bending actuators have several resonant frequencies relating to their length, width, thickness, and electrical properties. Two resonance peaks can be seen in Fig. 3A at 30 and 300 Hz. The frequency of least displacement can be seen at 80 Hz.

The acoustic emissions of the device were measured in a sound insulated room with a background noise of 37.3 dB (Fig. 3C). A BK Precision 732A Digital SPL meter (www.bkprecision.com) was used to take the measurements. The SPL meter used the IEC651 Type 2 standard, with slow time weighting and a period of 1 second. The bending actuator was positioned one foot away from the SPL meter, with the flat side facing the meter. All measurements were at 100Hz or higher, since lower frequencies did not produce a significant SPL relative to the background SPL of the sound insulated room. In the sound insulated room, the piezos were audible at higher frequencies. However in the MR scanner subjects wear hearing protection (SPL in MR scanner >90 dB), and are not able to hear the piezos.

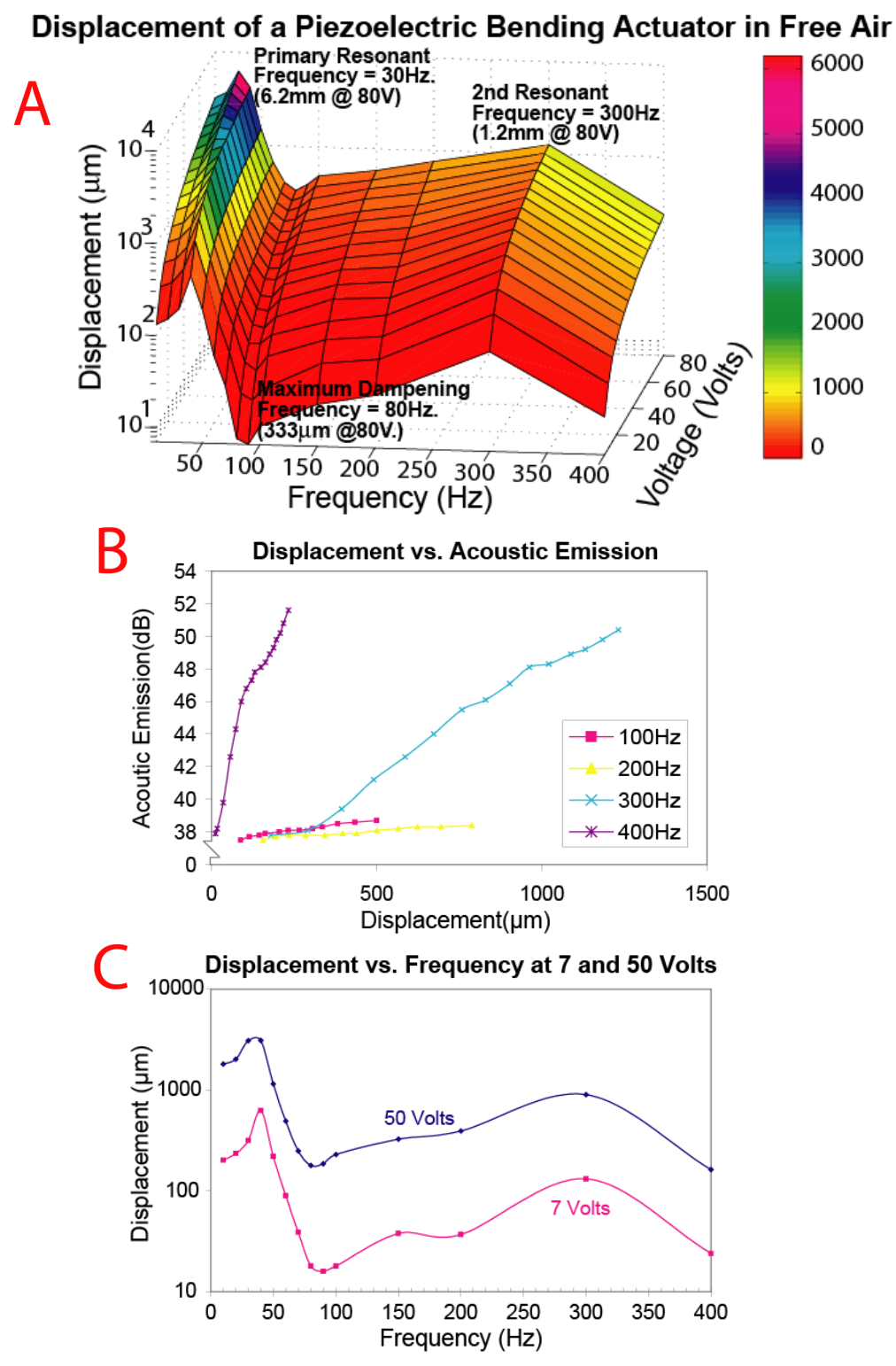


Figure 3 Performance graphs of the piezoelectric bending actuators. (A) Displacement of the piezo as a function of frequency and voltage. (B) The acoustic emissions of the piezo as a function of displacement at different frequencies. Frequencies below 100Hz did not produce any acoustic emissions significantly greater than the background noise. (C) Displacement as a function of frequency at two voltages. This graph highlights the resonant peaks at 30 and 300Hz.

Signal Delivery Cable for Piezo Actuators

The signal-delivery cable (Figure 4) was designed to be used inside the MRI room without interfering with the MRI signal, or receiving significant interference itself. It is made of eight two-conductor, shielded cables, and is terminated with a male DB25 on one end and eight pairs of male TA3M Switchcraft Q-G mini-XLR connectors on the other for connection to the piezoelectric bending actuators.



Figure 4 The signal-delivery cable. On the right is a close up showing termination.

High Intensity, Single Signal, Multi-positional Stimulation

In experiments where the subject will not be receiving more than one frequency of stimulation at any one time, it is more practical and economical to use a single amplifier capable of high voltages since multi-channel high-voltage amplifiers are very expensive, and generally use step-up transformers which cause very non-linear behavior. In this case a computer-controlled switch box is used to relay source to the areas to be stimulated (Fig. 5).

The control box is capable of delivering up to eight channels of tactile stimulation. It receives eight bit instructions from a computer through a DB25 port, and receives the signal for driving the piezoelectric bending actuators through a pair of banana plug jacks. Each pair of banana plug jacks drives four channels, allowing two different signals to be used, or the same signal can drive all eight channels if the pairs are jumpered. Each channel can be manually activated by lighted buttons and individually attenuated by potentiometers, providing a simple way to calibrate the device.

The operation of the box is simple. The instruction byte is received through the activation buttons to a 12-volt, eight-bit line driver. When the buttons are depressed the line driver receives the instruction byte, when a buttons is pressed the line driver instead receives a "high" signal. Each output of the line driver is connected to the 12-volt activation pin of a 250-volt relay. The relays themselves connect the input signal to

the attenuating potentiometers when activated, which in turn are connected to the pins of the output port. (Fig. 6)

When using this configuration, the signal was amplified by a Krohn-Hite 7500 variable-gain amplifier capable of delivering up to 200 volts peak.



Figure 5 The control box. The top view shows activation buttons, attenuating potentiometers, and protection fuses. The front and rear views on the right show the computer and signal input.

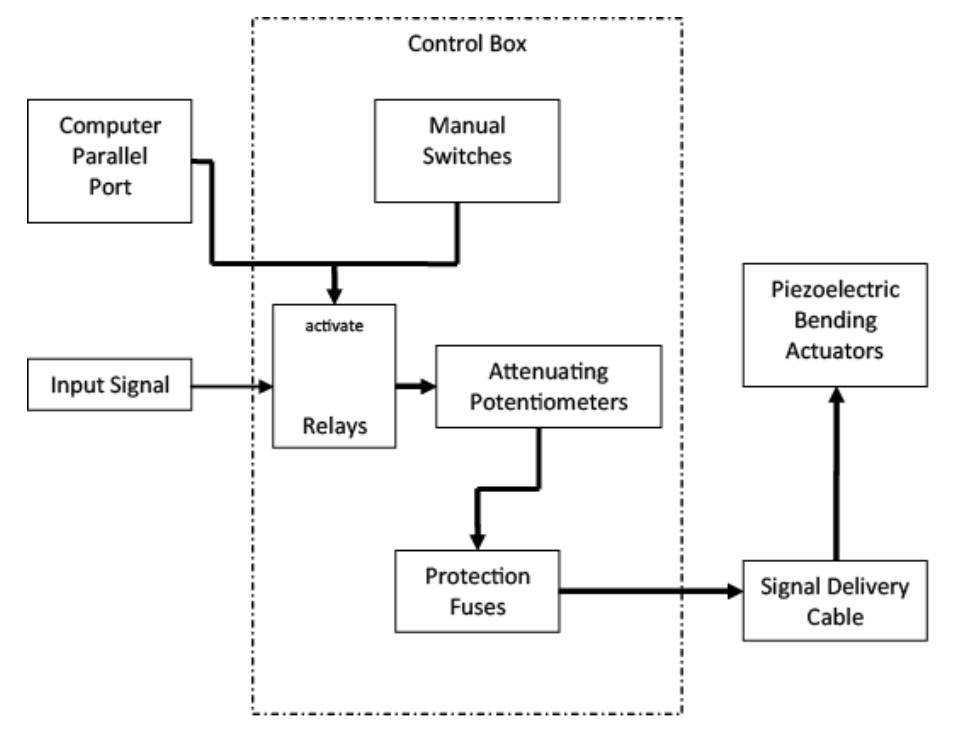


Figure 6 Block diagram of the stimulation apparatus

Lower Intensity, Multi-concurrent Signal, Multi-positional Stimulation

In cases where a very strong stimulus is not needed (such as threshold studies), but it is necessary to stimulate more than one body part at a time with different signals (i.e. it is necessary to stimulate the right hand with 100Hz sinusoid and the left with a 200Hz sinusoid), a cheaper, less powerful multichannel amplifier can be used along with a multi-channel sound card. When using this configuration a Sony STG-5500 home theatre receiver (www.sony.com) was used, providing up to 55 volts-peak.

Signal Generation

During experiments, one of two types of stimulus is desired, either a long pulse at a specific frequency of sinusoid, which creates a "buzzing" sensation, or an instantaneous "tap" stimulus.

Pulse generation

The pulse signal is constructed by the software used to run the experiments, Presentation (www.neurobs.com). The signal is created as a sound and then fed into an amplifier from the sound card's headphone jack. However, when Presentation generates sinusoids, it starts the sinusoid at an unknown phase, which can result in extreme ramp rates at the onset and cessation of the sinusoid (Fig. 7A). This causes a very rapid flex in the piezoelectric bending actuator that creates a loud click and a strong tactile impulse. To correct this the sinusoid is multiplied by a windowing function constructed by playing the first quarter phase of a 5Hz sinusoid, followed by a DC signal, followed by the second quarter phase of a 5Hz sinusoid (Fig. 7B), giving the waveform shown in Fig. 7C. The results in an electrical signal that still has a relatively pure frequency spectrum (Fig. 8), in fact more pure than the waveform shown in 2.1.7A, and eliminates the high ramp rates that cause the mechanical disturbances in the piezoelectric bending actuator. An example of a generated 100Hz pulse as recorded by oscilloscope is shown if Fig. 8.

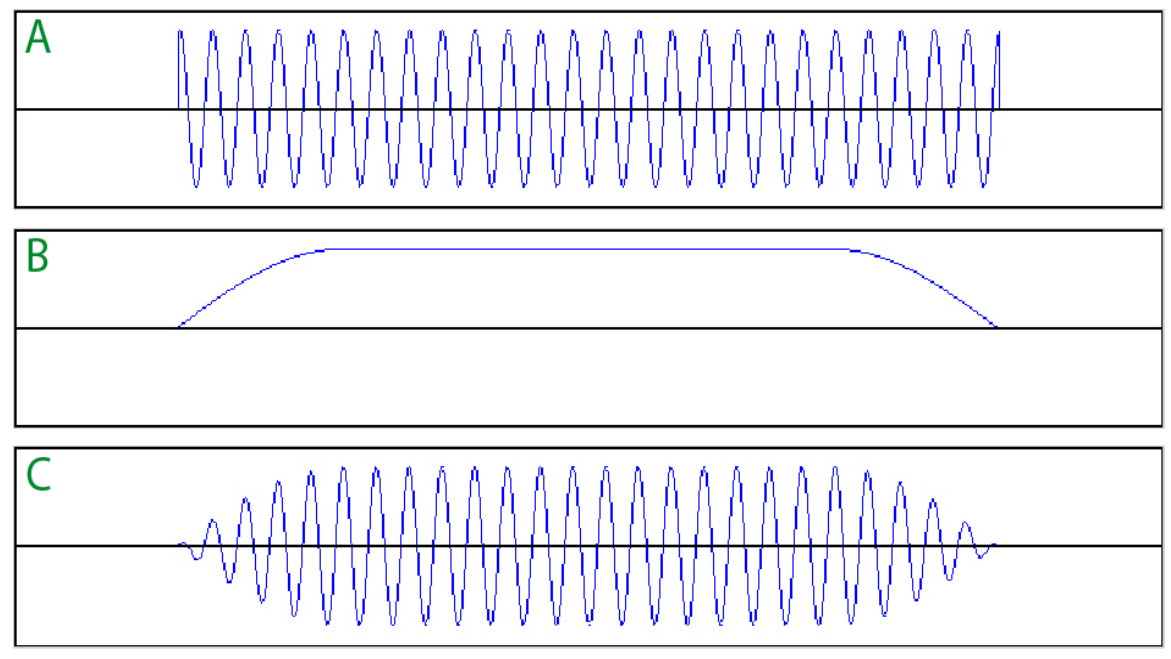


Figure 7 Waveform generation. (A) A 100Hz sinusoid generated by Presentation. Presentation starts the waveform at a random phase, which causes clicking at onset and termination of playback. (B) Windowing waveform which is multiplied by fig. A to produce fig. C. The waveform consists of the first and second quarter phases of a 5Hz sinusoid with a flat DC voltage in between. (C) The pulse waveform. The tapered ends prevent the clicking caused by (A).

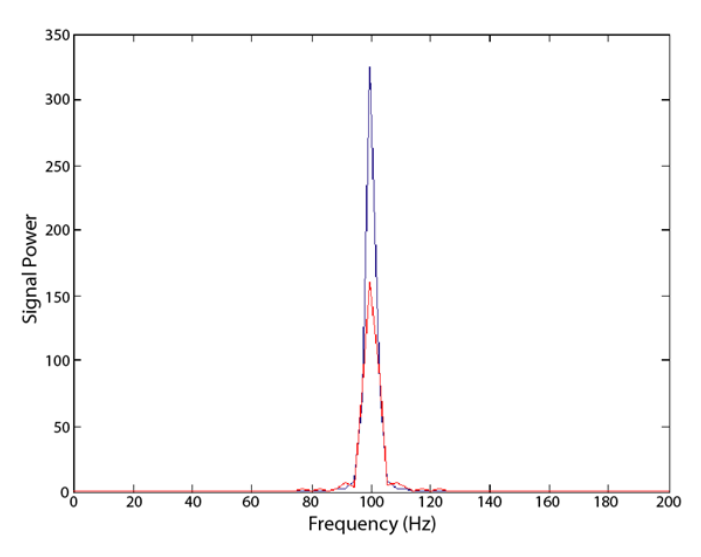


Figure 8 Spectral analysis of the waveforms shown in Fig. 7. The red line represents the finite sinusoid shown Fig. 7A, while the blue line represents Fig. 7C.

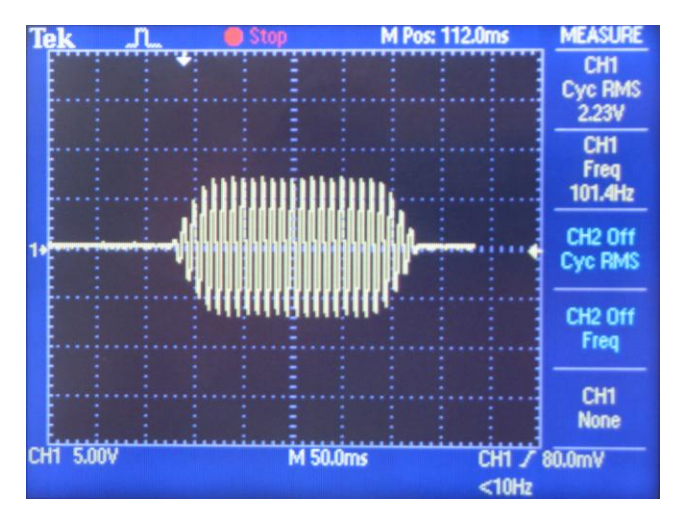


Figure 9 An example of a 100Hz pulse as captured by a Tektronix TDS 2002 oscilloscope (www.tek.com).

"Tap" generation

A tap on the skin can be generated by having the bending actuator flex just once against the skin. However if the bending actuator were to only flex away from the subject's skin, very little sensation would be created. By using a bipolar waveform the bending actuator will flex once each way, guaranteeing stimulation regardless of the orientation of the bending actuator. A Gaussian monopulse was selected since this waveform is continuous and provides a very strong flex in the bending actuator without creating clicks or damaging it. The center frequency of the monopulse can be varied based on the time constraints of the needed stimulus, although in most cases a 200Hz monopulse provides a sufficiently instantaneous stimulus (~6ms) that is also robust and does not produce a noticeable amount of sound.

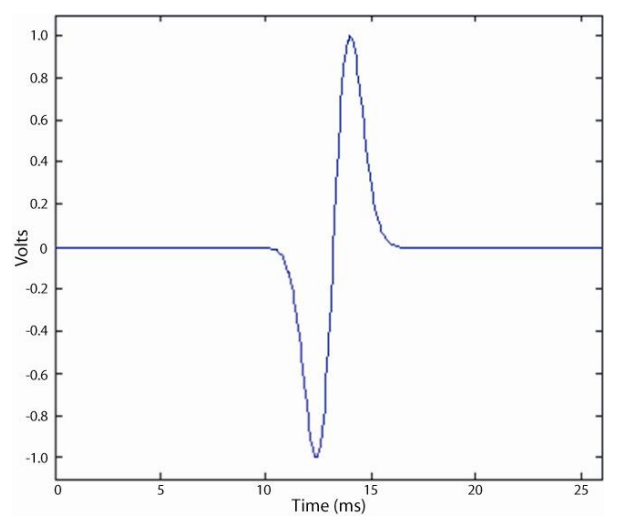


Figure 10 The 200Hz Gaussian monopulse as generated by Matlab.

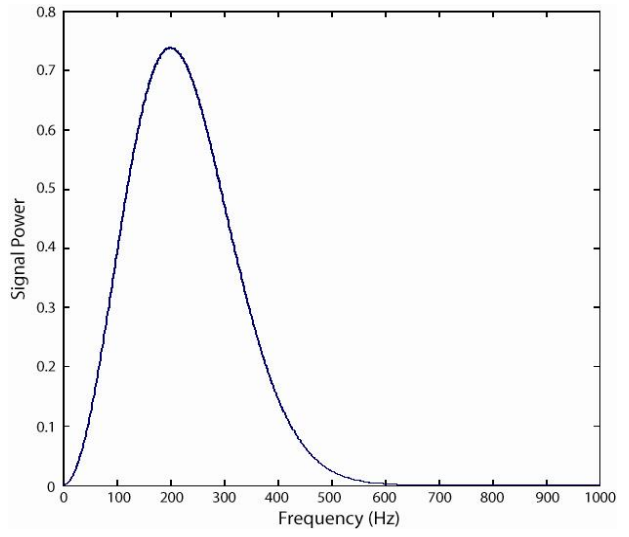


Figure 11 Spectral analysis of the Gaussian monopulse shown in Figure 10.

Chapter 2: Human MST But Not MT Responds to Tactile Stimulation

Based on manuscript:

Beauchamp, M.S., Yasar, N.E., Kishan, T., Ro, T. (2007). Human MST but not MT responds to tactile stimulation. Journal of Neuroscience 27 (31), 8261-8267

Introduction

The strategies used by the brain to integrate information from different sensory modalities are a question at the heart of cognitive neuroscience. One view is that all of sensory cortex is essentially multisensory (Ghazanfar and Schroeder 2006; Grefkes, et al. 2001). In support of this idea, functional neuroimaging studies have reported responses to tactile stimuli in regions of occipital lobe traditionally regarded as purely visual (Amedi, et al. 2001; Eickhoff, et al. 2005; Sathian, et al. 1997). More recently, two groups have reported responses to tactile stimuli in area MT, a region considered to be essential for processing visual motion (Blake, et al. 2004; Hagen, et al. 2002). In these studies, responses in MT were observed to complex moving tactile stimuli: a brush stroking the arm (Hagen, et al. 2002) or a rotating three-dimensional globe (Blake, et al. 2004). However, it is known that simply imagining a moving stimulus evokes activity in MT (Goebel, et al. 1998) and that visual imagery in general is a powerful, specific activator of visual cortex (Ishai, et al. 2000; O'Craven and Kanwisher 2000). If in previous studies subjects engaged in visual motion imagery (such as imagining the movement of the brush as it traveled up and down the arm or the motion of the globe as it rotated), activation in MT could have been an indirect result of visual imagery rather than a direct result of somatosensory stimulation.

The standard MT localizers used in previous studies identify a region (which we henceforth refer to as MT+) (Beauchamp, et al. 1997) that contains at least two distinct areas, MT and MST. In nonhuman primates, MT and MST have distinct functional specializations and different patterns of anatomical connectivity (Komatsu and Wurtz

1988) (Lewis and Van Essen 2000a). Therefore, we used anatomical and functional criteria to fractionate MT+ into MT and MST to separately measure tactile responses in each area. Because tactile responses have also been reported in the lateral occipital complex (LOC) (Amedi, et al. 2002; Amedi, et al. 2001), a region that overlaps MT+ (Kourtzi, et al. 2002), we also mapped the LOC in each subject to allow independent measurements of activity in MT, MST, and LOC.

We adopted two strategies to test whether somatosensory responses independent of visual imagery exist in MT+. First, we used vibrotactile stimuli delivered by piezoelectric bending elements to widely separated sites on the body surface. Because these stimuli do not contain any motion (real or apparent) relative to the body surface, although they do move perpendicular to the skin surface (a necessary precondition for activating mechanoreceptors), they are unlikely to induce the visual imagery of motion known to activate MT+. Second, we delivered vibrotactile stimulation to the ipsilateral and contralateral hands and feet of the subjects. If tactile activation in MT+ is produced by visual imagery of the tactile stimulus, the site of somatosensory stimulation should have relatively little effect. For instance, touching a rotating globe with the left hand or the right hand should induce similar amounts of visual motion imagery and concomitant activation in MT+. In contrast, one of the organizing principles of the somatosensory system is somatotopy, a map of the body surface. If MT+ tactile responses are not produced by imagery of visual motion, MT+ should show modulation by the body site of stimulation.

Methods

Subjects were recruited and informed consent was obtained in accordance with the University of Texas Committee for the Protection of Human Subjects. Four male participants and four female participants were scanned using a 3 tesla whole-body magnetic resonance (MR) scanner (Phillips Medical Systems, Bothell, WA). Anatomical images were collected using a magnetization-prepared 180° radio-frequency pulses and rapid gradient echo sequence optimized for gray—white matter contrast with 1-mm-thick sagittal slices and in-plane resolution of 0.938 X 0.938 mm. Functional images were collected using a gradient recalled-echo echo-planar-imaging sequence sensitive to the blood-oxygen level dependent (BOLD) signal. Thirty-three axial slices were collected in each 2 s repetition time (TR) with an echo time of 30 ms and a flip angle of 90°. Slice thickness was 3 mm, and in-plane resolution was 2.75 X 2.75 mm.

Vibrotactile stimulation

Somatosensory stimuli were delivered to subjects using a custom-built apparatus (Yasar and Beauchamp 2006). Five piezoelectric bending elements (Piezo Systems, Cambridge, MA) were attached, one each to the palm of the left and right hand, the sole of the left and right foot, and the right hip using nonslip silicon elastic bandages. A 200 Hz sinusoidal waveform was used to drive the piezoelectric bending elements (benders), based on behavioral data showing low detection thresholds at this frequency (Brisben, et al. 1999).

The qualitative percept of stimulation was akin to holding a ringing cell phone set to "vibrate" mode, without any accompanying auditory percept. The vibration of the benders was inaudible because of its low sound pressure level, the high ambient noise of the MR scanner, and the hearing protection sound reducers worn by the subjects.

An ultrapure sinusoidal oscillator and high-gain amplifier (both from Krohn-Hite, Brockton, MA) generated the waveform, which was delivered to the benders by a relay box under computer control. All stimuli were synchronized to the scanner via a transistor-transistor logic pulse sent every TR by the MR scanner to a PC running Presentation software (Neurobehavioral Systems, Albany, CA). Large piezoelectric benders (6.6 cm long and 3.3 cm wide) were used to stimulate a large territory of mechanoreceptors to produce a maximal BOLD functional magnetic resonance imaging (fMRI) response to the vibrotactile stimuli. Because fMRI measures neural activity integrated over time, we attempted to maximize the evoked BOLD response by delivering stimuli throughout each 2 s trial. Because both central and peripheral adaptation is observed to vibrotactile stimulation (Leung, et al. 2005; Tommerdahl, et al. 2005), a pulsed design was used (four repetitions of 250 ms ON/250 ms OFF). The driving voltage delivered to the benders was 50 V, producing a displacement of 0.5 mm. Before each experiment, the amplitude of each element was individually adjusted using the relay box potentiometers (in the range of 40–50 V, 0.4–0.5 mm) to equate the perceived intensity across benders. This served as a rough control for differences in efficacy caused by small differences in the placement, attachment, or manufacture of individual benders.

Visual stimulus presentation

The visual stimuli were back-projected from a liquid crystal display projector (Sony Electronics, San Diego, CA) onto a Lucite screen (Da-Lite, Warsaw, IN) and viewed through a mirror attached to the MR head coil. The visual stimuli for the MT/MST localizer consisted of low-contrast random dots presented in the left or right hemifields (Huk, et al. 2002). The dots moved radially in or out on sequential trials with slightly varying speeds (randomly chosen from 3–5°/s) to minimize adaptation. The visual stimuli for the LOC localizer consisted of photographs and scrambled photographs from a variety of object categories.

fMRI experimental design

The visual area localizer experiments were conducted using a block design. There were eight 30 s blocks in each 4 min scan series, with each block containing 20 s of stimulation (10 trials) of a single stimulation type followed by 10 s of baseline.

Regressors were created by convolving the timing of each type of stimulation block with a gamma-variate function to account for the BOLD hemodynamic response function.

The vibrotactile experiments were conducted using a rapid event-related design. There were 110 2 s stimulation trials in each 5 min scan series: 25 for each of left and right hand and foot and 10 catch (hip) trials (see below, Behavioral Task). Interspersed between stimulation trials were intervals of fixation (80 s total). An optimal stimulus sequence generator (optseq2) (Dale 1999) generated a pseudorandom ordering for the different trial types and fixation, resulting in a range of interstimulus intervals from 0 to

12 s. Event-related data were analyzed using the finite-impulse response (FIR) method, as implemented in the 3dDeconvolve program in the AFNI software package (Cox 1996). Tent shaped regressors were created for each of the nine images (18 s window with a TR of 2 s) after trial onset. Because a rapid event-related design was used, at any point in the MR time series the image intensity contained contributions from the overlapping responses evoked by many previous stimuli. By assuming linearity and time invariance, the FIR method deconvolved the overlapping responses into separate responses, one for each stimulus type, that were equivalent to those that would be measured with a slow event-related design.

In the general linear model, regressors of no interest consisted of the motion estimates from volume registration and polynomial regressors to account for baseline shifts and linear drifts in each scan series. The ratio of variance accounted for by the stimulus regressors and regressors of no interest to the regressors of no interest alone was used to calculate an *F*-ratio and associated significance for each voxel.

Cortical surface models

Individual cortical surface models were created using FreeSurfer software (Fischl, et al. 1999). Surfaces were visualized and average cortical surface models created using SUMA software (Argall, et al. 2006). To visualize activity buried in sulcal depths, the surface was partially inflated using 500 iterations of a smoothing algorithm. Anatomical features on the partially inflated surface were visualized by colorizing the surface with a

sulcal depth index derived from the distance of each node from the brain's bounding ellipsoid (Van Essen 2004).

Identified visual areas

To locate area MT and MST, anatomical and functional criteria were used (Beauchamp, et al. 1997; Beauchamp, et al. 2001; Dumoulin, et al. 2000; Huk, et al. 2002; Tootell, et al. 1995). First, an MT+ region of interest (ROI) was created containing voxels showing a significant response to left or right hemifield stimulation ($p<10^{-6}$) in the ascending portion of posterior inferior temporal sulcus (pITS). Second, contiguous voxels that showed no significant response to ipsilateral visual stimulation (p<0.05) were classified as MT; these voxels were concentrated on the posterior bank of the pITS in the posterior and ventral portion of the MT+ ROI. Contiguous voxels that showed a significant response to ipsilateral visual stimulation (p < 0.05) were classified as MST; these voxels were concentrated on the anterior bank of the pITS. To locate the LOC, voxels showing a significant response to real or scrambled photographs ($p<10^{-6}$) were identified, followed by a second stage of thresholding to find only voxels with a significant (p<0.05) preference for real versus scrambled photographs (Beauchamp 2005b; Grill-Spector, et al. 2001). All active voxels directly adjacent to the localizer defined visual regions (i.e., within 3 mm) were included in the ROI under the assumption that these were likely to represent regions of MT, MST, or LOC not mapped by the localizer because they represented peripheral parts of the visual field not accessible with our visual stimulation apparatus.

Voxels were classified as being somatosensory responsive if any combination of left and right hand or foot regressors showed a significant (*p*<0.01) effect. Group average somatosensory time series were created by calculating the average time series in each individual hemisphere, reordering the time series so that right (contralateral) hand and foot responses in left hemisphere were averaged with left (contralateral) responses in right hemisphere, and ipsilateral responses in left hemisphere were averaged with ipsilateral responses in right hemisphere, averaging across hemispheres to create individual subject time series, and then collapsing into a grand mean. In each individual, the MST time series was created from only those voxels that showed a significant vibrotactile response. In many hemispheres, there were no voxels in MT with significant vibrotactile responses, so the time series was created from all voxels in the MT ROI.

Behavioral task

To ensure that subjects remained alert and attentive throughout the experiment, we used a catch trial design adapted from magnetoencephalography experimental designs. Infrequently (10 trials per 5 min scan series), the piezoelectric bender affixed to the subject's hip (the catch stimulus) would be activated. This signaled the subject to make an eye movement to a visual target (white fixation crosshairs) placed in the upper right corner of the display screen, which was otherwise blank except for the target. BOLD data from catch trials and any false alarm trials were analyzed separately from all other trials, so that oculomotor and visual brain activations produced

by eye movements would not contaminate the activations measured in hand and foot trials. The visual display, including the target, remained constant at all times. With the exception of catch trials, subjects were not required to make any overt or covert behavioral responses.

Behavioral response collection

In all experiments, an MR-compatible eye-tracking system (Applied Science Laboratories, Bedford, MA) was used to monitor the subjects' behavioral state and record behavioral responses. A brief training session and calibration of the eye tracker was performed before the start of scanning, and recalibration was performed as needed throughout the scanning session. A window was created around the visual target with a 100 pixel margin, and a response was scored if the subject's eye position entered this response window at any time during a trial. On average, there was less than one false alarm and less than one miss in each 5 min scan series. Across subjects, the average saccadic reaction time during catch trials was 573 ± 118 (SD) ms.

Results

To localize area MT and MST, BOLD fMRI was used to measure brain activity as subjects viewed moving random dots presented in the left or right visual field (Huk, et al. 2002). Visual motion responsive voxels were mapped to inflated cortical surface models (Fig. 1A). Within motion-responsive cortex, MST was identified as the area in the ascending limb of the posterior inferior temporal sulcus that responded strongly to

ipsilateral visual stimulation, and MT was identified as the caudally adjacent area on the cortical surface that did not respond to ipsilateral visual stimulation.

Somatosensory brain regions were identified with a rapid event-related fMRI experiment in which the palms and soles of the left and right hands and feet were stimulated with brief vibrotactile pulses (Burton, et al. 2004). As shown in Figure 1*B*, vibro-tactile stimulation evoked a vigorous response concentrated in the parietal operculum, the location of secondary somatosensory cortex and other somatosensory association areas (S2+).

Vibrotactile responses were also observed in "visual" regions of lateral occipitotemporal cortex. To determine the spatial relationship between tactile responses and the location of identified visual areas, composite activation maps were created for an individual subject (Fig. 1*C*) and for the group activation map (Fig. 1*D*,*E*).

Tactile responses were consistently observed in MST but not in MT. To quantify the relative areas of tactile activation in MT and MST, we counted the number of suprathreshold nodes in the group average cortical surface model. In the left hemisphere, 2% of MT nodes and 49% of MST nodes showed significant tactile activation, whereas in the right hemisphere, 7% of nodes in MT and 43% of nodes in MST were significantly active.

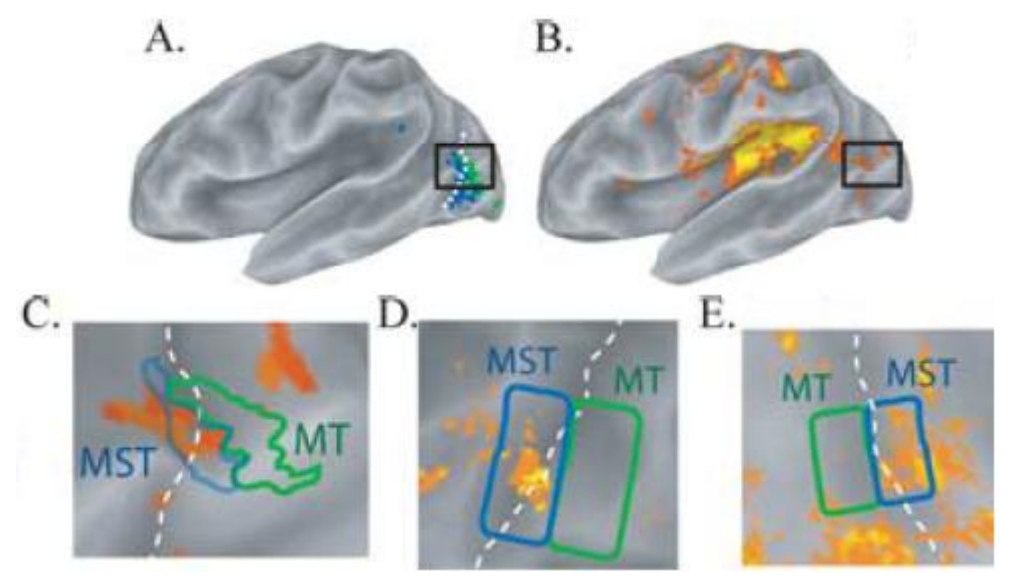


Figure 1. BOLD responses to visual and tactile stimulation (**A–C**, single subject; **D–E**, group data). **A**, Lateral view of the partially inflated left hemisphere. Brain areas responsive to visual motion that showed a response to ipsilateral stimulation (MST; blue) or no response to ipsilateral stimulation (MT; green) are shown. Dashed white line shows the fundus of the ascending limb of the posterior inferior temporal sulcus. **B**, Brain areas in the same subject responding to vibrotactile stimulation (orange-to-yellow color scale). **C**, Composite map showing MST (blue outline) and MT (green outline) overlaid on tactile activation map (enlarged view of black outlined region in **A** and **B**). **D**, Random-effects group average map (*n*=8 subjects) showing location of MST and MT relative to tactile activation in left hemisphere (anterior is left). **E**, Group average composite map for right hemisphere (anterior is right).

To more closely examine MST tactile responses, we calculated the average evoked response from all MST voxels that showed significant tactile responses (Fig. 2A). The temporal profile of the evoked response followed the classical BOLD hemodynamic response function, with a sharp peak 4 s after stimulus onset (2 s after stimulus offset) followed by a return to baseline within 4 s. There was a strong dependence on the location of stimulation. The largest response was to stimulation of the contralateral hand (mean of first and second time points, 0.16%) with smaller but still significant responses to stimulation of the ipsilateral hand and both feet (0.10, 0.11, and 0.09%, respectively). To measure the significance of these differences, we performed an ANOVA across subjects using two factors, body part of stimulation (hand vs. foot) and

side of stimulation (ipsilateral vs. contralateral) with percentage MR signal change as the dependent variable. There was a significant preference for contralateral versus ipsilateral stimulation (p=0.006) and for hand versus foot stimulation (p=0.04) but no interaction between them (p=0.11). For comparison with MST, we also calculated the average response in S2+ (Fig. 2B). The dynamics of the evoked hemodynamic response appeared similar to MST, with a peak 4 s after stimulus onset. As in MST, there was a significant preference for contralateral compared with ipsilateral stimulation (p=10⁻¹⁰) and hand compared with foot stimulation (p=0.02). In contrast to the strong tactile response observed in MST and S2+, the average time series from all voxels in MT showed only a weak response to tactile stimulation (Fig. 2C).

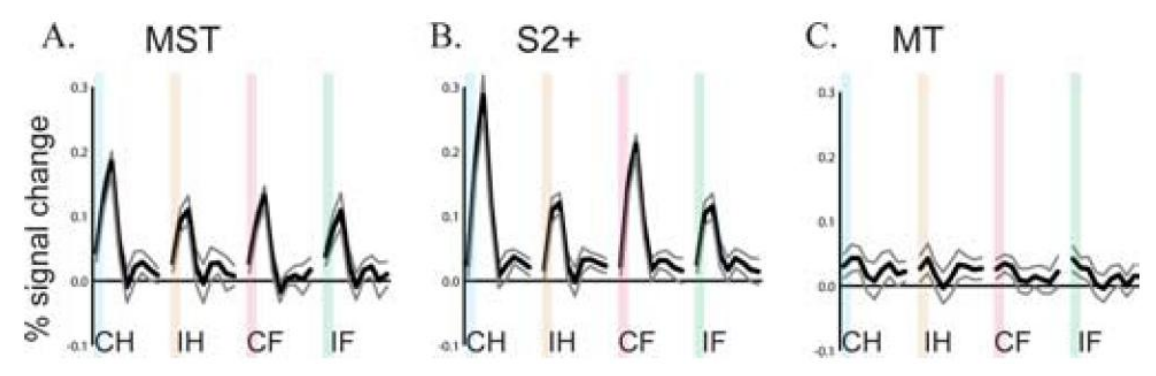


Figure 2. Time course of average evoked BOLD response (n = 8 subjects) to vibrotactile stimulation in MST (A), S2+ (B), and MT (C). Plots show evoked response to contralateral hand (CH), ipsilateral hand (IH), contralateral foot (CF), and ipsilateral foot (IF) stimulation. Colored bars illustrate 2 s stimulus duration. Black lines show mean signal change for 16 s after stimulus onset, and gray lines show ± 1 SEM.

Another well studied visual region is the LOC, defined as occipitotemporal cortex that prefers real visual images to scrambled visual images (Malach, et al. 1995). In a study in which subjects manipulated real objects, tactile responses were reported in a subregion of the LOC, labeled LOtv (tactile–visual) (Amedi, et al. 2001). There is overlap

between parts of the LOC and MT+ (Kourtzi, et al. 2002). This raises the question of whether the tactile MST responses observed in our study correspond to LOtv or represent a distinct focus of tactile activity. To answer this question, brain activity was measured as subjects viewed photographs and scrambled photographs. Cortex preferring real to scrambled photographs (the LOC) covered a large portion of lateral and ventral occipitotemporal lobes (Fig. 3A). An overlap map was created to show the relationship between LOC and other regions of interest (Fig. 3B). Superior portions of the LOC overlapped with inferior portions of MT. Tactile responses were observed in posterior and anterior portions of the LOC, corresponding to the previous descriptions of LOtv (Amedi, et al. 2002; Amedi, et al. 2001). In the single-subject and group maps (Fig. 3), the more anterior portion of LOtv was near the inferior border of MT. Therefore, the relatively few nodes in MT with a significant response to tactile stimulation likely share membership with LOtv. Tactile responses in MST were anterior and superior to LOtv and constituted a distinct focus of activity.

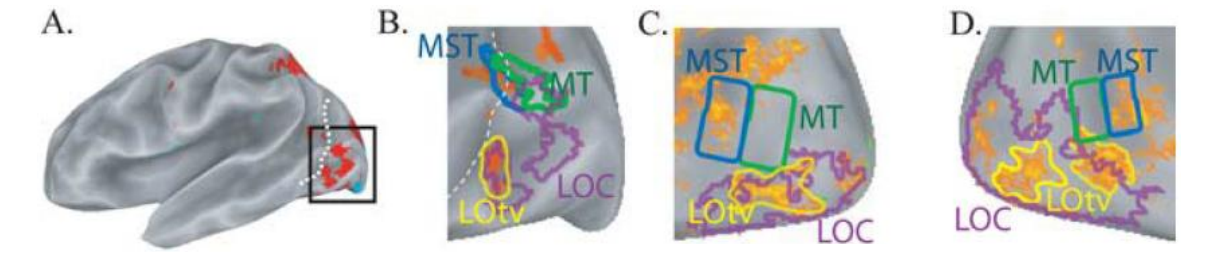


Figure 3. Relationship between tactile responses in MST and LOC (**A**, **B**, single subject; **C**, **D**, group data). **A**, Brain regions, in red, showing greater response to real pictures compared with scrambled controls in a single-subject left hemisphere. Dashed white line shows the fundus of the ascending limb of the posterior inferior temporal sulcus. **B**, Enlarged view of posterior lateral cortex (black region outlined in **A**). Shown is a composite map of LOC (outlined in purple), MST (blue), and MT (green) overlaid on tactile responses (orange). Portions of LOC, labeled as LOtv and outlined in yellow, responded to tactile stimulation. **C**, Group composite map showing identified visual areas overlaid on tactile activation in the left hemisphere (anterior is left). **D**, Group composite map of right hemisphere (anterior is right).

Previous studies of tactile responses in MT+ and LO have used only hand stimulation. To search for somatotopy in lateral occipital temporal cortex, we constructed individual and group maps of the contrast of contralateral hand versus contralateral foot stimulation (Fig. 4). The parietal operculum contained regions responsive to hand and foot stimulation organized in a mirror-symmetric manner, corresponding to the expected somatotopic organization of multiple representations of the body surface (Disbrow, et al. 2000; Eickhoff, et al. 2007). We did not observe somatotopic organization in MST. Most MST voxels preferred hand stimulation or showed no significant preference. We quantified the lack of somatotopy in MT+ as follows. If an area is somatotopic, there should be a spatial segregation between voxels that respond to hand stimulation and voxels that respond to foot stimulation. Mathematically, this can be quantified as the ratio between the number of voxels that respond to both hand and foot stimulation and the number of voxels that respond to either hand or foot stimulation. We calculated a relatively high ratio of 0.24 for MT+, indicating weak somatotopy (Young, et al. 2004).

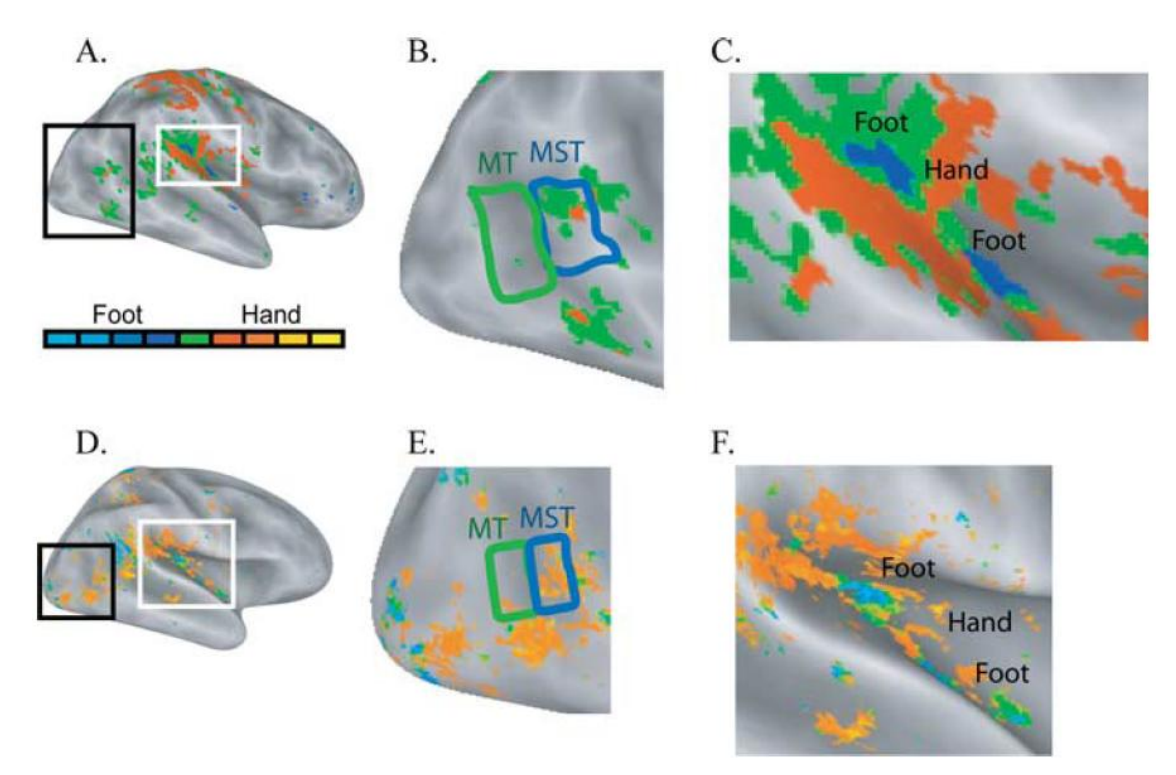


Figure 4. Location of hand- and foot-preferring regions (*A*–*C*, single subject; *D*–*F*, group data). *A*, Lateral view of right hemisphere. The color scale shows regions with a significant response to tactile stimulation and a preference for contralateral (left) foot stimulation (blue color scale), contralateral (left) hand stimulation (orange color scale), or no preference (green). The same color scale is used for *A*–*F*. *B*, Enlarged view of posterior lateral cortex (black region outlined in *A*). *C*, Enlarged view of operculum (white region outlined in *A*). A mirror-symmetric organization of foot- and hand-responsive areas was observed. *D*, Lateral view of group average dataset. *E*, Enlarged view of posterior cortex. *F*, Enlarged view of operculum.

Our analyses were conducted without any spatial smoothing to prevent the possibility that smoothing would blur activity from our visual areas of interest (MT, MST, and LOC), all of which are in close proximity. However, to obtain a global picture of brain areas responsive to vibrotactile stimulation, we performed a traditional SPM-style analysis in which a coarse (8 mm) Gaussian filter was applied to each individual subject's data before intersubject averaging. Then, a clustering technique was used to find the largest areas of activation on the group average cortical surface map. The results of this analysis are shown in Figure 5 and Table 1. As expected, the spatial smoothing blurred

together discrete activation foci (S2+, STS, MST, and LOC) into a single large patch of activation. The second largest area of activation was observed dorsally, in primary somatosensory cortex (S1) and adjacent areas, especially in a region in the postcentral sulcus. On the medial wall of the hemisphere, tactile responses were found in the supplementary motor area (Lim, et al. 1994) and posteriorly in the medial portion of S1.

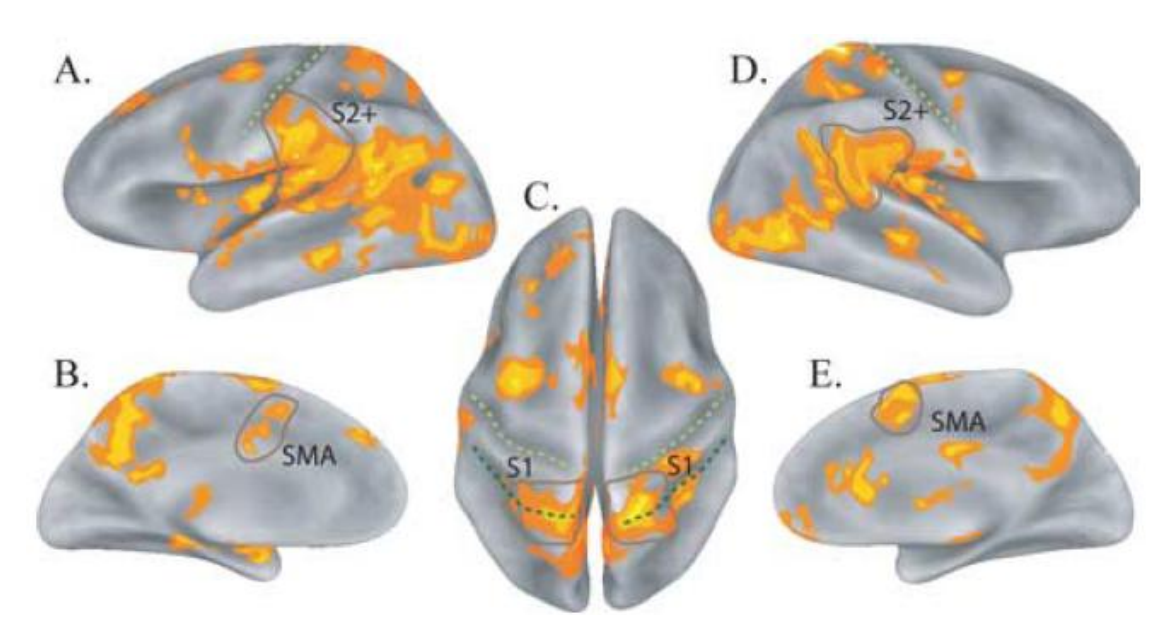


Figure 5. Group map of cortical tactile activations with spatial smoothing (8mmfull-width half-maximum Gaussian kernel). **A**, Lateral view of left hemisphere. **B**, Medial view of left hemisphere. **C**, Superior view of both hemispheres. **D**, Lateral view of right hemisphere. **E**, Medial view of right hemisphere. Outline shows selected regions. SMA, Supplementary motor area, located in the medial superior frontal cortex. Light green dashed line shows the fundus of the central sulcus, and dark green dashed line shows the fundus of the postcentral sulcus.

Table 1. Clustered-node analysis of the group average surface activation map shown in Figure 5

	Area (mm²)	Mean t statistic	Maximum t statistic	Coordinates o peak activity	f Location of peak activity	
Left hemisphere						
Lateral occipital-temporal-parietal	4545	4.9	18.2	(-54,-49,14)	Posterior superior temporal sulcus	
Postcentral gyrus	1834.25	4.4	8.7	(-15,-51,-59)	Postcentral gyrus and sulcus	
Right hemisphere						
Lateral occipital-temporal-parietal	2908	4.8	12.7	(40,-69,-2)	Lateral occipital (MST)	
Postcentral gyrus	1588	4.7	17.5	(21,-52,65)	Postcentral gyrus	

Subjects were not required to make any behavioral responses to the hand or foot vibrotactile stimuli, and little activation was observed in area MT. Because MT is known to be modulated by spatial attention (Beauchamp, et al. 1997; O'Craven, et al. 1997; Treue and Maunsell 1996), this raises the question of whether attending specifically to the vibrotactile stimulation would have resulted in increased activity in MT. To address this question, in a control experiment on a single subject, stimulation was delivered to different locations on the hand, and the subject made a behavioral response depending on the pattern of stimulation. As shown in Figure 6*B*, despite attention directed to the site of stimulation, activation was observed in MST but not in MT.

A second question concerns the relative amplitude of somatosensory and visual responses in MST. Because the visual localizer stimuli used a block design (20 s of stimulation), whereas the somatosensory experiment used a rapid event-related design (2 s of stimulation), it was not possible to directly compare the amplitudes of response. Therefore, in another control experiment on a single subject, a rapid event-related design was used to present point-light displays of biological motion, a stimulus known to evoke strong responses in MT+ (Beauchamp, et al. 2003; Peelen, et al. 2006). Consistent with amplitudes observed in previous studies, MST showed a 0.54% response to moving points. In the same subject, the MST response amplitude to vibrotactile stimulation of the contralateral hand was 0.26%, approximately one-half as large (Fig. 6C).

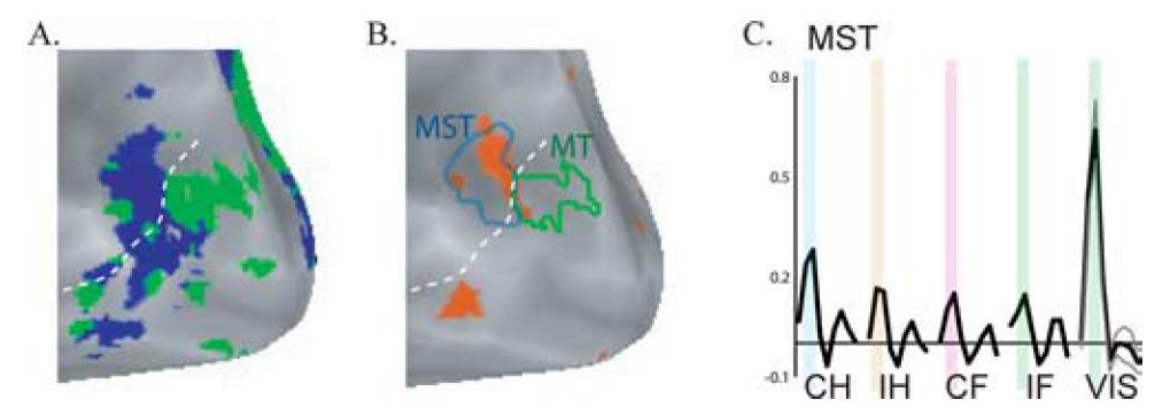


Figure 6. *A*, Brain areas responsive to visual motion that showed a response to ipsilateral visual stimulation (MST; blue) or no response to ipsilateral stimulation (MT; green) in a control subject (enlarged view of posterior left hemisphere). *B*, Composite map showing location of area MST and MT in the same subject overlaid on tactile activation map for an experiment in which all stimuli were delivered to the contralateral (right) hand. *C*, Results of a separate control experiment comparing responses to somatosensory and visual stimulation. Shown is an average time series from MST in a single subject for contralateral hand and ipsilateral hand (CH and IH, respectively) and foot (CF and IF, respectively) stimulation and for an average of six types of visual stimulation consisting of moving point-light figures (VIS).

Postmortem human brain studies have identified multiple cytoarchitectonically defined areas in the neighborhood of S1 and S2 (Eickhoff, et al. 2006a; Eickhoff, et al. 2007; Eickhoff, et al. 2006b; Geyer, et al. 1999; Grefkes, et al. 2001). To determine which of these areas were active in our study, we created an intersubject volume average and overlaid it on the publicly available standard-space map of cytoarchitectonic areas (Fig. 7). Near the superior portion of the central sulcus, activity was observed in areas 1, 2, and 3b, areas collectively referred to as the primary somatosensory cortex or S1. In the parietal operculum, activity was observed in OP1 (possible homolog of area SII), OP2 (possible homolog of PIVC), OP3 (possible homolog of area VS) and OP4 (possible homolog of area PV). To obtain a quantitative measure of which opercular areas were most active, we calculated the fraction of voxels within each region that exceeded our significance threshold of *p* < 0.01. A majority of voxels in OP1

(59.9%) and OP2 (59.8%) were significantly active, with a smaller fraction of active voxels in OP3 (19.1%) and OP4 (21.7%).

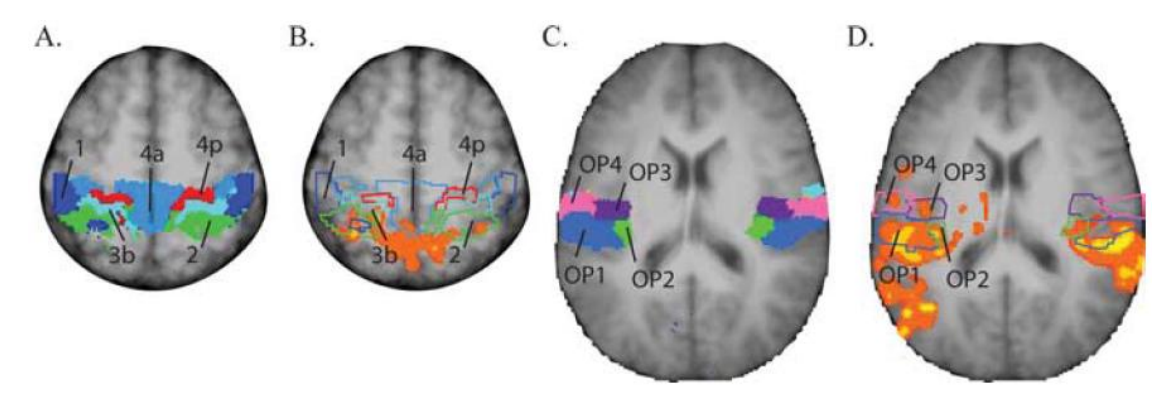


Figure 7. Relationship between cytoarchitectonically defined areas and somatosensory vibrotactile activation. A, Cytoarchitectonic regions in and near S1 from the Anatomy Toolbox (z=54 mm) (Eickhoff, et al. 2005; Geyer, et al. 1999; Grefkes, et al. 2001). B, Average somatosensory activation (orange-to-yellow color scale) under cytoarchitectonic boundaries (colored outlines). C, Cytoarchitectonic regions in and near S2 (z=18 mm) (Eickhoff, et al. 2006a; Eickhoff, et al. 2006b). D, Average somatosensory activations under cytoarchitectonic boundaries.

Discussion

These experiments demonstrate that simple vibrotactile stimuli evoke robust BOLD fMRI responses in MST but not in MT. A potential source for vibrotactile responses in MST is a projection from the ventral intraparietal area (VIP). In nonhuman primates, VIP receives input from hand and arm regions of S2, and in turn VIP projects to MST (Lewis and Van Essen, 2000). Connections from macaque VIP to MT are much sparser than those from VIP to MST, perhaps reflecting the weaker vibrotactile responses in MT than MST observed in the present study. Although the connectivity of human MST is uncertain, studies using diffusion tensor tractography (Rushworth, et al. 2006) and functional effective connectivity (Peltier, et al. 2007) offer promising avenues of exploration. Additional support for VIP contributions

to MST activation comes from a recent fMRI study, which proposed that the human homolog of VIP lies in the postcentral sulcus (Sereno and Huang 2006). Consistent with this proposal, we observed a strong focus of somatosensory activity in the mediolateral regions of the postcentral sulcus (Fig. 7). However, the homology between monkey and human parietal cortex is far from settled (Grefkes and Fink 2005), and other parietal areas must also be investigated as possible anatomical sources for tactile responses in MST.

In a meta-analysis of 57 functional imaging studies of S2, Eickhoff et al. (Eickhoff, et al. 2006a) found somatosensory activation in four cytoarchitectonically defined regions of parietal operculum (OP1–OP4), with the highest probability of activation in OP1 (putative S2). Consistent with this analysis, we also observed activation in each cytoarchitectonic region, with the highest fraction of active voxels in OP1/S2. There are likely to be important functional differences between the cytoarchitectonic subdivisions of the parietal operculum. In particular, OP2 may be equivalent to PIVC, the parietoinsular vestibular cortex. Our study found strong vibrotactile activation in OP2/PIVC, suggesting that multisensory convergence of tactile and vestibular information may occur in this region. Vibration applied to the neck can induce changes in steering of locomotion (Bove, et al. 2001) and perceived body orientation (Karnath, et al. 1994), demonstrating the behavioral relevance of vestibular—tactile integration. Additional studies examining the response of OP2 to the tactile and vestibular cues produced during natural behaviors, such as head movements (Petit and Beauchamp

2003), will be important to better understand the functional differences between the cytoarchitectonic subdivisions of the operculum.

Connections from many parietal regions to MST are considered to be "top-down" in the neuroanatomical sense, because they receive feed forward projections from MST and send feedback projections to MST, placing them higher in the visual processing hierarchy than MST (Felleman and Van Essen 1991). Top down has a quite different meaning in the psychological literature, in which it is used to describe perceptual phenomena that have a strong cognitive component, as opposed to bottom-up perceptual processes that are the direct result of sensory input. Although somatosensory responses in MST may arise from perceptual processing (bottom-up in the psychological sense), their potential substrates (e.g., VIP-to- MST feedback projections) is neuroanatomically top-down. We separately consider cognitive and perceptual processes that may be related to MST vibrotactile responses without labeling them as bottom-up or top-down.

The first cognitive factor that we consider is visual imagery. Previous studies reporting tactile activation in MT+ have used complex stimuli (such as a brush stroking the arm) and tasks (such as discriminating the direction of motion of a rotating sphere by touch) likely to induce imagery of visual motion. In our experiment, the piezoelectric vibrator was stationary relative to the body surface, so that there was no external cue to evoke imagery of visual motion. Imagery of the body site of stimulation is another possibility. In this view, tactile activation in MST is primarily an epiphenomenon of imagining the visual appearance of the touch or the body part being touched. However,

imagery is an active process engaged by demanding tasks, making this possibility unlikely: because there was no behavioral task for hand or foot stimulation in our study, there was no reason for subjects to engage in imagery. Furthermore, it is highly unlikely that over the hundreds of trials in our rapid event-related design, the subject would reliably (and in a time-locked manner) engage in visual imagery of the stimulus or the body part that was stimulated. Finally, it is also unlikely that imagining the visual appearance of the hand evokes stronger responses in MST than imagining the visual appearance of the foot, which is what was measured. Despite this evidence against an imagery explanation, we cannot definitively rule out a contribution of visual imagery without additional studies.

The second cognitive factor that we consider is attention. MT+ is part of the "attentional network" that shifts spatial attention to exogenous cues (Beauchamp, et al. 2001; Corbetta, et al. 1998). Tactile stimuli might produce a shift in the focus of attention to the body location of the stimulus. However, like visual imagery, shifting attention is a resource-demanding process. As argued for imagery, without a task requiring them to shift attention, it seems likely that subjects would habituate over the course of the hundreds of trials of passive stimulation.

We next consider perceptual processes that may explain MST activation. We now turn to more likely processes. The first perceptual process that may be an explanation for tactile MST activity is spatial transformation. An fMRI study suggests that anterior regions of MT+ (likely MST) code space in a spatiotopic (body centered) as opposed to retinotopic reference frame (d'Avossa, et al. 2007). MST might be part of a

brain network, including parietal areas such as VIP, that transform somatotopic touches on the body surface to spatiotopic coordinates. The second perceptual process that may explain tactile activation in MST is sensorimotor integration. Temporary inactivation of MST interferes with visually guided hand movements as well as smooth-pursuit eye movements (Ilg and Schumann 2007), and there are anatomical connections between MST and hand motor areas (Marconi, et al. 2001). Our finding that MST responds more strongly to hand than foot stimulation supports a link between MST and eye-hand coordination (Whitney, et al. 2007). Integrating visual and tactile signals in MST may be important for enabling the complex dynamics necessary to track and grasp a moving object. A third perceptual process that may explain tactile responses in MST is involvement in purely somatosensory processing. Just as MST is important for perceiving the direction and speed of visual stimuli (Celebrini and Newsome 1995), it may also be important for computing the direction and speed of tactile stimuli (Blake, et al. 2004; Hagen, et al. 2002). Although our vibrotactile stimuli were stationary relative to the body surface, they vibrated at a high frequency perpendicular to the skin surface. MT+ responds to visual flicker (Tootell, et al. 1995), which could be considered analogous to stationary vibrotactile stimulation. Therefore, responses in MST to simple vibrotactile stimulation do not rule out the involvement of MST in tactile motion processing.

Activity in MT and MST may also be dependent on the behavioral task. Although we did not observe MT activity in response to passive vibrotactile stimulation, it is possible that other kinds of tactile stimuli and tasks, such as direction discrimination of a

moving tactile stimulus, could evoke MT activity. However, a recent study demonstrated that passive presentation of a moving tactile stimulus activated only anterior regions of MT+ (likely corresponding to MST) in normal controls (Ricciardi, et al. 2007). Additional studies comparing the responses of MT and MST to stationary and moving tactile stimuli with different behavioral tasks will be important to determine the functional role of tactile responses in MT+.

Chapter 3: Touch, Sound and Vision in Human Superior Temporal Sulcus

Based on manuscript:

Beauchamp, M.S., Yasar, N.E., Frye, R.E., Ro, T. (2007). Touch, sound and vision in human superior temporal sulcus. Neuroimage 41 (3), 1011-1020

Introduction

In everyday life, perceptual events often occur in multiple sensory modalities: we may feel our cell phone vibrate, hear it ring, or see the display flash, all indicating an incoming call. Where and how such multisensory processing occurs has intrigued philosophers, psychologists, and neuroscientists since at least the time of Aristotle (Aristotle 350 B.C.E). In the macaque monkey, an important multisensory region lies along the fundus of the posterior superior temporal sulcus (STS). This region was originally labeled the superior temporal polysensory (STP) area because single units in this area respond to visual, auditory and somatosensory stimulation (Bruce, et al. 1981). Physiological and anatomical studies have delineated the cortical and subcortical connections and functional properties of macaque STP, also sometimes referred to as TPO (Padberg, et al. 2003). Identifying the human homolog of macaque STP will allow us to generate additional hypotheses about the functional and anatomical properties of human STS (Beauchamp 2005a).

In the banks of human posterior STS, neuroimaging studies have reported multisensory responses to auditory and visual stimulation (Beauchamp, et al. 2004b; Calvert 2001; Noesselt, et al. 2007; van Atteveldt, et al. 2004; Wright, et al. 2003). This region has been termed STSms, the STS multisensory region (Beauchamp, et al. 2004a). Guided by the macaque literature, we wanted to determine if STSms was also important for processing somatosensory information. Previous human fMRI studies examining responses to somatosensory, auditory and visual stimulation have found regions responsive to all three modalities in parietal and frontal cortex, but not in the STS

(Bremmer, et al. 2001; Downar, et al. 2000). Some studies of somatosensory processing have reported activity in STS (Burton, et al. 2006; Disbrow, et al. 2001; Golaszewski, et al. 2002)but it is unclear if somatosensory, auditory and visual responses occur in human STSms as they do in macaque STP.

The primary goal of our experiments was to test the hypothesis that human STSms responds to somatosensory, auditory and visual stimulation. A secondary goal, contingent on the presence of somatosensory responses in STSms, was to test the hypothesis that multisensory integration between touch and sound occurs in STSms.

Because a benchmark of multisensory integration is a differential response to multisensory compared with Unisensory stimulation (Beauchamp 2005b), we compared the response to multisensory and unisensory somatosensory and auditory stimulation.

The final goal of the experiments was to characterize somatosensory and visual responses in STSms to a broad range of stimuli to allow an assessment of whether human STSms has similar response properties as macaque STP, above and beyond simply responding to touch, sound and vision.

Methods

We used a single subject approach, identifying STSms on cortical surface models created for each individual subject. To allow us to devote the bulk of the experimental time to studying somatosensory responses in STSms, we used functional localizers (Saxe, et al. 2006) to map visual responses in STSms in Experiment 1 and visual and auditory

responses in STSms in Experiment 2. Table 1 lists a summary of the experimental conditions across experiments.

Subjects were recruited and informed consent was obtained in accordance with the University of Texas Committee for the Protection of Human Subjects. Eight subjects participated in experiment one (2M, 6F, mean age 26 years) and twelve subjects participated in experiment two (8M, 4F, mean age 27 years). Subjects' data was anonymized with two letter experiment codes not corresponding to the subjects' initials.

Table 1
Distribution of experimental conditions across subjects and experiments

Task	Scan series	Design	Conditions
Experiment 1: 12 subjects			
Visual localizer	1–3	BD	2
Vibrotactile somatosensory and auditory	3–6	RER	6
Experiment 2: 8 subjects			
Visual motion localizer	1	BD	3
Visual object localizer	1	BD	3
Auditory localizer	1	BD	2
Vibrotactile somatosensory	4–6	RER	6

Each task refers to a separate experimental condition undertaken in a separate MR scan series ("run"). Every subject performed every task, but the number of scan series devoted to each task varied from subject to subject. The number in the scan series column shows the range across subjects. The design column shows the type of stimulus presentation paradigm (BD: block design; RER: rapid event-related). The number in the conditions column shows the number of different conditions in each task, including fixation baseline.

General MRI Methods

Participants were scanned using a 3-tesla whole-body MR scanner (Phillips Medical Systems, Bothell, WA). Anatomical images were collected using a magnetization-prepared 180 degrees radio-frequency pulses and rapid gradient-echo

(MP-RAGE) sequence optimized for gray—white matter contrast with 1 mm thick sagittal slices and an in-plane resolution of 0.938×0.938 mm. Functional images were collected using a gradient-recalled-echo echo-planar-imaging sequence sensitive to the BOLD signal. Thirty-three axial slices were collected with an echo time (TE) of 30 ms and a flip angle of 90 degrees. Slice thickness was 3 mm and in-plane resolution was 2.75 mm×2.75.

Experiment 1

Experimental paradigm

As shown in Fig. 1, a three by two design was employed, with three categories of sensory stimulation (tactile-only, auditory-only, simultaneous tactile—auditory) and two intensities of stimulation (strong and weak). The trial duration was 2.75 s, corresponding to an MRI repetition time (TR) of 2.75 s. Within each TR, acquisition was clustered so that imaging (with its accompanying sound and vibration) was completed in the first 2 s of the TR, followed by 0.75 s of silence. During the middle 500 ms of this silent interval, the stimulus was presented. A rapid event-related design was used. Each 5-minute scan series contained 110 trials (corresponding to 110 TRs) with 15 trials of each type and 20 trials of fixation baseline with no auditory or tactile stimulation.

Vibrotactile somatosensory stimuli were delivered using a piezoelectric bending element (Piezo Systems, Inc., Cambridge, MA) attached to the left hand using non-slip silicon elastic bandages. The qualitative percept of stimulation was akin to holding a ringing cell phone set to "vibrate" mode, without any accompanying auditory percept

(the vibration of the benders was inaudible because of its low sound pressure level and the MR-compatible sound attenuating headphones worn by the subjects). Auditory stimuli were delivered to only the left channel (left ear) of the headphones to produce rough spatial correspondence with the left hand tactile stimulation.

The same waveform was used for vibrotactile stimulation (delivered via the piezoelectric benders) and auditory stimulation (delivered via headphones). A driving voltage was generated by a 24-bit PC sound card and amplified by a multichannel amplifier (Sony USA, New York, NY). The waveform consisted of a 200 Hz sinusoidal oscillation in a 500 ms envelope. To prevent onset and offset artifacts, the first and last 100 ms of the 500 ms envelope consisted of the first and second quarter-cycle of a 5 Hz sine wave, allowing the oscillation amplitude to gradually increase and decrease.

During experimental trials, subjects discriminated between the three trial types (tactile-only, auditory-only, or auditory-tactile) by pressing one of three buttons on a fiber optic response stick (Current Designs, Philadelphia, PA). No feedback was provided. Subjects were instructed to fixate central crosshairs, back-projected from an LCD projector (Sony Electronics, San Diego, CA) onto a Lucite screen (Da-Lite Inc., Warsaw, IN) and viewed through a mirror attached to the MR head coil. An MR-compatible eyetracking system (Applied Science Laboratories, Bedford, MA) was used to monitor fixation and behavioral state.

Two intensities of stimulation were used: strong and weak. The intensities were adjusted for each subject in the MR scanner just prior to fMRI data collection, using the same driving waveform as used in the fMRI experiment. A strong tactile stimulus was

delivered at a fixed intensity (10 dB attenuation equivalent to 30 V driving voltage and approximately 153 μm displacement for four subjects; 15 dB attenuation, 17V, 72 μm for three subjects; 17 dB, 13V, 72 μm for five subjects). To set the level of the strong auditory stimulus, an auditory stimulus was presented at the same time as the strong tactile stimulus. Subjects used the MR-compatible response buttons to adjust the intensity of the auditory stimulus until it matched the perceived magnitude of the strong tactile stimulus (mean attenuation 16 dB±2 dB SEM, mean sound pressure level 72 dB±2 dB). To set the level of the weak tactile stimulus, subjects decreased the intensity of the strong tactile stimulus until it was very weak but could still be detected on every presentation (50±1 dB attenuation, 0.3V±0.04V, 1.6±0.2 μm displacement). This threshold was consistent with previous psychophysical studies using 200 Hz vibrotactile stimulation (Brisben, et al. 1999). To set the level of the weak auditory stimulus, subjects adjusted the intensity of the auditory stimulus to match the intensity of a simultaneously presented weak tactile stimulus (42 dB±2 dB attenuation, 49±2 dB SPL).

Visual localizer

To identify visually-responsive brain regions, a block-design visual localizer was conducted, in which subjects performed no task but alternately viewed 30-second excerpts from a movie (Winged Migration, Sony Pictures Classics) and fixation baseline.

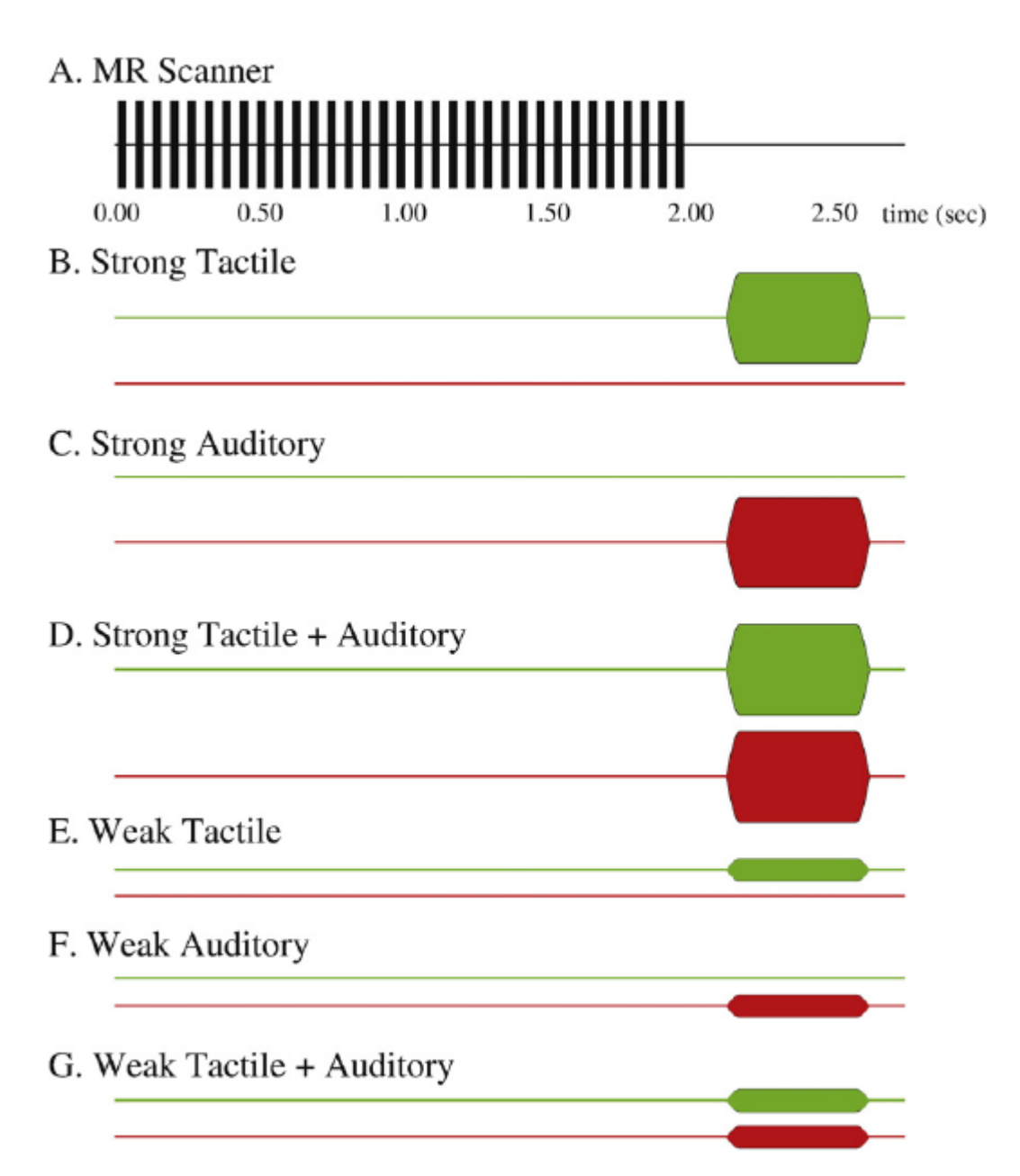


Figure 1. Structure of stimulation trials in Experiment 1. A. Clustered MRI acquisition protocol. During the first 2 s of each 2.75-second trial, 33 images were acquired. Each image acquisition (indicated with thick vertical bars) produced sound and vibration from the scanner. Experimental stimuli were presented in the final 0.75 s of the trial, when no MR image acquisition occurred. B. Sensory stimulus during strong tactile trials. Green line indicates tactile stimulation, red line indicates auditory stimulation. The thick green portion indicates duration of a 200 Hz sinusoidal vibrotactile stimulus applied to the left hand. Gradual rise and fall of the thick green portion reflects the 4 Hz sinusoidal envelope applied to the driving waveform. C. Sensory stimulus during strong auditory trials. The thick red portion indicates duration of a 200 Hz sinusoid played in the left ear. D. Sensory stimulus during strong tactile+auditory trials. Thick portions indicate simultaneous tactile+auditory stimulus presentation. E. Unisensory tactile stimulus presented at low intensity. G. Multisensory tactile+auditory stimulus presented at low intensity. Stimulus presented at low intensity.

Experiment 2

Experimental Paradigm

The vibrotactile somatosensory stimulus in Experiment 2 was delivered by five piezoelectric benders attached to the left and right hand and foot of the subject and the right hip. Trial duration and TR were both 2 s (clustered acquisition was not used) and there were five trial types, each containing stimulation of a single bender. The driving voltage consisted of a 200 Hz sine wave modulated by a 4 Hz square wave envelope. There was no task during hand or foot stimulation. Hip stimulation trials (catch trials) required subjects to make an eye movement to a visual target (the word "TARGET") in the upper right corner of the display screen, which was otherwise blank except for white fixation crosshairs (the target and fixation crosshairs were always present, so there were no visual transients associated with changes in the display). fMRI data from the catch trials were analyzed separately, so that oculomotor activations in catch trials would not confound the somatosensory activations measured in hand and foot trials; only the responses in hand and foot trials are reported here. In the rapid event-related design, each 5-minute scan series contained 150 trials (corresponding to 150 TRs) with 25 of each of the four types of hand and foot trials, 10 catch trials and 40 fixation baseline trials. Subjects performed 4–6 runs. A report on somatosensory responses in area MST using the data collected for Experiment 2 has been previously published (Beauchamp, et al. 2007).

Visual and auditory localizers

In separate scan series, subjects performed different auditory and visual localizers (see Table 1 for a summary). In the first localizer, subjects viewed low-contrast random moving dots presented in the left or right hemifields alternating with stationary dots. In the second localizer, subjects viewed real photographs of objects and scrambled photographs, alternating with fixation baseline. In the third localizer, subjects heard brief (1–2 s) recordings of a variety of non-linguistic stimuli, including recordings of animal calls, recordings of man—made objects (both manual and powered), scrambled versions of these recordings, and pure tones (Beauchamp, et al. 2004b). Subjects performed a simple detection task during each localizer to ensure attention to the stimulus.

Experiment 1 and 2: fMRI experimental design and data analysis

fMRI data was analyzed using AFNI (Cox 1996). Individual cortical surface models were created with FreeSurfer (Fischl, et al. 1999) and visualized in SUMA (Argall, et al. 2006). Localizer experiments were performed with a block design and analyzed with the general linear model by convolving the timing of each type of stimulation block with a gamma-variate function. Tactile experiments were conducted using a rapid event-related design, and analyzed with finite impulse response deconvolution. This allows estimation of the hemodynamic response to each trial type as if it had been presented in isolation in a slow event-related design.

To identify areas responding to auditory, visual and somatosensory stimulation, a modified conjunction analysis was used (Nichols, et al. 2005). In each subject, the tstatistic of the contrast between stimulation vs. rest was independently calculated for each sensory modality in every voxel. This contrast revealed voxels that showed either a positive or negative BOLD response to sensory stimulation. Because a task-independent network of brain areas is deactivated (negative BOLD response) during any kind of sensory stimulation (Raichle, et al. 2001) we selected only voxels showing a positive BOLD response to each sensory modality. This criterion was instantiated with the thresholding operation (Visual-t-statistic>x) AND (Auditory-t-statistic>x) AND (Tactile-tstatistic>x) where x is the unisensory threshold (Beauchamp 2005b). All voxels passing this test were classified as "multisensory", mapped to the cortical surface and classified as inside or outside the STS using an automated surface parcellation algorithm (Fischl, et al. 2004). The time series from all multisensory STS voxels were converted to percent signal change and averaged to create an average time series for each subject. These time series were then averaged across subjects to create a grand mean.

A conjunction analysis was also used to create the mixed effects group map.

Individual subject brains were converted to standard space (Brett, et al. 2002), and the percent signal change for each condition was entered into a voxel-wise ANOVA with subject as the random factor and condition as the fixed factor. A conjunction analysis was performed on the output of the ANOVA to find voxels showing a significant effect to each modality in isolation. All statistical inferences are based on between-subjects

variance using a mixed-effects model, with stimulus type as the fixed factor and subject as the random factor.

Most statistical tests were performed only on the average time series created from all active voxels in each subject's STS, mitigating the need to perform corrections for multiple comparisons. To create activation maps, a significance level of p<0.05 (single voxel, uncorrected for multiple comparisons) was used for the single modality activation maps and p<0.01 for the conjunction analysis. The actual probability of the observed STSms activations being due to chance fluctuations in the MR signal is considerably lower, approximately p<pⁿ, where p is the single-voxel p-value and n is the number of voxels in the STSms (Xiong, et al. 1995). For individual subjects, mean n=17; for the group map, n=55.

Results

Experiment 1

Subjects received vibrotactile somatosensory stimulation on their left hand and auditory stimulation in their left ear while making behavioral responses with their right hand. To determine brain areas responsive to sensory stimulation, we focused our analysis on the right hemisphere, collapsing across different intensities of stimulation. As shown in Fig. 2A, tactile-only trials activated a broad network of frontal, parietal and temporal, including the post-central gyrus (the location of primary somatosensory cortex, S1), the parietal operculum (the location of secondary somatosensory cortex, S2), intraparietal sulcus, and the STS. Auditory-only trials activated a similar network of

areas (including the STS) and the temporal plane, the location of core and belt areas of auditory cortex (Fig. 2B). The visual localizer activated occipital, temporal and parietal cortex, including the STS (Fig. 2C). To determine regions that responded to all three modalities, we performed a voxel-by-voxel conjunction analysis. Voxels concentrated in the parietal lobe and the STS were active in all three conditions (Fig. 2D). The mixed-effects group map showed a similar pattern, with a region of posterior STS responding to all three modalities (Fig. 2E). The center-of-mass of the STS activation in the group map was (52, 44, 15).

After identifying STSms, we measured the degree of multisensory integration in STSms between tactile and auditory modalities. The evoked response in STSms to unisensory and multisensory trials was computed in each subject and averaged across subjects (Figs. 2F, G). The response resembled a classical hemodynamic response with a sharp increase followed by a slow return to baseline. Due to the relatively long TR (2.75 s), the largest magnitude of response was observed in the second TR, 5.5 s following stimulus onset; this peak magnitude was used as a measure of the amplitude of response in different trials. Because the STSms was defined without reference to the multisensory response, unbiased statistical comparisons could be performed between multisensory and unisensory responses (Simmons, et al. 2007).

The response was similar in unisensory tactile and auditory trials (0.30% vs. 0.31%±0.02% SEM for both). In multisensory tactile—auditory trials, the response was significantly larger than the maximum unisensory response and the average unisensory response (multisensory response, 0.38%±0.02% SEM vs. max Unisensory response,

 $0.31\%\pm0.02\%$ SEM, paired t-test with 11 degrees of freedom, p=0.0001). The response in the STSms to each of the six trials types was also entered into a three-factor mixed-effect ANOVA with stimulus modality (tactile, auditory, tactile—auditory) and intensity (weak, strong) as fixed factors and subject as a random factor. The most significant effect was modality (F(2,22)=10.3, p=0.0007) driven by the increased response to multisensory stimulation. There was also a significant effect of intensity (F(1,11)=16.1, p=0.002), reflecting a larger response to strong compared with weak stimuli (0.37 $\%\pm0.02\%$ vs. 0.29 $\%\pm0.02\%$). The interaction between modality and intensity was not significant (F(2,22)=0.1, p=0.9) showing that the degree of multisensory enhancement did not differ between weak and strong multisensory trials.

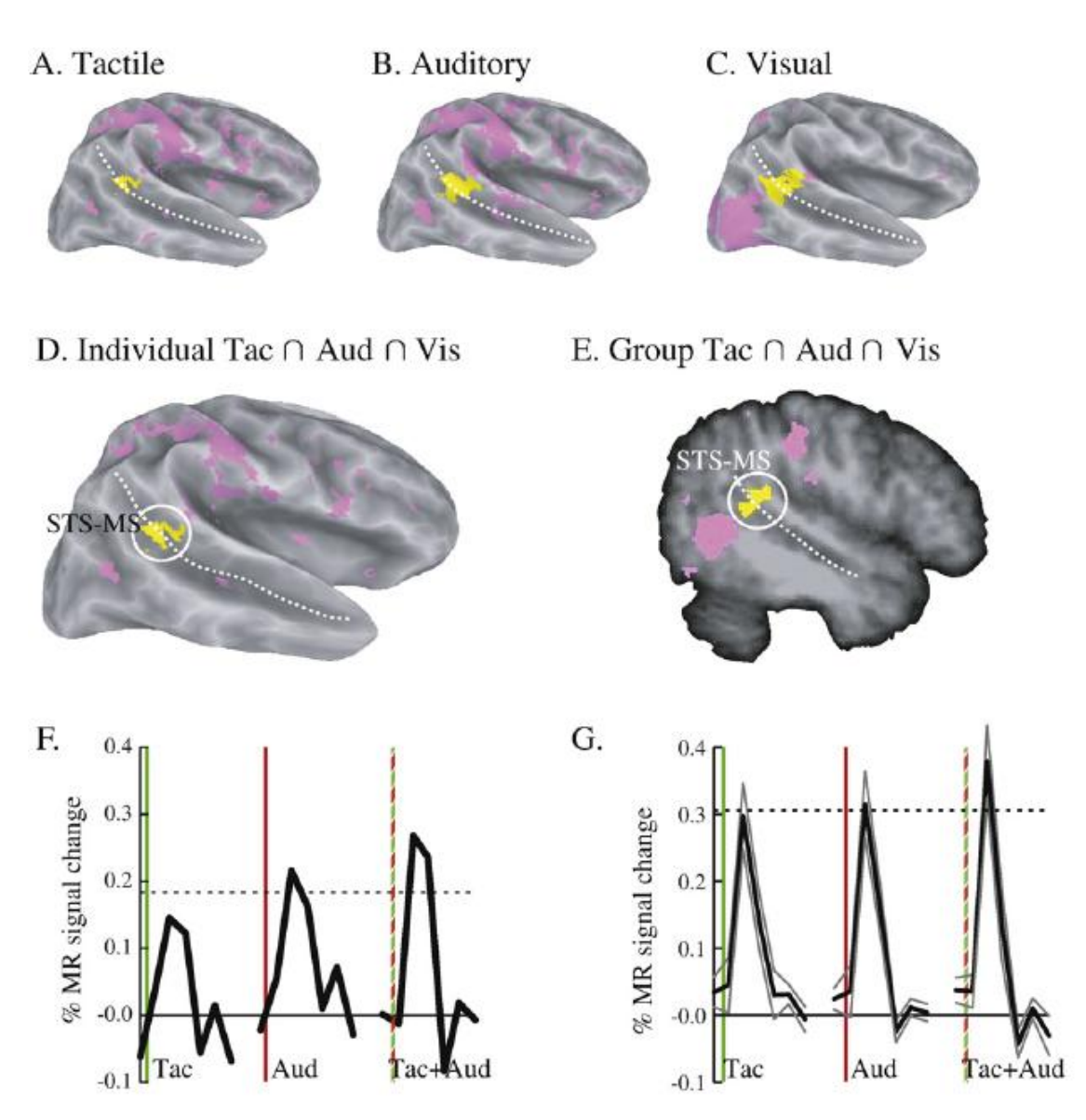


Figure 2. Responses to tactile, auditory and visual stimulation in Experiment 1. **A.** Lateral view of a single subject's partially inflated right hemisphere. Colored regions responded significantly to tactile stimulation. Active regions in posterior STS are colored yellow; other active regions are colored purple. The fundus of the STS is shown as a white dashed line. **B.** Single subject activation to auditory stimulation. **C.** Single subject activation to visual stimulation. **D.** Single subject conjunction map showing voxels responding to all three modalities. Circled yellow cluster shows the STS multisensory area, STSms. **E.** Mixed effects group map (n=12). Voxels showing a significant response to all three modalities. Yellow cluster shows the STSms, with center-of-mass (52, 44, 15). **F.** Single subject MR time series from STSms. The dark black line shows the deconvolved event related response in a 16.5-second window following stimulation onset for three kinds of trials, collapsed across intensity of stimulation: Tac, tactile stimulation; Aud, auditory stimulation; Tac+Aud, tactile and auditory stimulation. The dashed line shows the mean unisensory response. The colored bars show the 500 ms stimulus duration. **G.** Group average MR time series from STSms (n=12). The dark black line shows the mean deconvolved event-related response, the gray line shows±1 SEM.

Experiment 2

In Experiment 1, subjects performed a discrimination task, manually pressing a button in response to each sensory stimulus. It could be argued that the observed STS activations were the result of cognitive processes involved in task performance, rather than simple sensory responses. To address this possibility, in Experiment 2 subjects received somatosensory vibrotactile stimulation on their hands and feet that did not require a behavioral response (Beauchamp, et al. 2007).

Because tactile stimuli were delivered bilaterally, we expected responses to be evoked in both left and right hemispheres. Consistent with this, we observed activation in the left and right postcentral gyrus, parietal operculum and STS (Fig. 3A). Localizers were used to map auditory and visually-responsive brain regions. Auditory responses were observed in the temporal plane, inferior frontal cortex, and the STS (Fig. 3B) while visual responses were found primarily in the occipital lobe and the STS. A conjunction analysis revealed a focus of trisensory activation in posterior STS in the single subject (Fig. 3D) and group average activation maps (Fig. 3E). The center-of-mass of the average STS activation was (56, 41, 14) in the right hemisphere and (-44, 35, 13) in the left hemisphere.

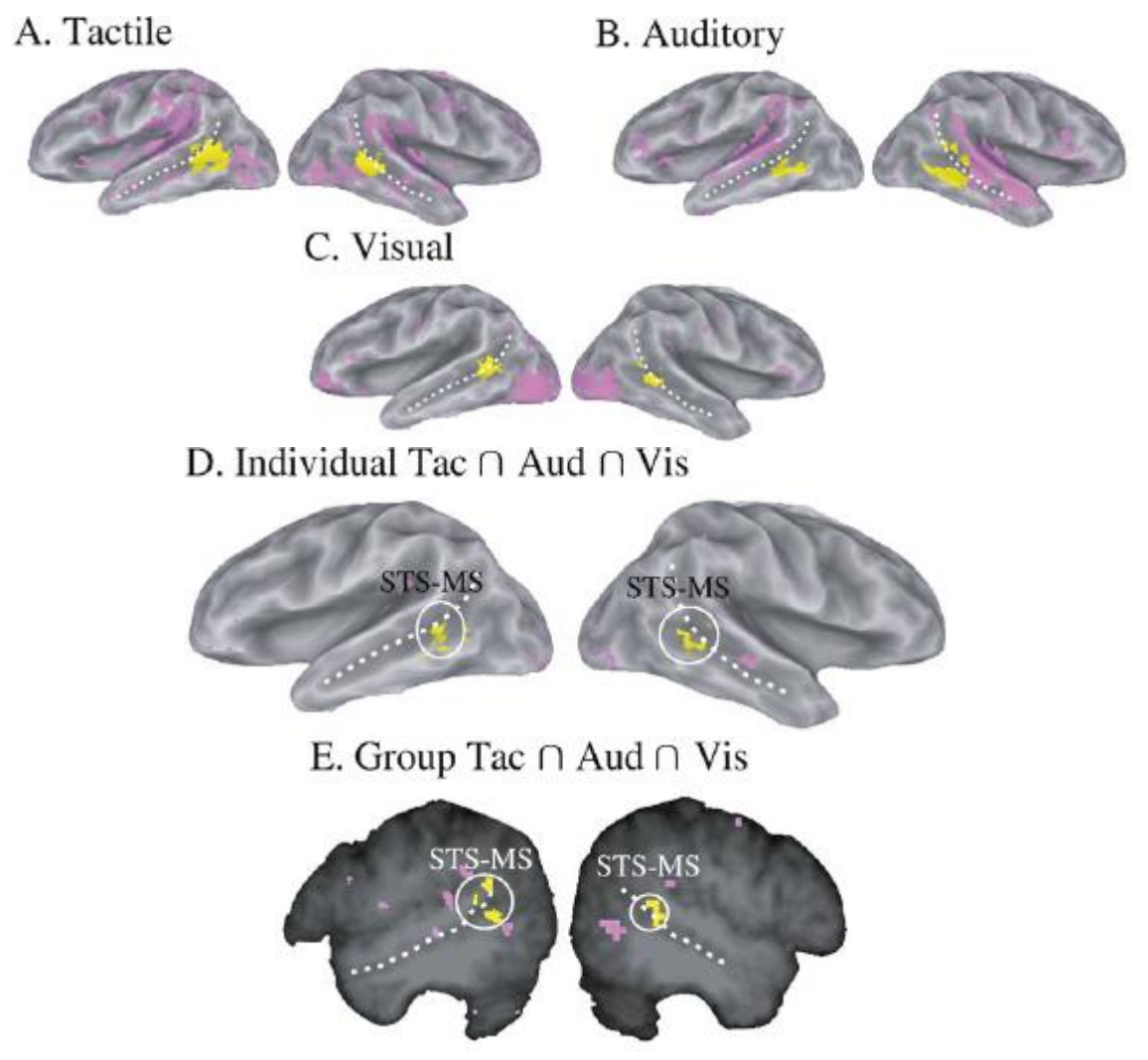
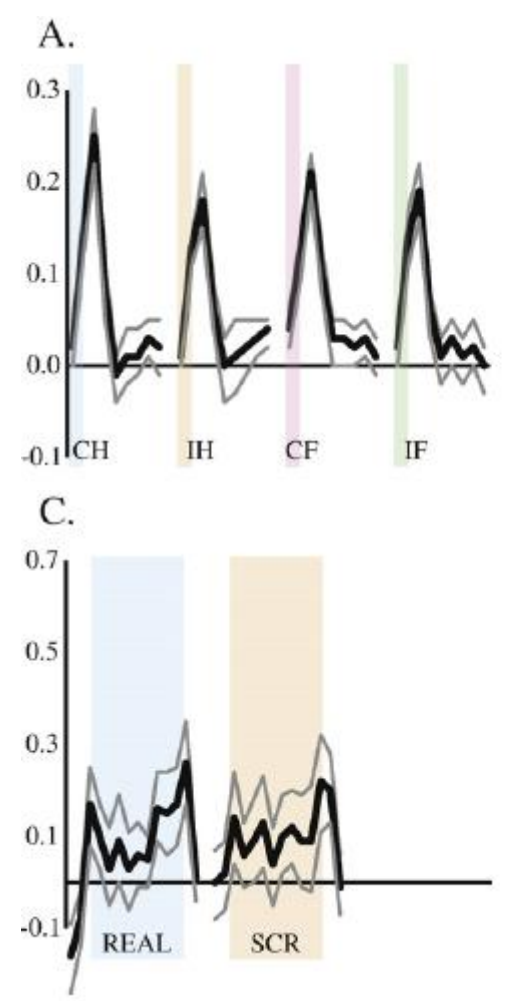


Figure 3. Brain areas responding to auditory, visual and tactile stimulation in Experiment 2. **A.** Lateral view of a single subject's partially inflated right hemisphere. Colored regions responded significantly to tactile stimulation. Active regions in posterior STS are colored yellow, other active regions are colored purple. The fundus of the STS is shown as a white dashed line. **B.** Single subject activation to auditory stimulation. **C.** Single subject activation to visual stimulation. **D.** Single subject conjunction map showing voxels responding to all three modalities. Circled yellow cluster shows the STS multisensory area, STSms. **E.** Mixed effects group map (n=8). Voxels showing a significant response to all three modalities. Yellow cluster shows the STSms, with center-of-mass (-44, 35, 13) in left hemisphere and (56, 41, 14) in right hemisphere.

The event-related design used for the tactile experiment allowed us to extract the average hemodynamic responses to single stimulation trials (Fig. 4A). The strongest response was to contralateral hand stimulation (0.25%), which was significantly greater than the response to ipsilateral hand stimulation (0.18%, paired t-test with 7 degrees of

freedom, p=0.02) contralateral foot stimulation (0.21%, p=0.02) and ipsilateral foot stimulation (0.19%, p=0.02). In order to determine the functional properties of the STSms, we also calculated the average evoked response during the different stimulus conditions presented in the visual and auditory block-design localizers. STSms showed a strong response to low-contrast moving points, with a greater response to contralateral than ipsilateral motion (Fig. 4B; 0.45% vs. 0.29%, p=0.004). STSms also responded to static images (Fig. 4C), although significantly weaker than the response to moving points (0.13%, p=0.03). There was no significant difference in the response to real photographs compared with the response to scrambled photographs (0.13% for both). Auditory stimulation produced a strong response that was equivalent in magnitude (0.41%, p=0.4) to the strongest visual stimulus (contralateral moving points) but was significantly greater than the response to the other visual stimuli (p=0.0004) although these comparisons must be interpreted cautiously because auditory and visual stimuli were presented in different scan series.



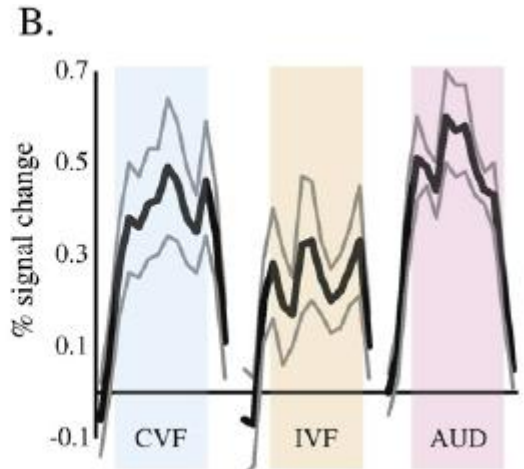


Figure 4. Time course of average evoked BOLD response (n=8 subjects) in the STS multisensory area. **A.** Response to contralateral hand (CH), ipsilateral hand (IH), contralateral foot (CF), and ipsilateral foot (IF) stimulation. Colored bars illustrate 2-second stimulus duration. Black lines show mean, gray lines show ±1 SEM. **B.** Response to low-contrast moving points in the contralateral (CVF) and ipsilateral (IVF) visual field. Response to auditory stimuli (AUD) is shown for comparison. Colored bars illustrate 20-second stimulus duration (followed by fixation baseline). **C.** Response to real (REAL) and scrambled (SCR) photographs.

In macaque monkeys, area STP is located anterior and superior to areas MST and MT. To determine the relationship between human MT, MST and STSms, previously described techniques (Beauchamp, et al. 2007; Huk, et al. 2002) were used to create maps of all three areas in two hemispheres (Fig. 5). MT was located in the posterior bank of the ascending limb of the posterior inferior temporal sulcus. MST was located anterior in the ascending limb of the sulcus, extending onto middle temporal gyrus. STSms was located on the posterior bank and fundus of the STS, just anterior to MST. Across subjects, a consistent anatomical landmark for STSms was the inflection point in

the posterior superior temporal sulcus where it angles upwards towards the parietal lobe. The anatomical positioning of MT, MST and STSms in human cortex was similar to that of MT, MST and STP in macaque cortex (Fig. 5D).

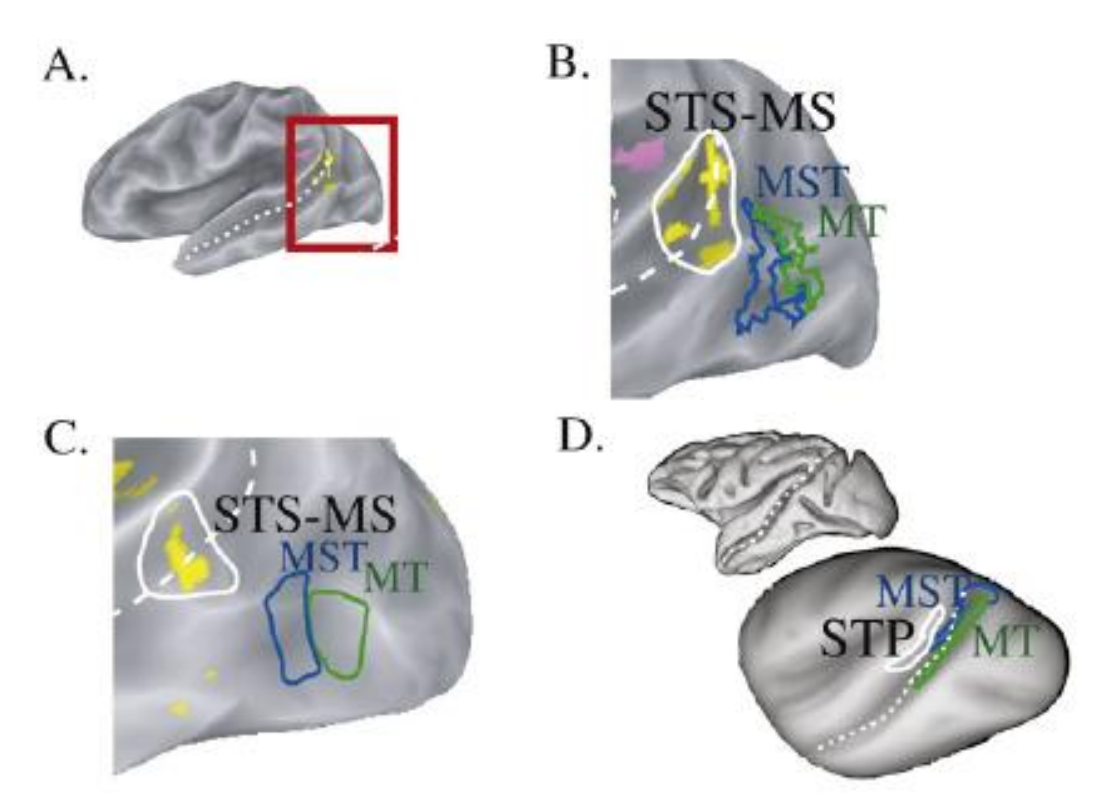


Figure 5. Relationship between the STS multisensory area (STSms) and areas MT and MST. **A.** Lateral view of a single subject's partially inflated left hemisphere. Colored regions responded significantly to all three modalities. Active regions in posterior STS are colored yellow, other active regions are colored purple. The fundus of the STS is shown as a white dashed line. Red box indicates the region enlarged in B. **B.** Composite map showing multisensory activation and localizer defined MT and MST. White outline shows STSms, blue outline shows MST, green outline shows MT. **C.** Composite map in an additional hemisphere from a different subject. **D.** Relationship between macaque area STP and macaque areas MTand MST. The top panel shows a lateral view of a macaque brain (Dickson, et al. 2001). The fundus of the STS is shown as a white dashed line. The bottom panel shows an inflated view of the brain, with labeled areas from (Lewis and Van Essen 2000b): MT, MST (MSTdp+MSTm) and STP (TPOi+TPOc).

Discussion

Guided by the literature on macaque STP, we hypothesized that human STS should contain an area that responds to somatosensory, auditory and visual stimulation.

Data from twenty subjects in two separate imaging experiments supported this hypothesis.

Tactile responses in STSms

Previous studies have reported somatosensory responses in human STS (Burton, et al. 2006; Disbrow, et al. 2001; Golaszewski, et al. 2002). The present results are the first to show that these responses are co-localized with auditory and visual responses. The results of Experiment 1 might have reflected a general cognitive process important for the behavioral task rather than a modality-specific sensory response in STS.

However, passive presentation of somatosensory stimuli in Experiment 2 evoked a similar magnitude of response as Experiment 1 suggesting that a behavioral task is not required for somatosensory STS responses. The magnitude of STSms response was modulated by the intensity of the tactile stimulation and by the body site of stimulation, further supporting the conclusion that STSms responses reflect sensory processing rather than task performance.

Multisensory integration in STSms

Previous studies have shown that posterior STS responds more to multisensory auditory—visual stimuli than to unisensory auditory or visual stimuli (Beauchamp, et al. 2004b; Calvert 2001; Noesselt, et al. 2007; Raij, et al. 2000; van Atteveldt, et al. 2004). Consistent with these results, we observed a larger response for multisensory auditory—tactile stimuli than unisensory auditory or tactile stimulation. The degree of

enhancement for auditory—tactile multisensory stimulation compared to the maximum unisensory response in the present study was 23%, similar to the 17% enhancement for auditory—visual multisensory stimuli in STSms observed in a previous study (Beauchamp, et al. 2004b). These results add to a body of evidence showing multisensory interactions between touch and sound in auditory cortex, sometimes extending into the STS (Foxe, et al. 2002; Kayser, et al. 2005; Murray, et al. 2005; Schroeder, et al. 2001).

In the present study, "super-additive" multisensory responses were not observed. That is, the response to auditory-tactile stimuli was greater than the response to auditory or tactile stimuli in isolation, but was not greater than the summed response to auditory and tactile unisensory stimuli (Stein and Meredith 1993). Previous fMRI studies of auditory-visual integration in STS (Beauchamp, et al. 2004a; Beauchamp, et al. 2004b; Hein, et al. 2007; van Atteveldt, et al. 2004; van Atteveldt, et al. 2007) and auditory—tactile integration in auditory cortex (Kayser, et al. 2005) have also not observed super-additive changes in the BOLD signal, perhaps because only a few single neurons show superadditivity (Laurienti, et al. 2005; Perrault, et al. 2005). Supporting this idea, in single-unit recording studies, only a small fraction of STP neurons respond to both auditory and tactile stimulation (Bruce, et al. 1981; Hikosaka, et al. 1988); the same is true in multisensory regions of cat cortex (Clemo, et al. 2007). Conversely, many single neurons may show no response to a sensory stimulus in isolation, but the same stimulus may modulate responses when presented with other sensory modalities (Allman and Meredith 2007). In macaque auditory cortex, auditory tactile integration increases as the auditory stimulus decreases in intensity (Lakatos, et

al. 2007) consistent with the so-called law of inverse effectiveness (Stein and Meredith 1993). In the present experiment, differences in auditory–tactile integration were not observed for weak and strong tactile stimuli, possibly because all of the auditory stimuli were well above threshold.

Double label studies show that projections into STP from parietal and temporal lobe (carrying visual and auditory information, respectively) project to non-overlapping, but often adjacent, patches of cortex (Hackett, et al. 2007; Seltzer, et al. 1996; Smiley, et al. 2007). Functional responses in macaque STP are also unevenly distributed (Dahl, et al. 2007). Consistent with these findings, in a high resolution fMRI study, human STSms was observed to contain a patchy distribution of auditory, visual and multisensory auditory—visual responses (Beauchamp, et al. 2004a). It is not clear whether macaque STP or human STSms contains an additional, dedicated set of patches that respond preferentially to somatosensory stimulation, or whether somatosensory stimuli arrive in STSms within the previously described auditory, visual and multisensory patches.

Homology between macague STP and the human STS multisensory area

We hypothesized that if human STSms is the homolog of macaque STP, it should share the same anatomical relationship with nearby identified areas, especially the adjacent area MST. Detailed functional mapping showed that human STSms was located just anterior to areas MST and MT, the same anatomical relationship that exists between MT, MST and STP in macaque cortex (Fig. 5D) (Lewis and Van Essen 2000a).

If STSms is homologous to macaque STP, it should also have similar functional properties, above and beyond simply responding to the same three sensory modalities. We used previous electrophysiological and fMRI studies of macaque STP as a gauge to compare the functional properties of macaque STP with the functional activation of the human STS as measured in this study; simultaneous electrophysiological and fMRI studies have shown good correlation between multiunit activity, local field potentials and the BOLD response (Logothetis, et al. 2001). Retinotopy in macaque STP, as measured with fMRI, is relatively crude (Nelissen, et al. 2006). Receptive fields of single units in STP are large; most are limited to the contralateral visual field but about a third also respond to the ipsilateral visual field (Hikosaka, et al. 1988). This would predict a significant ensemble BOLD fMRI response for ipsilateral stimulation, and a larger response for contralateral stimulation. This is exactly the BOLD signal we recorded from STSms: ipsilateral responses were significantly greater than zero, but significantly weaker than the response to contralateral visual stimulation. Macaque STP shows a significant fMRI response to moving compared with static stimuli (Nelissen, et al. 2006) and visually-responsive macaque STP neurons are best activated by moving stimuli (Bruce, et al. 1981; Hikosaka, et al. 1988). Consistent with this finding, we observed significantly greater responses to moving compared with stationary stimuli in STSms, with only a weak response to static images. Macaque STP shows only a weak BOLD preference for shapes compared with scrambled shapes (Nelissen, et al. 2006) and single STP neurons show little or no selectivity for shape (Bruce, et al. 1981; Hikosaka, et al. 1988). This matches our finding of no significant difference between real and

scrambled static images in STSms. However, some neurons in TPO are face-selective (Baylis, et al. 1987; Bruce, et al. 1981) and human fMRI studies have described face selectivity in the posterior STS (Kanwisher, et al. 1997).

In addition to similar visual processing profiles, the response selectivity of STSms to auditory and tactile stimuli was similar to that of macaque STP. Auditory-responsive STP neurons show broad-spectrum responses, with similar activity to very different sounds, such as pure tones, voices, white noise, and hand clapping (Bruce, et al. 1981; Hikosaka, et al. 1988). Consistent with this result, we saw robust activity in STSms to our auditory stimuli, which were pure tones in Experiment 1 and a variety of animal, human and mechanical sounds in Experiment 2. In tactile STP neurons, strong responses are evoked by cutaneous stimuli (Bruce, et al. 1981; Hikosaka, et al. 1988). The spatial preference of these neurons varies widely, from neurons that represent the entire body surface, to neurons that represent the contralateral body surface, to neurons that represent only the contralateral hand and arm. Estimating the ensemble response of these neurons, we would predict the largest responses to contralateral hand stimulation (which would activate all neurons) with the smallest responses to ipsilateral stimulation (which would activate only whole-body neurons). Consistent with this analysis, we observed the greatest BOLD activation in STSms for contralateral hand stimulation, and significantly weaker BOLD activation for ipsilateral hand and contralateral foot stimulation.

The role of multisensory responses in STSms

Visual biological motion is an especially potent activator of posterior STS (Beauchamp, et al. 2002; Grossman and Blake 2002). The STS is also important for processing speech, one of the main auditory cues used by humans to communicate (Price 2000), with a special role for the integration of auditory and visual language cues (Callan, et al. 2004; Calvert, et al. 2000; Macaluso, et al. 2004; Miller and D'Esposito 2005; Saito, et al. 2005; Schroeder, et al. 2008; Sekiyama, et al. 2003; van Atteveldt, et al. 2007). STSms prefers real auditory stimuli to scrambled auditory stimuli (Beauchamp, et al. 2004b) consistent with its role in the representation of sensory stimuli with meaning for the individual.

Some of the most important and meaningful types of sensory stimuli are social cues. The STS is thought to be an important node in the brain network for social cognition (Adolphs 2003; Allison, et al. 2000). Both human and non-human primates use visual, auditory and somatosensory cues to convey social information (Hauser and Konishi 1999). Therefore, we speculate that multisensory integration of tactile responses in STSms might exist in the service of understanding the actions and intents of others. A firm pat on the back might be interpreted differently in the context of either a friendly greeting or a sharp reprimand. Integrating across modalities would allow the STSms to aid the individual in interpreting the ambiguous cues that abound in social interactions.

Chapter 4: Distributed Representation of Single Touches in Somatosensory and Visual Cortex

Based on manuscript:

Beauchamp, M.S., LaConte, S., Yasar, N.E. (2009) Distributed representation of single touches in somatosensory and visual cortex. Human Brain Mapping *In Press*

Introduction

Traditional neuroimaging analyses use information about the sensory stimulus or behavioral state of the subject to calculate a measure of activation in a single brain voxel at a time. Recently, techniques have been developed to measure distributed patterns of activity across the brain, referred to as multi-voxel pattern analysis (MVPA) (Norman, et al. 2006). With MVPA, the traditional analysis is reversed and measurements of brain activity are used to decode the sensory stimulus presented to the subject or the mental or behavioral state of the subject (Cox and Savoy 2003; Haynes and Rees 2006; Kamitani and Tong 2005; Kriegeskorte, et al. 2006; LaConte, et al. 2005).

Most distributed pattern analysis studies have focused on decoding visually presented stimuli. Visual cortex is anatomically the largest of the early sensory cortices, and even simple visual stimuli evoke activity in many visual areas (Grill-Spector and Malach 2004). This distributed representation makes visual cortex an ideal laboratory for MVPA, because it provides many active voxels across which to pool information. However, it raises the question of whether other sensory modalities whose cortical representations are smaller or less distributed than visual cortex are amenable to MVPA. We performed two experiments to investigate whether MVPA could be used to decode individual stimuli presented in a different sensory modality, namely the somatosensory system.

In both experiments, a simple vibrotactile somatosensory stimulus (touch) was delivered to different locations on the body surface. In the first experiment, widely

separated touches were delivered to the left or right hand or foot of the subject. In the second experiment, closely spaced touches were delivered to three fingers on the right hand and to the right foot. Our analyses focused on three regions of the somatosensory network: primary somatosensory cortex (S1), secondary somatosensory cortex (S2), and a region of lateral occipital-temporal cortex, MST/STP, that has traditionally been labeled as visual association cortex but also responds to touch (Beauchamp, et al. 2008; Beauchamp, et al. 2007; Blake, et al. 2004; Hagen, et al. 2002; Ricciardi, et al. 2007).

Most MVPA studies have used blocked designs, in which stimuli from the same category are grouped. Block designs are problematic in the somatosensory system, where adaptation is pronounced both peripherally and centrally (Leung, et al. 2005; Tommerdahl, et al. 2005). Rapid event-related designs are an efficient way to present many different stimuli while minimizing adaptation. We developed a simple technique to analyze single trials of somatosensory stimulation presented in a rapid event-related design using support vector machines (SVMs), a supervised learning method that performs efficiently at high-dimensional classification tasks like those found in fMRI (Cox and Savoy 2003; LaConte, et al. 2005).

Methods

Subjects were recruited and informed consent was obtained in accordance with the University of Texas Committee for the Protection of Human Subjects. Subjects were scanned using a 3 tesla whole-body MR scanner (Phillips Medical Systems, Bothell, WA). Seven subjects participated in experiment 1, and eight subjects participated in experiment 2. In both experiment, vibrotactile somatosensory stimuli were delivered by five piezoelectric benders. In experiment 1, the five benders were attached to the left palm, the right palm, the sole of the left foot, the sole of the right foot, and the right hip (Fig. 1A). In experiment 2, the benders were attached to the thumb (D1), the third (middle) finger (D3), and the fifth (pinky) finger (D5) of the right hand (adjacent fingers were not stimulated because of mechanical constraints introduced by the benders); the right foot; and the right hip (Fig. 1B). A similar rapid event-related design was used for both experiments (Fig. 1C). Each 5-minute scan series contained 150 two-second trials (corresponding to the MRI repetition time, TR, of 2 sec) with 10 hip target trials, 40 fixation baseline trials with no somatosensory stimulus, and 25 of each of the other four benders. Trial ordering was counter-balanced so that each trial type was equally likely to be preceded by any other trial type, and experimental power was maximized by jittering (randomizing) the interval between two trials of the same type (Dale 1999). Six scan series were collected from each subject. There was no task during hand or foot stimulation, other than to maintain visual fixation on central crosshairs. During hip stimulation trials, subjects were required to make an eye movement to a visually presented target. This ensured that subjects remained alert and attentive throughout the experiment. Because hip trials were analyzed separately (and not used for the classification analysis) any brain activity related to the eye movement responses could not contribute to classification performance.

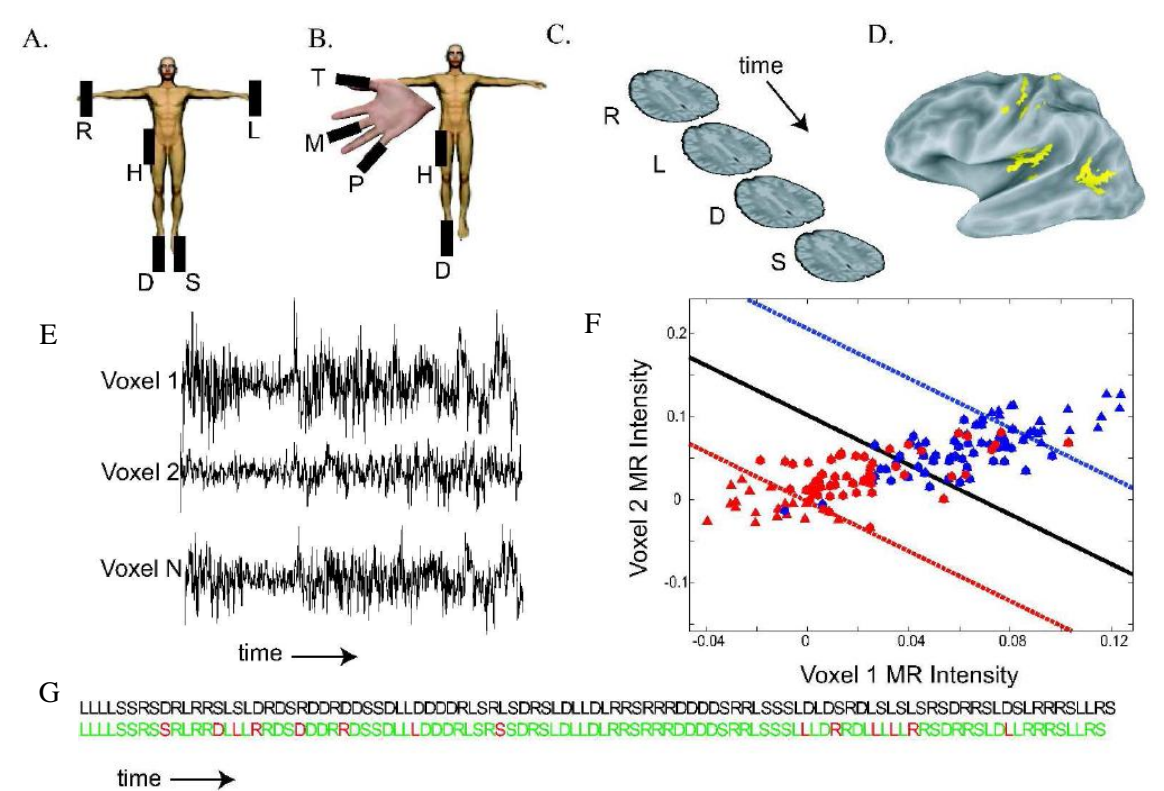


Figure 1. Methods used for somatosensory multivoxel pattern analysis.

- **A.** Somatosensory stimuli were delivered by five piezoelectric benders. In experiment 1, the benders were located on the palm of the right hand (R), the palm of the left hand (L), the sole of the right foot (D), the sole of the left foot (S), and the right hip (H).
- **B.** In experiment 2, the benders were located on the right thumb (T), the right middle finger (M), the right fifth pinky finger (P), the right hip (H) and the right foot (D).
- **C.** During the course of an MRI scan series, brain volumes were acquired (shown schematically by single brain slices) every 2 sec. Each acquisition corresponded to a single stimulation trial in which a single body site was stimulated, shown by a letter corresponding to the body plan shown in (A). Some trials (not shown) contained target bender stimulation or fixation baseline with no somatosensory stimulation.
- **D.** Using the MR data, an activation map was constructed of voxels responding significantly more (p < 10-6) to somatosensory stimulation than to fixation baseline. A lateral view of a partially inflated left hemisphere is shown, yellow color shows active areas (Argall, et al. 2006).
- **E.** Over the course of a scan series, 150 brain volumes were acquired. The three black traces show the image intensity over the course of a scan series in three active voxels selected from the yellow voxels in (C).
- **F.** The time series from all active voxels (E) and the stimulus ordering (C) were used to train an N-dimensional support vector machine. For illustration, a simplified training dataset is shown, with only two voxels and two stimulus categories (right hand and left hand). Each symbol shows the normalized MR image intensity during a single trial. The red triangles show the MR image intensity in all right hand stimulation trials and the blue triangles show the intensity in all left hand stimulation trials. The solid line shows the separating hyperplane $\mathbf{W}^T \mathbf{X}_i + \mathbf{w}_0 = 0$ calculated by the classifier. The dashed lines show the canonical hyperplanes $\mathbf{W}^T \mathbf{X}_i + \mathbf{w}_0$ \mathbf{E} ±1 Trials falling between the separating and canonical hyperplanes were used as support vectors (indicated by circles). An unknown test trial is classified as "right hand" if it falls below the solid line and "left hand" if it lies above the solid line.
- **G.** Result of the experiment 1 classifier when tested on a different scan series not used for training. The actual stimulus ordering presented to the subject is shown in the top row in all black, body part abbreviations as in (A). The classifier prediction of the stimulus ordering is shown in the bottom row: green for correct classification, red for incorrect classification. Performance of the classifier in this scan series was 86% correct (p < 10-38).

A finite impulse response model was used to fit the MR time series in the context of the general linear model using the AFNI program 3dDeconvolve (Cox 1996). The average response to each trial type in each voxel was determined with nine individual tent functions that modeled the entire BOLD response from 0 seconds to 16 seconds post stimulus, accounting for overlapping responses from consecutive trials without any assumptions about the shape of the hemodynamic response (Glover 1999). An F-test was used to find active voxels, defined as those in which the tent functions for the hand and foot stimulation trials accounted for a significant fraction ($p < 10^{-6}$) of the variance.

Classifier Training and Testing

Separate classifiers, as implemented in SVMlight (Joachims 1999) were constructed for each subject. Complementary analyses with a different package, LibSVM (Chang and Lin 2001), gave very similar results. Within each subject, the SVM was trained using one set of data from the subject. Then, the SVM was tested on additional data not used for training.

The input to the SVM consisted of a matrix of pattern vectors, **X***y,i* . **X** had *N* rows corresponding to the number of active voxels, with *y* corresponding to the trial type and *i* corresponding to the trial index of that trial type. Since the feature dimension *N* was high, a linear kernel was used to lower the computation time (LaConte, et al. 2005; LaConte, et al. 2007). Separate classifiers were constructed for each pair of stimuli and combined using a decision directed acyclic graph (Platt, et al. 2000).

In each subject, six scan series were collected, each containing a random sequence of somatosensory stimuli. This allowed the use of leave-one-out cross-validation to assess classification performance. Within each subject, six different SVMs were constructed, each trained on a different set of five scan series collected from the subject. Then, each SVM was tested on the single left-out scan series not used for training. Arranging the samples in this way avoids splitting samples from one run into both training and test sets which may be problematic due to dependency among successive samples within each run (Haxby, et al. 2001).

Because the BOLD response to brief somatosensory stimulation was relatively punctate (Fig. 6A), in order to estimate the response to individual trials we made the simplifying assumption that the image intensity in a voxel at a given time reflected only the somatosensory stimulus delivered two TRs (4 seconds) previously; this meant that the estimated response to a single trial contained small contributions from previous trials. This did not introduce bias into the classifier for two reasons. Most importantly, all training trials were from different five-minute scan series (separated by 30 seconds – 30 minutes) from the trial being classified, preventing BOLD spillover between testing and training trials. Any BOLD response spillover could only hurt classification performance (by providing a less accurate estimate of the true response), and not help classification performance (by introducing a classification signal into neighboring trials, as would occur if training and testing was performed within a single scan series).

Second, first order counterbalancing was used when designing the stimulus sequence, and the stimulus sequence for each scan series was randomized independently,

ensuring that there were no systematic order effects that could help classification performance.

The image intensity used for classification was obtained from the adjusted MR time series, which had regressors of no interest removed in order to reduce temporal variation. The regressors of no interest included a mean and linear trend for each scan series (accounting for slow drifts in the MR time series); head motion estimates from the image registration algorithm; and the estimated hip trial responses. For two-way classification, estimates of the response to the unclassified trial types were also considered to be regressors of no interest. To the extent that noise from the regressors of no interest remained in the MR time series, classification performance will be impaired, resulting in an underestimate of classifier performance.

Additional Analyses

To identify voxels for classification, a leave-one-out procedure was used to identify voxels that responded to somatosensory stimulation ($p < 10^{-6}$) in the five scan series used for training each classifier. Data in the left-out scan series was not used to construct the activation map for the corresponding classifier to avoid introducing bias. For further analysis, the active voxels were grouped into different regions of interest (ROIs) based on anatomical and functional criteria using the same leave-one-out procedure (Fig. 2). The primary somatosensory cortex (S1) ROI was created from all active voxels in and near the central sulcus, postcentral gyrus and postcentral sulcus. The secondary somatosensory cortex (S2) ROI was created from all active voxels in and near the parietal operculum. A visual association ROI was created from all active voxels

in and near posterior superior temporal sulcus, middle temporal gyrus, and inferior temporal sulcus. Because this brain region contains the medial superior temporal area (MST) and the superior temporal polysensory (STP) areas, we labeled it the MST/STP ROI. Two additional ROIs were created from subsets of voxels in S1. The S1foot ROI was created from all contiguous voxels on the vertex and medial face of the hemisphere that showed a significantly greater response to foot than to hand stimulation (p < 0.05). The S1hand ROI was created from all contiguous voxels near the so-called hand knob (Yousry, et al. 1997) that showed a significantly greater response to hand than to foot stimulation (p < 0.05). In order to study the effect of ROI size on classification performance, permutation testing was used (Haynes and Rees 2005b). For a given ROI size s, s voxels were randomly selected from the ROI and used to train and test a classifier. This process was repeated 100 times (with different pools of s randomly selected voxels) to give the average performance of the ROI at size s. Across subjects, the performance was averaged at size s and the between-subjects variance was used to calculate the SD. This process was then repeated across values of s.

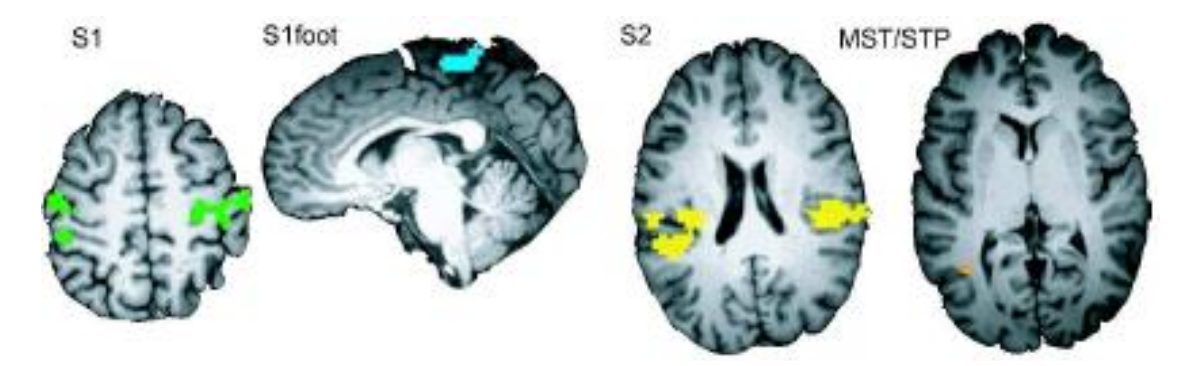


Figure 2. Regions of interest (ROIs). Regions of interest were defined individually in each subject. Colored voxels responded significantly more to somatosensory stimulation on the hands and feet than to fixation baseline ($p < 10^{-6}$). Different colors indicate different ROIs. S1 (green), primary somatosensory cortex; S1foot (blue), foot sub-region of S1; S2 (yellow), secondary somatosensory cortex and associated areas; MST/STP (orange), areas MST and STP.

Results

In each subject, somatosensory stimulation activated somatosensory cortex in the postcentral gyrus and parietal operculum and regions of visual association cortex in lateral occipitotemporal lobe (Fig. 1D). The response in these areas was used to train a classifier, which in turn was used to decode the body site of somatosensory stimulation for individual trials not used for training. The classifier prediction across all trials in a single scan series is shown in Fig. 1F. The classifier successfully predicted the correct body site for stimulation for 85% of the trials (shown in green) and incorrectly classified 15% of the trials (shown in red). Because classification was performed on each trial separately, this level of prediction accuracy was highly unlikely to be due to chance. For 100 hand and foot trials in the example scan series, the chance likelihood under the binomial distribution of at least 85 correct trials was p < 10⁻³⁸ (success probability per

trial of 25%). For the same subject, five additional classifiers were trained and tested, producing a total classification across six scan series of 462 correct and 138 incorrect (77%); the chance likelihood of this performance was vanishingly small (p < 10^{-99}). In every one of 7 subjects, decoding performance was much greater than chance, with a mean of 68% \pm 3% SEM across subjects. Changing the ratio of training to testing data (from five scan series for training and one scan series for testing to three scan series for training and three scan series for testing) did not change classification accuracy. We also examined the ability of separate sets of classifiers to perform two-way discriminations between the left and right hand of stimulation, and the left and right foot of stimulation. Across subjects, the mean classification performance was 91% \pm 2% SEM for two-way hand decoding and 85% \pm 1% for two-way foot decoding (both p < 10^{-99} under the binomial distribution with success probability per trial of 50%).

Having shown that MVPA across all active areas could successfully decode the body site of stimulation, we wished to determine if different brain areas differed in their decoding ability. Classifiers were separately trained and tested using only the voxels in each of three ROIs: S1, S2 and MST/STP. The four-way decoding performance across subjects was $60\% \pm 1\%$ for the S1 ROI; $60\% \pm 1\%$ for the S2 ROI and $30 \pm 0.4\%$ for the MST/STP ROI (Fig. 3A). The scores of the S1, S2 and MST/STP ROIs were entered into a one-factor ANOVA, which revealed a significant effect of area (F(2,18)=51, p<10⁻⁷).

To study distributed representations in somatosensory cortex, we created two additional ROIs consisting of voxels in the foot region of S1 (S1foot) and voxels in the hand region of S1 (S1hand), as determined by their anatomical location and preference

for foot vs. hand stimulation. The ability of both ROIs to perform two-way classification (left vs. right) was tested (Fig. 3B,C). S1hand was better at predicting side of hand stimulation than side of foot stimulation (75% vs. 54%, p < 0.001). S1foot was significantly better at predicting side of foot stimulation than side of hand stimulation (73% vs. 60%, p < 10^{-4}).

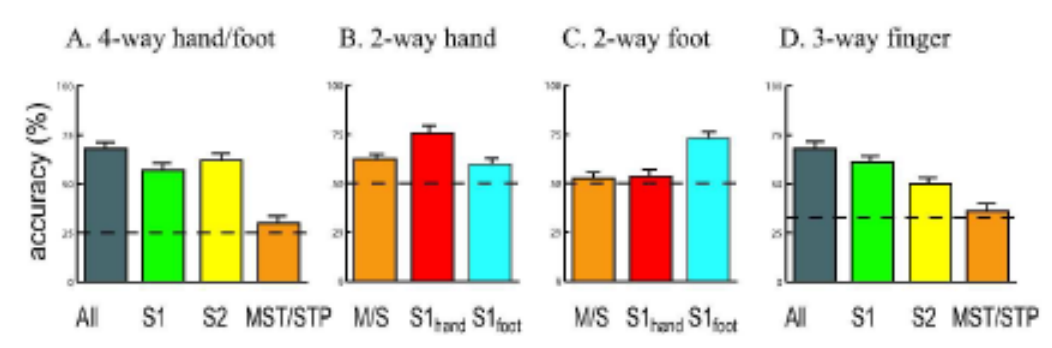


Figure 3. Classification performance.

A. Performance for four-way classification (right hand, left hand, right foot, left foot). The mean performance of the classifier when classifying single trials in a scan series not used for training, averaged across 8 subjects (error bars shows the SEM). The gray bar shows the performance when the classifier was trained and tested on voxels in all ROIs; colored bars show performance when classifier was trained and tested only on voxels in a single ROI (S1, S2, MST/STP). Chance performance was 25% (dashed line).

- **B.** Accuracy of two-way classification (left hand vs. right) in three ROIs.
- **C.** Accuracy of two-way classification (left foot vs. right foot) in three ROIs.
- D. Accuracy of three-way classification in experiment 2 (thumb vs. middle finger vs. pinky finger).

In a previous study, MST significantly preferred hand stimulation to foot stimulation, perhaps because of a role in eye-hand coordination (Beauchamp, et al. 2007). We hypothesized that the relatively poor MST/STP performance in 4-way classification might reflect differential performance on hand and foot classification. Therefore, the ability of MST/STP to classify hand stimuli (left vs. right) and foot stimuli (left vs. right) was also separately tested. MST/STP classification performance was

significantly greater for hand classification than for foot classification (62% vs. 53%, p < 0.001).

To avoid assumptions introduced by predefining regions of interest, we trained additional classifiers with whole brain data. Because a linear SVM was used, the decision boundary can be mapped directly to image space (LaConte, et al. 2007). This provides an assumptions-free map (without predefined ROIs) of voxels that contain significant information about the body site of stimulation. As shown in Fig. 4, voxels with high feature space weights were found in S1, S1foot, and S2, similar to the functional activation maps obtained from the traditional univariate methods.



Figure 4. Support vector weight maps. Map of the support vector weights (|weights|>10 colored yellow) assigned to each voxel in an ROI-free analysis, for the same subject as shown in Figure 2. Note the high weights for voxels in S1 (left), S1foot (middle) and S2 (right).

To study how classification performance changed with ROI size across all subjects, classifiers were trained and tested with sub-ROIs consisting of from 1 to 70 voxels randomly selected from S1, S2 and MST/STP (Figs. 5A, B, and C, respectively). The accuracy with one voxel was low but performance increased as more voxels were added to the ROI. The increase had a rapid initial phase followed by a slow, nearly linear

component, which was fit with a sum of two exponential functions $y = ae^{bx} + ce^{dx}$. The function produced a good fit (mean $r^2 = 0.996$), with the slow linear component fit by the first exponential and the rapid initial phase fit by the second exponential. The number of voxels required to reach 75% of the rapid initial maximum was calculated as $N_{\%} = -\frac{2\ln 2}{d}$. Averaged across subjects, 8.3 voxels was required to reach 75% of the initial maximum, with no significant difference between areas according to an ANOVA (F(2,21)=0.9, p=0.4).

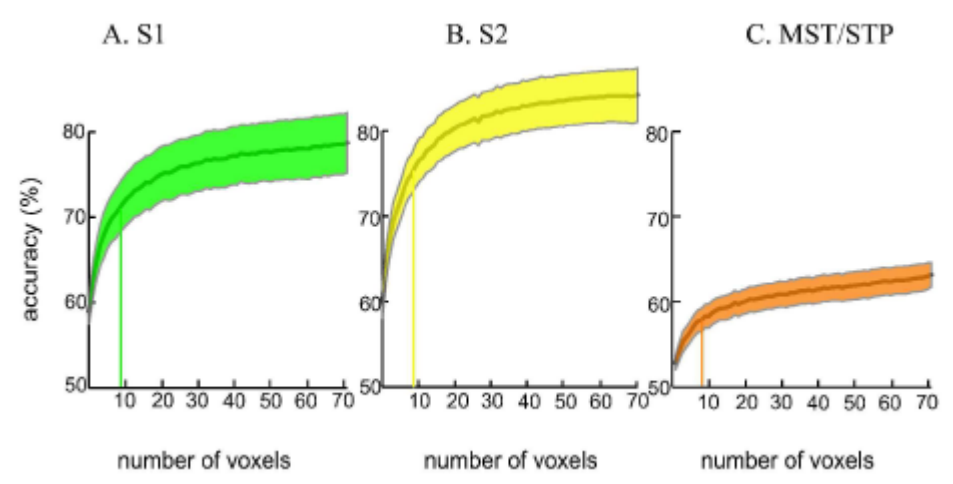


Figure 5. Relationship between region of interest size and classification performance. **A.** Classification accuracy for subsets of voxels from S1. Two-way classification (left hand vs. right hand) was performed using randomly selected subsets of voxels. The y-axis shows the classification accuracy for an ROI containing the number of voxels shown on the x-axis. The center gray line shows the mean performance across subjects, the shaded area shows ±1 SEM across subjects (the color of the shaded area corresponds to the color used to illustrate the corresponding ROI in Figure 2). The initial rise in the accuracy curve was fit with an exponential function. The vertical bar in each curve shows the number of voxels required to reach 75% of the peak of the exponential function.

- **B.** Classification accuracy for subsets of voxels from S2.
- C. Classification accuracy for subsets of voxels from MST/STP

The results of experiment 1 demonstrated that MVPA could be used to decode somatosensory stimuli widely separated on the body surface (left and right hand and

foot). In order to determine whether MVPA could also be successful in a more difficult somatosensory classification task, in experiment 2 touches were delivered to closely spaced locations on the body surface (different digits on the same hand and the foot).

In every one of 8 subjects, decoding performance was much greater than chance, with a mean of $56\% \pm 4\%$ SEM across subjects (chance performance of 25% for 4-way decoding). As a more rigorous test, we measured decoding performance for 3-way decoding of different fingers on the same hand. Performance was good for finger decoding, with a mean of $68\% \pm 3\%$ SEM across subjects (chance performance of 33%). Subdividing the active voxels revealed significant differences in decoding performance between ROIs (Fig. 3D; F(4,39)=7.3, p = 0.0002). The best performance was found in S1 (61% \pm 4% for the S1 ROI) and S2 (50% \pm 3%).

The MVPA analysis used multivariate information from many voxels to successfully classify *individual* stimulation trials. Traditional univariate methods examine the *average* BOLD response to different trial types averaged across voxels in an ROI. Could classification be performed with the BOLD response to individual trials in an ROI? First, we examined the easier classification task of experiment 1. Figure 6A shows the average response to left hand and right hand touches in left hemisphere S2 of a single subject. The response, averaged across all trials, was significantly greater for right hand than left hand touches. Next, we measured the response to each individual trial in left hemisphere S2 (Fig. 6B). While on average the BOLD signal change was greater in right hand than left hand trials, the distributions of the signal changes were largely overlapping. The optimal classification boundary was calculated as the average of the

contralateral and ipsilateral response means, weighted by their variance. Because of the large variance in the individual trial responses, many trials were wrongly classified by the boundary. The univariate classification performance was calculated by creating a boundary from training runs, and then measuring accuracy on testing runs, to ensure an unbiased comparison with the equivalent leave-one-out analysis used for MVPA. The univariate S2 classification performance was 66%, much less than the 95% accuracy achieved with multivariate analysis for left S2 in this subject. A similar analysis for left S1 showed univariate accuracy of 66%, less than the 92% accuracy for MVPA in the same ROI. Next, we examined the more difficult classification task of experiment 2. In left S2 of a single subject the average response to D1, D3 and D5 touches was similar in amplitude (Fig. 6C) and the distributions of the individual trial responses were almost completely overlapping (Fig. 6D); a similar pattern was seen in S1. Classification accuracy for the univariate analysis was 43% for left S2 in this subject and 47% for S1, much less than the MVPA accuracy of 55% for S2 and 69% for S1.

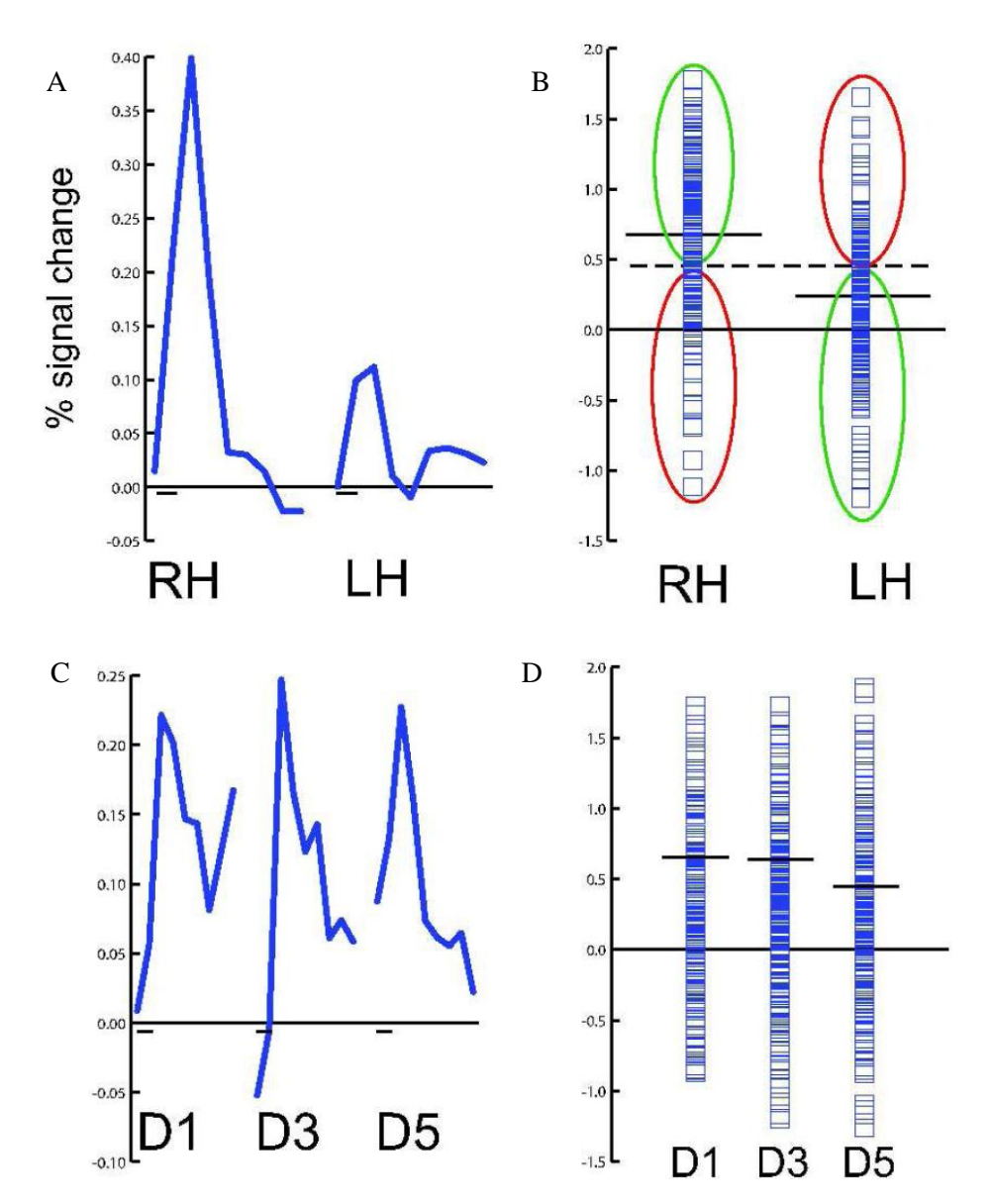


Figure 6. Classification performance with univariate analysis.

A. The solid blue line shows the BOLD response averaged across all trials to right hand (RH) and left hand (LH) touch in the left hemisphere S2 of an individual subject in experiment 1. The duration of each response is 16 seconds; the small black bar on the x-axis shows the stimulus duration of 2 seconds.

B. Each blue symbol show the BOLD response in a single trial of right hand (RH) touch (left column of symbols) and left hand (LH) touch (right column) in left S2 (same subject as A). The solid black lines show the mean response to RH and LH touch. The optimal classification boundary is midway between the two means (dashed line). This boundary correctly classifies all RH trials above it and all LH trials below it (66%, green ellipses) and incorrectly classifies all RH trials below it and all LH trials above it (34%, red ellipses).

C. The BOLD response, averaged across all trials, to thumb (D1), middle finger (D3), and pinky finger (D5) touch in the left hemisphere S2 of an individual subject in experiment 2.

D. Individual trial responses (blue squares) and means (black lines) in S2 to single finger touch.

Discussion

For single, two-second trials of somatosensory stimulation, MVPA was able to decode the body site of somatosensory stimulation at levels far above chance performance. Two-way decoding performance of hand stimulation was particularly accurate, with a mean of 92% performance, similar to performance levels reported in two-way decoding tasks with visual stimulation (e.g. 80% accuracy for an orthogonal orientation decoding task in (Haynes and Rees 2005a)). As in visual studies, increasing the difficulty of the classification task decreased classifier performance (Kay, et al. 2008). However, even for closely spaced touches on the same hand, performance was still well above chance (68% compared with 33% chance performance). Also similar to MVPA studies of visual decoding, accuracy increased sharply as more voxels were included in the analysis, with the increase slowing as the number of voxels increased beyond ten to twenty (Haynes and Rees 2005a).

In a visual MVPA study, V1 and V2 were both able to accurately decode stimulus orientation (Kamitani and Tong 2005). In the present study, S1 and S2 were able to decode the body site of stimulation with high levels of accuracy. Receptive fields in S1 are small and highly somatotopic, while receptive fields in S2 are much larger and less well-organized (Nelson, et al. 1980). This may correspond to the dissociation in classification accuracy observed between the experiments. In experiment 1, in which the stimuli were widely separated on the body surface, S2 and S1 classified the stimuli with similar accuracy (both 60%). In contrast, in the 3-way finger decoding task of experiment 2, the stimuli were closely spaced on the body surface and S1 was more

accurate than S2 (61% vs. 50%, p = 0.01). S1 and S2 both contain multiple subdivisions (Eickhoff, et al. 2006a; Kaas, et al. 1979) and in future experiments at higher resolution it will be important to study the ability of these subdivisions to discriminate somatosensory stimuli.

Previous studies have reported responses to somatosensory stimuli in "visual" cortex (Amedi, et al. 2001; Sathian, et al. 1997). In particular, tactile responses have been reported in a region of lateral occipital-temporal cortex that contains area MST and the possible human homolog of area STP (Beauchamp 2005a; Beauchamp, et al. 2008; Beauchamp, et al. 2007; Blake, et al. 2004; Hagen, et al. 2002; Ricciardi, et al. 2007). Previous MVPA studies have shown that MST and nearby areas can decode the direction of motion, but not the orientation, of visual stimuli (Kamitani and Tong 2005; Kamitani and Tong 2006). Here, we extend these findings by showing that fMRI activation patterns in MST/STP are able to decode information about the hand of somatosensory stimulation. Inactivation of monkey MST interferes with visually-guided hand movements (Ilg and Schumann 2007) and transcranial magnetic stimulation of human MT/MST reduces reaching accuracy (Whitney, et al. 2007). While visual signals provide an accurate initial targeting signal during reaching movements, determining whether a target has actually been touched is most easily accomplished by the somatosensory system. Consistent with this idea, MVPA of area MST/STP was able to determine the location of hand stimulation (left vs. right) with performance far above chance. However, MST/STP was not able to decode the finger of touch for fingers on the same hand, suggesting that tactile inputs into MST/STP are not highly specific, perhaps

signaling only that a touch has occurred. Decoding performance in MST/STP was also poor for foot touches, consistent with a role in eye-hand coordination. While eye-foot coordination is important in some tasks, such as directing a ball with the foot, these tasks may be subserved by other brain areas.

Building on the previous literature (Haynes and Rees 2006; Kamitani and Tong 2005; Kriegeskorte, et al. 2006; LaConte, et al. 2005; Norman, et al. 2006), we performed MVPA on individual trials presented in a rapid event-related somatosensory stimulation design. The ability to classify single trials has several important advantages. First, it results in a large testing and training set, important for good classification performance (Mitchel, et al. 2004). Second, it allows for real-time designs that provide feedback to the subject or make adjustments in the task difficulty (LaConte, et al. 2007). Third, it is a necessity for correlating behavior and information content on a trial-by-trial basis (Wagner, et al. 1998). In the somatosensory modality, event-related designs are particularly critical because there is a great amount of adaptation both peripherally and centrally (Deuchert, et al. 2002). Taken together, these studies illustrate how MVPA allows a closer investigation of the function of different cortical areas by examining their information content, above and beyond simple fMRI activation maps of single voxels responding to a sensory stimulus (Kriegeskorte and Bandettini 2007).

Chapter 5: Sound Enhances Touch Perception

Based on manuscript:

Ro, T., Hsu, J., Yasar, N.E., Elmore, L.C., Beauchamp, M.S. Sound Enhances Touch Perception. Experimental Brain Research *In Press*

Introduction

Our perceptual systems are frequently confronted with simultaneous information from multiple sensory modalities. For example, while hearing the buzzing sound of a mosquito, we may also feel the mosquito attempting to land on our neck. Although there have been numerous studies of auditory-visual (Bertelson 1999; Bertelson and Aschersleben 1998; Recanzone 1998; Vroomen and Gelder 2000) and visual-tactile interactions (Ernst, et al. 2000; Kennett, et al. 2001; Pavani, et al. 2000; Ro, et al. 2004; Rock, et al. 1965; Rock and Victor 1964; Tipper, et al. 1998; Tipper, et al. 2001), little is known about the psychological rules governing the interactions between sound and touch.

This is not because the two modalities are unrelated. Indeed, some studies have shown that certain types of sounds can affect some aspects of touch perception in systematic ways (Gescheider, et al. 1969; Guest, et al. 2002; Hotting and Roder 2004; Jousmaki and Hari 1998; Navarra, et al. 2007; Serino, et al. 2007; Sherrick 1976) and that touch can also affect sound perception (Gillmeister and Eimer 2007). In fact, under some conditions sound alone can invoke certain somatosensory percepts, such as the sound of fingernails scratching a chalkboard (Halpern, et al. 1986). We may also feel the vibrations from a loud car stereo, experience tingling sensations from a ringing phone, or feel sharpness from the sound of breaking glass. These strong associations between sound and touch may be a consequence of similar encoding mechanisms: both senses process information that produces mechanical displacements of tissue (i.e. the tympanic

membrane for auditory and the skin for somatosensory) and are processed in frequency-based codes in adjacent regions of the cerebral cortex.

In addition to cortical proximity, the somatosensory cortex projects to regions of auditory cortex (Schroeder, et al. 2001) and neuroimaging studies have demonstrated interactions between the somatosensory and auditory modalities in some regions of auditory cortex (Foxe, et al. 2002). Other studies have also shown direct anatomical connections between auditory and visual cortex at early stages of the cortical processing hierarchy (Bizley, et al. 2007; Clavagnier, et al. 2004; Falchier, et al. 2002; Rockland and Ojima 2003). These demonstrations of interconnectivity between the primary sensory cortices of different sensory modalities have led some to question whether any cortex is truly unisensory (Ghazanfar and Schroeder 2006; Macaluso and Driver 2005; Schroeder and Foxe 2005) and suggest that the perceptual processing of information in one sensory modality may have systematic effects on the processing of information in a different sensory modality.

To assess the perceptual interactions between sound and touch, we conducted three psychophysical experiments examining the effects of a task-irrelevant auditory stimulus on the perception of weak somatosensory events. Weak somatosensory stimuli were used because multisensory interactions are known to be most potent for near threshold stimuli (Stein and Meredith 1993). Experiment 1 examined whether a simultaneously presented tone affects somatosensory perception. Experiment 2 examined whether the spatial location of the sound affects somatosensory processing in a spatially specific manner. Experiment 3 examined whether the effects of sound on

vibrotactile perception are frequency specific. All three experiments found systematic enhancing effects of sound on somatosensory perception.

Experiment 1

Experiment 1 examined whether an auditory tone affects somatosensory perception. Thus, a centrally perceived behaviorally-irrelevant sound was simultaneously presented with a near threshold electrical cutaneous stimulus on the critical trials. In the baseline trials, the somatosensory stimulus was delivered without any sound. The detection rates for detecting the somatosensory stimulus with sounds was compared to the detection rates for detecting it alone.

Methods

After informed consent, twenty participants (10 males; 10 females; mean age = 19.05 years) completed this experiment in exchange for course credit. All subjects were neurologically normal and reported no hearing or somatosensory deficits.

The somatosensory stimulus, which was generated using an optically isolated Grass SD9 stimulator, was a 0.3 ms square-wave electrical current that was passed through a pair of ring electrodes that was attached to the middle finger of the left hand. The participants comfortably rested their left hand on the armrest of a chair below the left speaker. In each subject, the intensity of this electrical cutaneous stimulus, which felt like a faint tap or pulse in the finger, was adjusted to a near-threshold level of 50% detection by varying intensities across blocks of trials until between 4 and 6 stimuli out

of ten were detected. The auditory stimulus, which was a pure 500 Hz sine-wave tone, was delivered via two computer speakers that were approximately 30 cm to the left and right of a centrally located fixation light emitting diode (LED). The tone was 200 ms in duration, 59 dB in intensity, and produced the percept of a central sound.

Participants fixated the central LED, which signaled the start of each trial with a 200 ms flash. Three hundred ms after fixation offset, one of four conditions was delivered: auditory stimulus alone, somatosensory stimulus alone, auditory stimulus with somatosensory stimulus, or no stimuli. Participants performed a two-alternative force choice (2-AFC) task; they verbally reported on each trial whether or not they felt the somatosensory stimulus and were instructed to ignore the auditory stimulus. Once the verbal response of the participant was entered into the computer by the experimenter, the next trial commenced after 500 ms. A total of 160 trials (40 trials for each condition) was completed by each participant.

Results and Discussion

An ANOVA was conducted on the behavioral responses, with auditory stimulus (present vs. absent) and somatosensory stimulus (present vs. absent) as the two withinsubject factors and the proportion of trials that resulted in a somatosensory percept as the dependent variable. There was a highly significant main effect of the somatosensory stimulus on detection ($F_{1,19} = 96.32$, p < .001), demonstrating that the electrical current successfully produced a somatosensory percept. The main effect of the auditory stimulus was not significant ($F_{1,19} = 2.25$, p = .15), indicating that sound

alone could not reliably produce a somatosensory percept. However, there was a significant interaction between the auditory stimulus and somatosensory stimulus factors ($F_{1,19} = 6.69$, p = .02), showing that sound can modulate somatosensory perception. As shown in Figure 1 and Table 1, this interaction was due to a significant increase in the detection rate for somatosensory stimuli when they were accompanied by an auditory stimulus (61.6% vs. 57.4%; $t_{19} = 2.121$, p = .047). Importantly, although the sound increased the detection rate when a somatosensory stimulus was presented, the sound did not increase the false alarm rate for reporting a somatosensory stimulus when none was presented (3.4% for sound present vs. 3.4% for sound absent; F < 1). This shows that increase in the detection rate for somatosensory stimuli with sounds was not due to confounding factors, such as feeling mechanical vibrations or air pressure from the speakers.

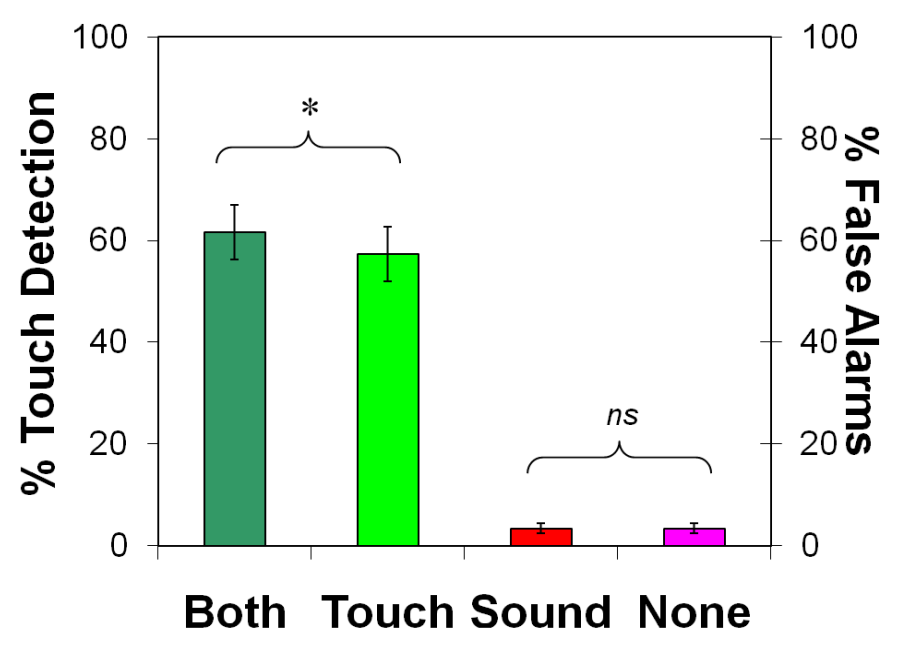


Figure 1. The data from Experiment 1 examining the effects of audition on touch perception. The left half of the figure shows the hit rates, whereas the right half of the figure illustrates the false alarm rates. Error bars reflect ±1 standard error of the mean.

Table 1. The mean hit and false alarm rates, along with the d' and c values, for Experiments 1 and 2. Only hit rates were measured in the two-alternative forced-choice task of Experiment 3. Standard deviations are in parentheses.

are in parentileses.			.,	
	<u>Hits</u>	False Alarms	<u>d'</u>	<u>C</u>
Experiment 1				
Sound Present	.62 (.24)	.03 (.09)	2.81 (1.13)	.99 (.56)
Sound Absent	.57 (.24)	.03 (.06)	2.40 (.90)	.97 (.53)
Experiment 2				
Touch Left-Sound Left	.51 (.21)	.02 (.04) ^a	2.38 (.95)	1.18 (.30)
Touch Left-Sound Right	.47 (.18)	.04 (.07) ^b	2.04 (.94)	1.11 (.40)
Touch Left-No Sound	.46 (.19)	.02 (.05) ^c	2.29 (.92)	1.26 (.32)
Touch Right-Sound Left	.38 (.18)	.03 (.06) ^a	1.93 (.78)	1.28 (.42)
Touch Right-Sound Right	.42 (.15)	.03 (.04) ^b	1.99 (.68)	1.20 (.34)
Touch Right-No Sound	.37 (.17)	.03 (.05) ^c	1.87 (.90)	1.33 (.35)
	(/	(100)		()
No Touch-Sound Left	-	.05 (.06) .04 (.05) ^d	-	-
No Touch-Sound Right	_	.03 (.03) .07 (.10) ^d	-	-
No Touch-No Sound	_	.03 (.04) .03 (.05) ^d	_	_
rto rodon rto bodina		103 (101) 103 (103)		
Experiment 3				
<u>Experiment 5</u>				
100 Hz Touch-100 Hz Sound	.78 (.21)	_	_	_
100 Hz Touch-200 Hz Sound	.49 (.30)	_	_	_
100 Hz Touch-No Sound	.57 (.31)	_	_	_
100 Hz Touch-No Sound	.57 (.51)	_	_	_
200 Hz Touch-100 Hz Sound	.37 (.17)	_	_	_
200 Hz Touch-200 Hz Sound		-	-	-
200 Hz Touch-No Sound	.71 (.19)	-	-	-
200 HZ 100CH-NO 300NO	.67 (.33)	<u>-</u>	-	

^a This false alarm rate reflects the mean proportion of trials that participants incorrectly reported feeling a sensation on the hand opposite the sound and touch

^b This false alarm rate reflects the mean proportion of trials that participants incorrectly reported feeling a sensation on the hand opposite the touch, but on the same side as the sound

^c This false alarm rate reflects the mean proportion of trials that participants incorrectly reported feeling a sensation on the hand opposite the touch

^d The left false alarm rate reflect the mean proportion of trials that participants incorrectly reported feeling a sensation on the left hand whereas the right false alarm rate reflects the mean proportion of trials that participants incorrectly reported feeling a sensation on the right hand

Signal detection analyses were also conducted to assess the changes in sensitivity independent of or at least with minimal influences from response biases. For this analysis, d' values for the two auditory stimulus conditions were calculated from the hit (detection report when a somatosensory stimulus present) and false alarm (detection report with no somatosensory stimulus) rates and subjected to a two-tailed paired t-test. There were significantly higher d' values for detecting the somatosensory stimulus with the sound present (d' = 2.81) as compared to the sound absent conditions (d' = 2.40; $t_{19} = 2.721$, p = .014). The c values to measure any potential response biases were also calculated for each auditory stimulus condition. There were no differences in response biases between the sound present (c = .99) vs. sound absent (c = .97) conditions ($t_{19} = 0.16$, p = .88), indicating that the effects of the sound were not a consequence of shifts in response criteria.

These results indicate that a task-irrelevant sound can enhance somatosensory perception. The sounds in this experiment were perceived to come from directly in front of the subject, while the somatosensory stimuli were delivered to only the left hand. This spatial separation might have limited the increase in somatosensory perception because previous studies in our laboratory have shown that the enhancing effects of vision on somatosensory perception are spatially specific (Johnson, et al. 2006). Therefore, Experiment 2 asked whether spatial congruence is important for the effects of audition on somatosensation.

Experiment 2

Experiment 2 examined whether the effects of sound on somatosensory perception are lateralized. Instead of a central sound and a left-hand somatosensory stimulus, as in Experiment 1, the auditory and somatosensory stimuli were delivered to either the left or right of the subject. Thus, the auditory and somatosensory stimuli could be on the same or opposite sides when the sound was presented. Furthermore, Experiment 2 used a set of sound-isolating headphones rather than speakers to lateralize the sounds and to eliminate any potential effects or interactions on somatosensory processing from air pressure. We hypothesized that, compared with the no auditory stimulus condition, a congruent auditory stimulus on the same side as the somatosensory stimulus would improve somatosensory discrimination while an incongruent sound on the opposite side would result in poorer discrimination.

Methods

After informed consent, twenty participants (8 males; 12 females; mean age = 19.15 years) who did not participate in Experiment 1 completed this experiment in exchange for course credit. All subjects were neurologically normal and reported no hearing or somatosensory deficits.

As in Experiment 1, the somatosensory stimuli were near-threshold electrical stimuli that were delivered through ring electrodes attached to the middle finger of the left and right hands. Each subject comfortably positioned their left and right hands on the arms of their chair. The somatosensory stimulation intensity was first adjusted

separately for each hand to a near-threshold level at which 4 to 6 stimuli out of ten were felt. The behaviorally-irrelevant auditory stimulus, which was a pure 500 Hz sinewave tone of 200 ms duration, was delivered to either the left or the right ear via Direct Sound EX-29 Extreme sound-isolating headphones. Because headphones were used, the intensity of the sound (80 dB) was louder than Experiment 1.

This experiment used a 3 auditory stimulus (none, left, right) x 3 somatosensory stimulus (none, left, right) factorial design for a total of 9 conditions. Participants fixated a centrally located light emitting diode (LED), which flashed for 200 ms to signal the start of each trial. Three hundred ms after fixation offset, one of the nine conditions was randomly presented with the constraint that no more than two trials in a row were identical. The participants performed a three-alternative force choice (3-AFC) task, reporting to the experimenter (who entered the response into the computer) whether a left somatosensory stimulus, a right somatosensory stimulus, or no somatosensory stimulus was felt by saying "left," "right," or "none". The next trial began 500 ms after response input.

A total of 360 trials were completed by each subject in this experiment.

Collapsed over left and right stimulation sides, this yielded 80 trials for each of the three conditions of main interest: somatosensory stimulus without auditory stimulus, somatosensory stimulus with auditory stimulus on the same side, and somatosensory stimulus with auditory stimulus on the opposite side of space. The remaining trial types (the 120 no somatosensory stimulus trials) were included for signal detection analyses.

Results and Discussion

Table 1 provides the data for each of the nine conditions in this experiment. An initial two-way ANOVA was conducted for all of the trials on which a somatosensory stimulus was delivered, with auditory stimulus (left, right, none) and side of somatosensory stimulus (left, right) as the two within subject factors. The main effects of auditory stimulus and side of somatosensory stimulus were not significant (both ps > 10). However, there was a significant interaction between these two factors ($F_{2,38} = 10$), which was mainly due to better somatosensory localization rates when the auditory stimulus was on the same side as the sound (i.e., left auditory stimulus with left somatosensory stimulus and right with right) than when they were on opposite sides (i.e., left with right and right with left).

To further assess the nature of this interaction, side of stimulation was collapsed in a subsequent one-way ANOVA, resulting in three levels of auditory stimulation with respect to somatosensory stimulation (same side as somatosensory stimulus, opposite side as somatosensory stimulus, none). This additional analysis further confirmed a significant main effect of auditory stimulation on somatosensory localization accuracy ($F_{2,38} = 3.90$, p = .029). As shown in Figure 2, when the sound was presented on the same side as the somatosensory stimulus, discrimination rates (46.5%) were significantly greater than when the sound was presented on the opposite side (42.6%; $t_{19} = 2.387$, p = .028) and greater than when no sound was delivered (41.6%; $t_{19} = 2.691$, p = .014). The difference in somatosensory discrimination rates between the no sound and the opposite sound conditions was not significant ($t_{19} = .495$, p = .626), indicating that there

was no cost associated with sounds delivered to the side opposite the cutaneous stimulus. These results indicate that when an auditory stimulus was delivered to the same side as the somatosensory stimulus, there was a significant enhancement for spatially discriminating the side of the somatosensory stimulus with this simultaneous irrelevant sound.

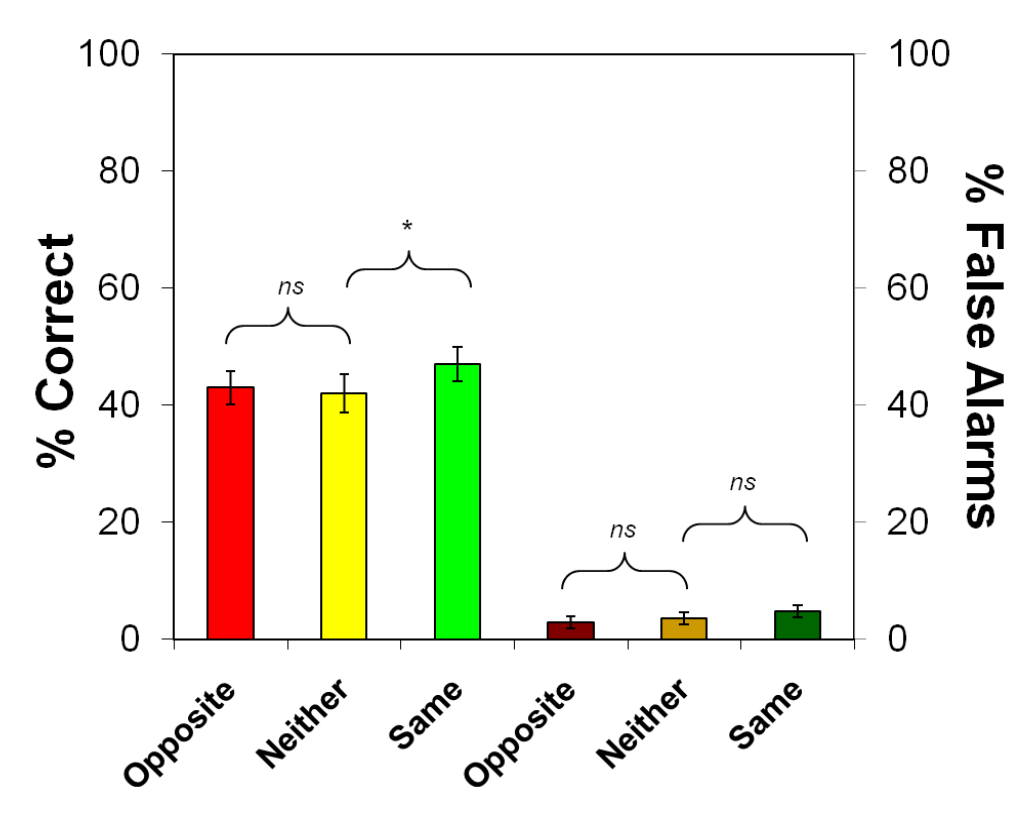


Figure 2. The data from Experiment 2 examining the spatial specificity of auditory influences on touch perception. The left half of the figure shows the hit rates, whereas the right half of the figure illustrates the false alarm rates. Error bars reflect ±1 standard error of the mean.

Since subjects reported on each trial whether they felt something on the left, right, or on neither side, false alarms occurred when participants reported feeling something that was not actually presented (i.e., erroneous reports of a somatosensory percept on one hand when no somatosensory stimulus was delivered or when it was

delivered to the opposite hand). The false alarm rates were low for all auditory stimulation conditions (see Table 1). An initial two-way ANOVA on the false alarm rates was conducted, with auditory stimulus (left, right, none) and side of false alarm (left, right) as the two within-subject factors. There was a significant main effect of auditory stimulus that was mainly due to higher false alarm rates for trials with a sound as compared to trials without any sound ($F_{2,38} = 5.45$, p = .009). The main effect of side of false alarm was not significant (p > .10). However, the interaction between auditory stimulus and side of false alarm was significant ($F_{2,38} = 5.63$, p = .007). This interaction was primarily due to subjects making more left-sided false alarms when the auditory stimulus was on the left side and more right-sided false alarms when the auditory stimulus was on the right side.

To further assess the nature of this interaction, we averaged the false alarm rates across left and right sides and classified the false alarms as being same-sided when a subject reported feeling something on the same side as the sound when no cutaneous stimulus was provided or reported feeling something on same side as the sound even though the cutaneous stimulus was delivered to the opposite hand. Similarly, opposite-sided false alarms were computed by averaging across trials on which participants reported feeling a somatosensory stimulus on a hand opposite a sound, regardless of whether a somatosensory stimulus was delivered to the other hand or not. For the no sound trials, the false alarm rates were averaged across the no somatosensory stimulus and the somatosensory stimulus on the opposite hand trials. When a false alarm was made on a trial in which a sound was delivered, participants were more likely to report

it on the same side as the sound as compared to the opposite side (4.8% vs. 2.8%; t_{19} = 2.447, p = .024), regardless of whether or not a somatosensory stimulus was delivered to the opposite hand. However, there was only a marginally significant difference between false reports of somatosensation on the same side as the sound and the no sound conditions (4.8% vs. 3.5%; t_{19} = 2.054, p = .054). The difference in false alarm rates between the no sound condition and the false reports of somatosensation on the opposite side of the sound also was not significant (3.5% vs. 2.8%; t_{19} = 1.209, p = .241).

Although the design of this experiment was not perfectly suited to conduct signal detection analyses, and not all response biases could be ruled out with this design, we nonetheless conducted signal detection analyses to obtain an estimate of bias free changes in sensitivity to somatosensory perception with sound. The d' values were calculated from the hit (correct localization of the somatosensory stimulus) and false alarm (see above and Table 1) rates for each subject and subjected to the same statistical analyses as the percent correct data. Consistent with the analyses on the discrimination and false alarm rates, an ANOVA revealed a significant difference in sensitivity between the three auditory stimulus conditions ($F_{1.19} = 7.05$, p = .002). There was significantly higher sensitivity for discriminating the side of the somatosensory stimulus when the sound was on the same side (d' = 2.00) as compared to the opposite side (d' = 1.30; $t_{19} = 3.689$, p = .002) and the no sound conditions (d' = 1.14; $t_{19} = 3.352$, p= .003). There was no decrease in sensitivity when the sound was delivered to the hand opposite the somatosensory stimulus as compared to the no sound conditions ($t_{19} =$.561, p = .581). These differences in d' values indicate that perceptual sensitivity,

independent of any response or decisional biases, was enhanced when the somatosensory stimulus was on the same side as the auditory one.

There was also a marginally significant difference in criterion between the three main conditions (F(1,19) = 2.99, p = .062). To assess the source of this marginal effect, we conducted further paired t-tests on the c values, which should be interpreted with caution since the main effect did not achieve significance. On the trials when no somatosensory stimulus was delivered, participants were more likely to report feeling an illusory somatosensory stimulus on the same side as the sound (c = 1.09) as compared to the opposite side (c = .84; $t_{19} = 2.509$, p = .021) and no sound conditions (c = .79; c = .79; c = .79; c = .79). There was no difference in response biases for the opposite side sound vs. the no sound conditions (c = .562, c = .581).

The analyses of d' values indicate that a sound on the same side as the somatosensory stimulus significantly enhances discrimination, regardless of any response or decisional biases that may or may not have been present. Unlike any contributions from response biases, which have been ruled out by our signal detection analyses, these results could have been affected by an enhanced alerting, temporal marking, or attentional orienting effect from the sound that increased touch perception (cf. Spence, et al. 1998). However, unlike the cross-modal attention studies by Spence, Driver, and colleagues (Driver and Spence 1998a; Driver and Spence 1998b), in which auditory stimuli preceded tactile ones, our stimuli were simultaneously presented, making an alerting, marking, or orienting account of our results less likely. We return to this issue in the General Discussion.

Sound on the opposite side from the cutaneous event did not produce a decrease or cost in its discrimination. Our previous work on vision and touch (Ingeholm, et al. 2006), using a similar design and paradigm, revealed a large decrement in performance when a somatosensory stimulus was delivered to the opposite side from vision. This difference may be explained by the poorer spatial localization capabilities of the auditory as compared to the visual system, or the fact that the sounds were not emitted from the precise location of the electrical cutaneous stimuli (i.e. the middle finger of the hands).

Since auditory coding is more dependent on frequency-based information rather than precise spatial localization, the enhancing effects on somatosensory processing from audition may be more readily measured in the frequency-domain. Experiment 3 examined the effects of different frequencies of auditory information on somatosensory processing.

Experiment 3

This experiment used different frequencies of auditory and somatosensory stimuli to assess whether the direct effects of sounds on touch perception are frequency-dependent. We hypothesized that the effects of sound on vibrotactile perception might be restricted to specific frequencies. Indeed, a recent study suggested that delayed auditory feedback at the same frequency as a vibrotactile stimuli improved tactile discrimination performance via acoustic imagery (Iguchi, et al. 2007). To test our hypothesis, we used either congruent or incongruent frequencies of sound and touch in

a two-alternative, forced-choice (2AFC) tactile discrimination paradigm. For Experiment 3, we developed a somatosensory stimulation apparatus that used piezoelectric vibrators to allow for precise control of vibrotactile stimulation frequency and to extend our results from the previous two experiments to other types of somatosensory stimuli.

Methods

After informed consent, nineteen undergraduate students (9 males; 10 females; mean age =19.9 years) from Rice University participated in this experiment in exchange for course credit. All subjects reported having no auditory or somatosensory deficits.

Somatosensory stimuli were delivered using a piezoelectric bending element (bender). The element was affixed to the dorsal surface of the left hand in each subject using a cloth bandage wrap. A 100 or 200 Hz sinusoidal voltage was applied to the bender, causing it to oscillate at one of these two frequencies. The duration of the oscillation was 250 ms, producing the percept of a brief "buzz" similar to that of a cell phone in vibrate mode. Because of the low intensity of the tactile stimulus and the further attenuation of any sounds from the bandage wrap, the piezoelectric bender did not produce audible vibrations (undetectable increase in sound pressure level as measured with a SPL meter).

For each subject, the amplitude of the applied voltage to the bender was adjusted to near-threshold levels and the perceived intensities of the two stimulation frequencies were equated. The voltage for the 100 Hz vibration was first adjusted to produce a moderately intense percept. Then, the 200 Hz and the 100 Hz vibrations were

alternately presented as the subject adjusted the voltage of the 200 Hz vibration to match the perceived intensity of the 100 Hz vibration. This modified staircase procedure (with random initial voltages for the 200 Hz vibration) was performed three times, with the mean voltage used for the experiment.

The auditory stimulus, when delivered, was either a 100 Hz or a 200 Hz pure frequency tone (59 dB or 60 db in intensity, respectively) delivered for 250 ms over a speaker placed 50 cm in front of the left hand. Thus, the auditory stimulus could either be congruent or incongruent with the tactile stimulus. The position and distance of the speaker from the hand was such that no air pressure was felt on the hand from the sounds. As in Experiments 1 and 2, the participants' left hands rested on the armrest of their chair.

A 3 sound (100 Hz, 200 Hz, or no sound) x 2 touch (100 Hz or 200 Hz) factorial design was used. The start of each trial was signaled by a white fixation cross that was presented for 500 ms at the center of a blank LCD monitor. The participant's performed a 2-AFC task, reporting whether the tactile stimulus on each trial was the low (i.e. 100 Hz) or high (i.e. 200 Hz) tactile stimulus frequency, ignoring any auditory stimulation. Each subject performed 20 trials for each of the 6 conditions for a total of 120 trials. The data were collapsed across stimulation frequency, resulting in 40 trials for congruent auditory and tactile stimulation, 40 trials of incongruent auditory and tactile stimulation, and 40 trials for tactile stimulation with no auditory stimulus.

Results and Discussion

When the sound was the same frequency as the touch, tactile discrimination performance increased by 12.8%, and when the sound was the opposite frequency as the touch, tactile discrimination performance *decreased* by 18.8% in comparison to the no sound condition (see Figure 3 and Table 1). A two-way ANOVA with auditory stimulus (none, same frequency, different frequency) and vibrotactile frequency (100 Hz, 200 Hz) as the two within subject factors revealed a highly significant main effect of sound ($F_{1,18} = 21.008$, p < 0.001). This main effect was driven both by an increase in discrimination performance with congruent sounds as compared to the no sound conditions ($t_{18} = 3.010$, p < 0.001) and a decrease in performance with incongruent sounds as compared to the no sound conditions ($t_{18} = 4.442$, p < 0.001). The main effect of vibrotactile frequency ($F_{1,18} = .440$, p = 0.516) and the sound x tactile frequency interaction ($F_{1,18} = 1.434$, p = 0.252) were not significant. These results demonstrate a frequency-specific effect of sound on touch perception.

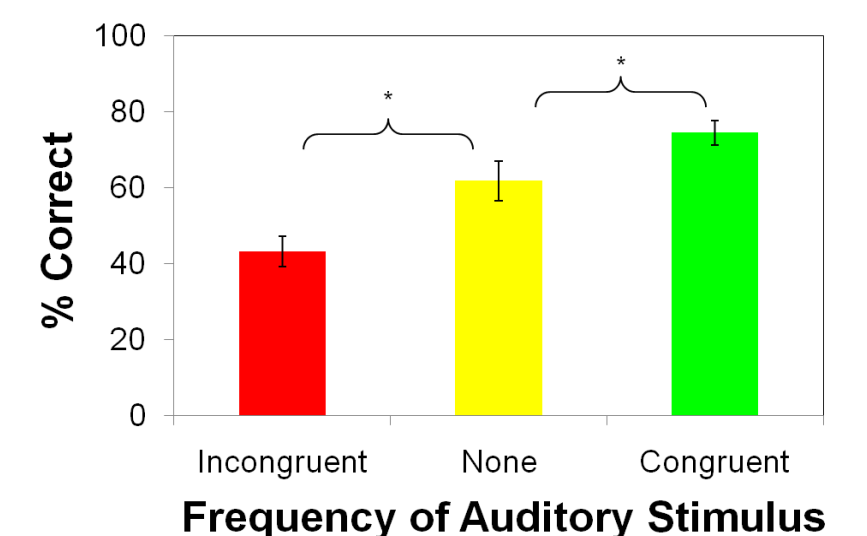


Figure 3. The data from Experiment 3 examining frequency-specific effects of audition on touch. Error bars reflect ±1 standard error of the mean.

General Discussion

Three experiments examined the effects of a task-irrelevant auditory stimulus on somatosensory perception. In Experiment 1, a simultaneously presented auditory stimulus increased sensitivity to a near-threshold touch stimulus. Experiment 2 showed that the enhancing effects of sounds on touch perception are spatially specific; only sounds that occurred on the same side as the touch enhanced spatial discrimination. In Experiment 3, a somatosensory stimulus containing frequency was used to show that the effects of sound on touch are frequency-dependent: discrimination performance increased when a sound was the same frequency as the tactile stimulus and decreased when the sound was of a different frequency.

All three experiments show a significant effect of sound on touch perception, even though different experimental paradigms were used. This consistency is important because it demonstrates the robustness of the auditory influences on touch perception, and suggests that there are likely to be a variety of interesting neural interactions underlying these behavioral effects. For instance, Experiment 1 shows that simultaneous sound enhances somatosensory perception, with the increases in d' indicating that the effect is not due to a response bias. However, the results of Experiment 1 could have been due to an increase in arousal, which could arise from a simultaneous stimulus in any modality (not necessarily auditory-somatosensory). But Experiment 2 shows that the interaction between audition and somatosensation is spatially lateralized, with signal detection analyses confirming that this lateralized enhancement was not a consequence of a response bias. These results suggest neural interactions occurring in

brain regions that have spatial maps and indicate that these effects are not an effect on general arousal. The fact that performance was worse in Experiment 2 than Experiment 1 is relatively uninformative because subjects performed a more difficult discrimination task (deciding between two hands) as opposed to the simple detection task (on only one hand) in Experiment 1.

Although there was not a correspondence between somatosensory frequency and auditory frequency in the first two experiments, the onset of the electrical cutaneous stimulus used in those experiments coincided with the onset of the auditory stimulus and auditory-somatosensory interactions were observed. Unlike Experiments 1 and 2, Experiment 3 used piezoelectric vibrotactile stimulation of much longer temporal durations and specific frequencies. However, due to potential variations in mechanical inertia of the stimulators and the skin, the mechanical deflection of the vibrotactile device may not have been precisely in phase with the sound. Nonetheless, the use of a vibrotactile stimulus allowed us to study auditory-tactile interactions in the frequency domain, which is more precisely coded by the auditory and somatosensory systems, and robust auditory-tactile interactions were measured. This suggests that there may be three separate dimensions along which auditory-tactile multisensory integration may occur (temporal synchrony, spatial concordance, and frequency concordance). In future studies, it will be important to explore these dimensions. For instance, is the integration between spatially congruent and frequency congruent auditory-tactile stimuli additive and do harmonics of the sounds produce similar effects on vibrotactile frequency discrimination?

These systematic effects of sound on touch perception may be a consequence of neuronal interactions within and between several different brain areas. The organization of the cerebral cortex is well-suited for integrating sound and touch information since a) primary auditory cortex is adjacent to secondary somatosensory areas, b) there are anatomical connections from somatosensory cortex into auditory cortex (Schroeder, et al. 2001), c) functional imaging studies show common cortical activation sites for auditory and somatosensory information (Beauchamp and Ro 2008; Foxe, et al. 2002; Ozcan, et al. 2005; Schurmann, et al. 2006), and d) even unisensory cortex may be driven by different sensory modalities (Ghazanfar and Schroeder 2006; Macaluso and Driver 2005). This anatomical proximity and functional interconnectivity may provide the neural basis for the interactions between audition and touch measured in these experiments; connections between nearby areas of cortex are more extensive than connections between distant areas.

The interactions between the auditory and somatosensory systems may reflect a special case of multisensory integration for information in peripersonal space. Previous studies have shown that auditory-somatosensory interactions may be specific to information around the body (Serino, et al. 2007), regardless of whether the peripersonal auditory information comes from in front of or behind the subject (Farne and Ladavas 2002; Zampini, et al. 2007). Since in our experiments the auditory information was always presented through headphones or in peripersonal space, we cannot assess whether the increases in sensitivity to somatosensory information would also extend for auditory information in far, extrapersonal space. Further experiments

directly modulating the distance of the auditory information, as well as the intensity (Occelli, et al. 2008), might be informative regarding some of the boundary conditions of these enhancing effects on somatosensation from audition.

It is important to note that our experiments used simultaneous auditory and tactile stimuli. Therefore, it is unlikely that our results are a consequence of a spatial orienting of attention effect of the sound on touch, as has been shown in other studies (cf. Spence and Driver 1997). In contrast to spatial orienting, which requires some time for attention to move to the locus of an event (Posner 1980), our results could have been influenced by an increased level of general alerting and/or arousal when an auditory stimulus was presented. However, the fact that the enhancements of touch from sound were spatially- and frequency-specific rather than more generally enhancing suggests that a general alerting or arousal account for these results is insufficient. In some of our previous work, we have also demonstrated that a simultaneous visual stimulus can affect tactile processing in similar ways (Johnson, et al. 2006). Taken together, these findings suggest that these multisensory enhancement effects may be a result of superadditive processing of vision, audition, and touch in brain areas coding for all of these sensory modalities (e.g., the superior colliculus and the posterior parietal cortex). We are currently examining these enhancing effects of sound on touch using functional magnetic resonance imaging, which may provide further clues to the neural mechanisms underlying these effects.

Recently, we reported a patient with an interesting linkage between touch and sound (Ro, et al. 2007). Following a thalamic stroke, the patient had somatosensory

processing deficits on the left side of her body. Gradually, the patient came to feel touches when she heard certain sounds. A possible explanation for these results is that latent connections from auditory cortex to somatosensory cortex are now hyperactive, as further suggested by neuroimaging experiments on this patient (Beauchamp and Ro 2008). As a result, sounds activate somatosensory cortex, which result in the perceptions of touch. The results from this patient further support a tight link between sound and touch, and suggest some degree of interchangeability between these two sensory modalities.

In addition to demonstrating some of the ways in which sounds interact with touch perception, the current results suggest another systematic and more general medium through which multisensory information might be integrated. Specifically, our studies extend the work demonstrating spatial and temporal specificity in multisensory integration and attention (e.g. see Driver and Noesselt 2008; Driver and Spence 1998b; Stein and Meredith 1993) into the frequency domain. By integrating information from different sensory modalities based on stimulus frequency, perception might be further optimized through this frequency-specific form of multisensory integration. Further work examining frequency-dependent visual-auditory and visual-tactile integration may provide the boundary conditions for multisensory interactions based on frequency information.

Chapter 6: Providing Transcranial Magnetic Stimulation (TMS) in an MRI Environment

Introduction

While fMRI can tell us whether or not a brain region is activated during a task, it cannot tell us if that brain region is essential to the task or merely associated with it. For instance, if a subject were to count while being scanned activity in visual cortex may be observed from the subject visualizing the numbers. Unfortunately the only way to determine if a brain area is essential for a given task is to deactivate that area and see if that interferes with a subject's ability to perform the task. This is commonly done in experiments with animals and with humans about to undergo cortical resection surgery by using cortical cooling techniques or by applying electric current directly to the brain; although for obvious reasons these methods can't be used on healthy human subjects which are the focus of the bulk of our research. However, the cortex can be inductively stimulated using eddy currents as a non-invasive way of suppressing cortical areas. This can be accomplished by placing an inductive coil on the skull of a subject and applying a high-current pulse to the coil (Barker, et al. 1985); the high ramp-rate of the pulse creates a magnetic field around the coil which will in turn induce currents the cortical tissue below the skull.

The use of this technique, called Transcranial Magnetic Stimulation (TMS) has become a popular complement to fMRI, although currently fMRI and TMS experiments must be run separately as fMRI compatible TMS systems are not yet available. This is unfortunate because concurrent fMRI and TMS can provide a simple and verifiable way to determine that the correct brain area was targeted by the TMS, as well the extent and duration of suppression. So with this in mind we have adapted a commercially

available TMS system, the Magstim Rapid (www.magstim.com) for use in an MRI environment. To accomplish this we had to overcome two challenges, first the Magstim Rapid is designed to be controlled manually by the experimenter (although it does include features for rapid stimulation that make computer control possible), so we had to devise a way to control the system using a computer so it could be synchronized with fMRI experimental stimuli and the scanner. Second, both systems rely on magnetic fields to operate, we therefore had to devise methods to prevent interference between the TMS and fMRI.

Adapting the TMS system for computer control

Controlling the TMS system through a Parallel Port

The Magstim Rapid is designed to be able to provide rapid trains of pulses of up to 100Hz. Since it is impossible for a human to signal such a rapid sequence with button presses, and since the TMS system does not have an internal sequence generator, the system includes a port for external control to connect to a pulse train generator. We were able to use this interface to provide the computer control necessary for syncing up the TMS pulses, experimental stimuli, and fMRI scanner.

The software we use to run our fMRI experiments is Presentation (www.neurobs.com). This software provides a large library of functions for delivering visual and auditory stimuli, but is limited in its use of the parallel port; it can only control pins 2-9 as outputs and pin 10 as an input. The TMS console uses a Centronics 36 port for input control, and requires eleven lines of control for our purposes (Table 1 below).

In order to expand the output lines a control box was built centered around a 74HC595 serial-in, parallel out shift register (Fig. 1). This allows all seven of the Power Level Control inputs to be controlled by only four pins (2-5) of the parallel port (Fig. 2). Pins 7, 8, and 9 are used to arm, disarm, and trigger the Magstim Rapid.

Pin Number	Description		
1	Data Direction Control (Apply +5V here to select external control)		
2	Power Level Control (LSB, Value 1)		
3	Power Level Control (Value 2)		
4	Power Level Control (Value 4)		
5	Power Level Control (Value 8)		
6	Power Level Control (Value 16)		
7	Power Level Control (Value 32)		
8	Power Level Control (MSB, Value 64)		
9	Trigger Input ("0" triggers the Magstim Rapid)		
10	Ready Output ("1" when Rapid is armed, charged and ready)		
11	Replace Coil Output ("1" means coil is disconnected or faulty)		
12	Coil Temperature Output ("1" means temperature has exceeded 36°C)		
13	Coil Active Output ("0" means that the coil button is pressed)		
14	Run Input (Applying a "0" briefly arms the Magstim Rapid)		
15	outputs +12VDC at 250mA		
16	Analog Ground		
17	Chassis Ground		
18	Capacitor Voltage (1V per kV)		
19-30	Ground		
31	Stop Input (Applying a "0" briefly places the Magstim Rapid in standby)		
32	Armed Output ("1" when unit is armed, "0" when unit is in standby)		
33	Trigger Output		
34	No connection		
35	Trigger Input ("0" triggers the Magstim Rapid)		
36	Coil Temperature Output (analog output of 10mv/°C from 5-80°C)		
Chassis	Ground		

Table 1. Input/output table for the Magstim Rapid. The items in bold are the control lines necessary for our purposes.



Figure 1 The TMS control box. The LEDs on the face of the box are used to show the contents of the output latches, which is very useful during debugging.

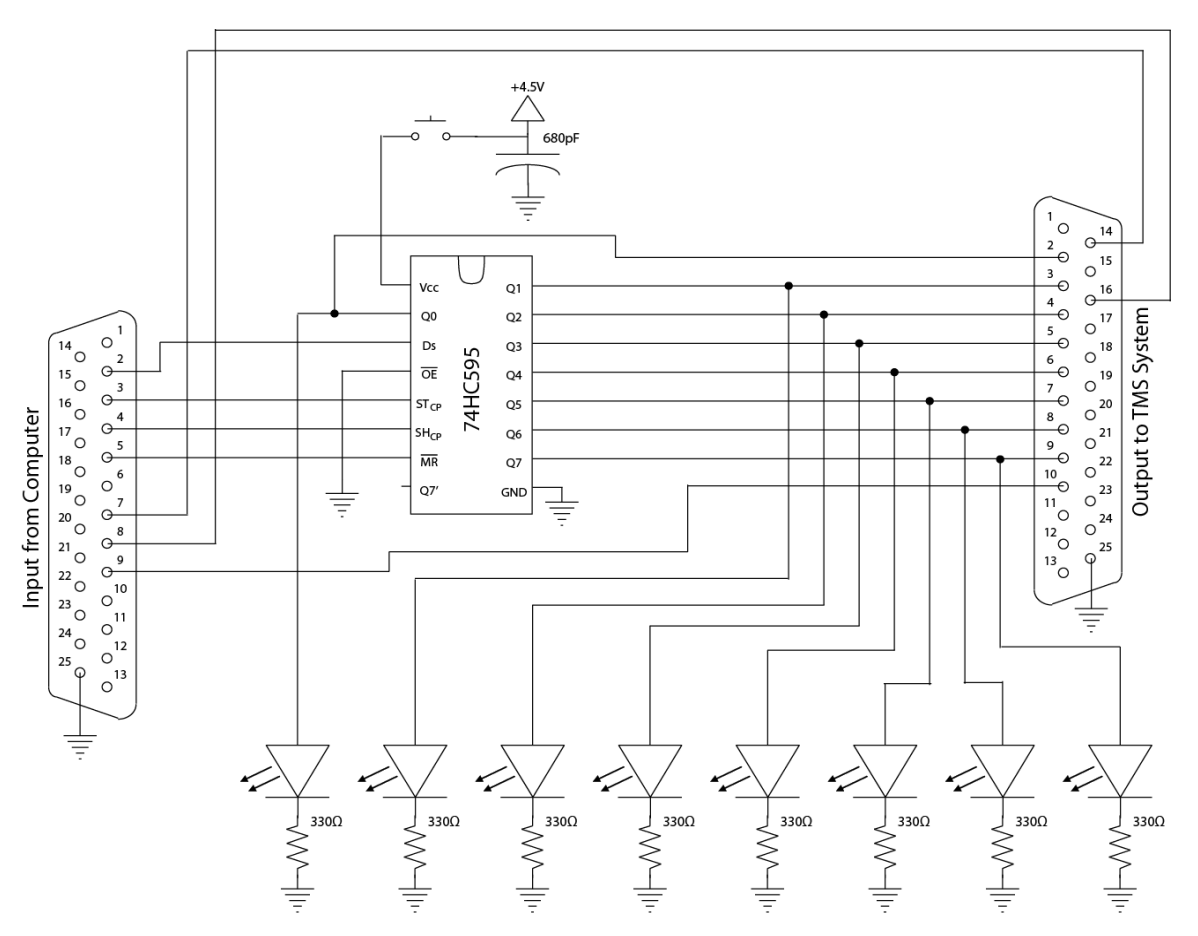


Figure 2 Schematic for the TMS control box. The output is also a DB25 connector, a DB25 to Centronics 36 cable was constructed to connect the control box to the TMS system.

In order to pass a number to the Power Control Lines, it is converted into binary and the digits are passed to the serial data input of the shift register (D_s) from pin 2 of the parallel port. The chip is signaled to input a bit at each digit through the shift register clock input (SH_{CP}) from pin 4 of the parallel port. After the shift register has been filled the storage register clock input (ST_{CP}), connected to pin 5 of the parallel, is signaled to send the contents of the shift register to the output latches, which connect to the Power Control Lines of the TMS. Figure 3 shows an example of setting the power level to 83%.

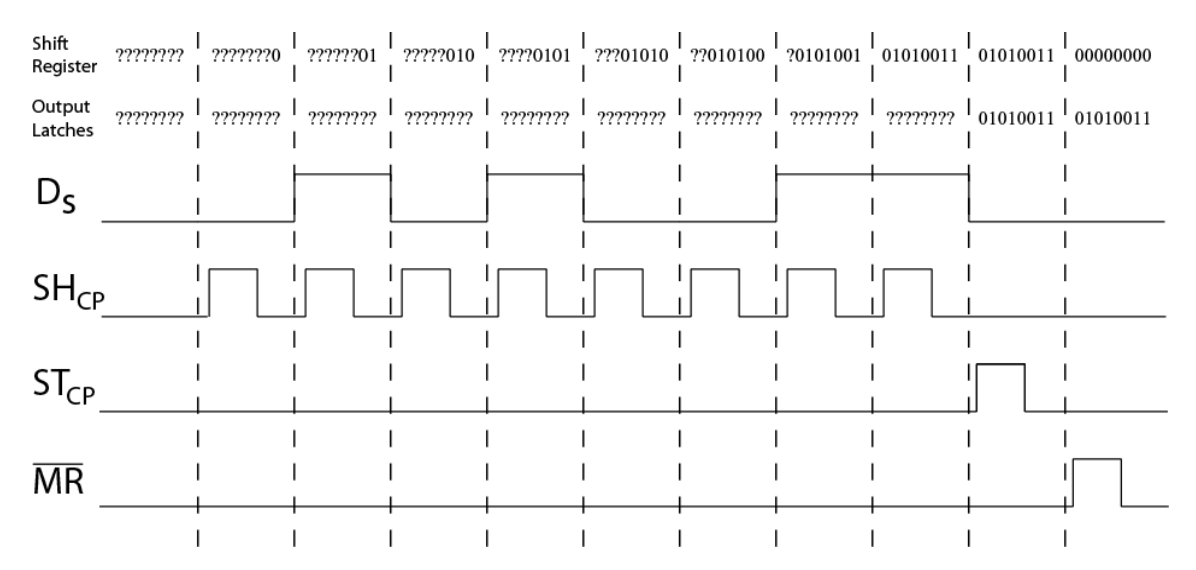


Figure 3 Control diagram of the control box. This example shows the steps to set the TMS strength to 83%, or 01010011_2 in binary. The inputs D_s , SH_{cp} , ST_{cp} , and \overline{MR} correspond to pins 2, 4, 5, and 6 of the computer's parallel port when connected.

Bypassing safety systems for manual control and adding safety systems for computer control

The Magstim Rapid uses a pneumatic foot pedal that connects to the coil control box to prevent accidental discharges (Fig. 4). This foot pedal has to be depressed in order for the TMS system to trigger, which is not practical for computer control.

Therefore a new coil control box was built which adapted the circuitry for the foot pedal to use a large button instead (Fig. 5). When struck, the button halts the system in the same way that taking your foot off of the pneumatic pedal would with the old coil control box. This feature is necessary in order to provide a quick way to end TMS stimulation in the event that a subject has a seizure, which is a possibility although very unlikely unless the subject is epileptic or very high stimulation frequencies are used.

Next to the switch is an LED that is used to indicate whether or not the system is halted by the emergency switch. The new coil control box also has a button to switch between manual and computer control. This switch is connected to pin 1 of the TMS console's centronic port (Table 1), and when depressed signals the Magstim Rapid to ignore the front panel button interface and instead respond to computer control. This switch allows the TMS system to be easily converted for use inside or outside the scanner.

Besides these features, the new coil control box also contains additional circuitry for noise elimination, which is described in the next section.



Figure 4 Coil control box showing the pneumatic foot pedal. The Magstim Rapid will not operate unless the foot pedal is depressed.



Figure 5 The new coil control box with the pneumatic foot pedal removed and the new safety switch installed. This box also contains added noise elimination circuitry that is described below. The button in the top left corner switches between manual and computer control; manual control is useful for debugging and experiments outside the scanner. The large red button will immediately disconnect the coil when struck, this may be necessary if the subject has a seizure.

Noise Elimination

Noise inherent to TMS

The very function of the TMS critically interferes with the function of the MRI; activation of the coils can create a field of up to two teslas at its focal point. This is on

the same order of magnitude as the field in the bore of the scanner (the scanner used in our research is a three tesla scanner) and significantly distorts it, thereby greatly distorting the MRI image. Additionally the rapid pulses of the TMS also emit a high amount of RF noise, drowning out the MRI signal. A TMS pulse therefore cannot be given during acquisition of an image, and enough time must be given between image acquisitions to give a TMS pulse. To accomplish this a clustered acquisition protocol must be used, with the TR extended by 250ms (roughly the time needed to arm the TMS, set the strength level, and trigger a pulse) during which time the scanner is inactive.

Noise caused by the recharging capacitor bank

The TMS system uses a large bank of capacitors to build up enough charge to produce the TMS pulse. After each pulse the capacitors have to recharge before another pulse can be given. Since the coil is connected to the bank of capacitors, the rising voltage of the capacitors creates a current through the coil. This current is relatively small, however because of the large inductance of the TMS coil, its position inside the bore of the scanner, and the extreme sensitivity of MRI scanner, it creates more than enough noise to drown out any useful signal. To illustrate this we scanned a phantom while delivering TMS pulses in between image acquisitions. We initially set the strength of the pulse to 10% and gradually increased it after every image until the maximum strength was reached. The resulting time series is shown in figure 6. As you

can see, even low levels produce a significant amount noise, and the level increases approximately linearly with pulse intensity.

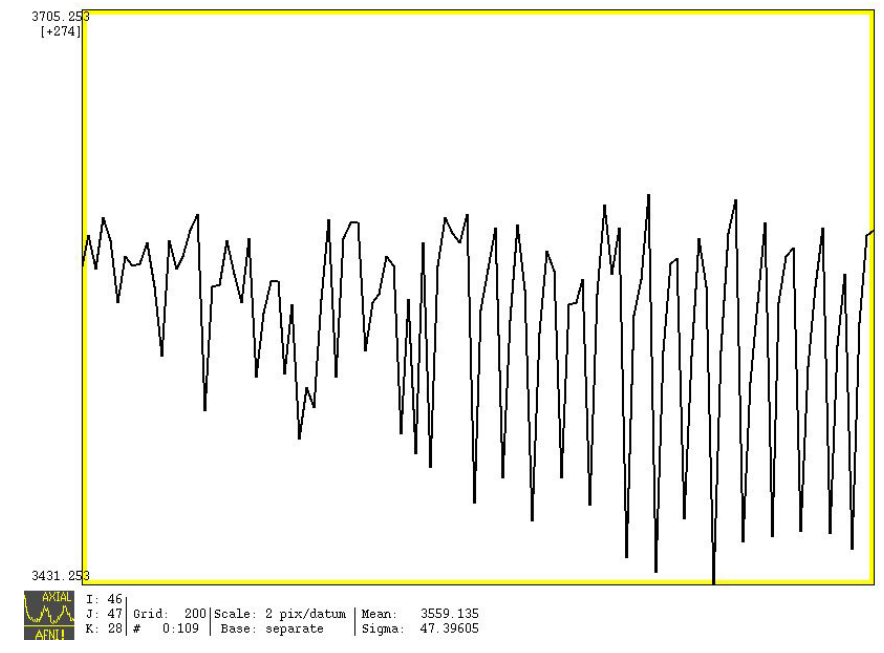


Figure 6 Time series of the noise created by recharging of the pulse-generating capacitors. Here the TMS was triggered between pulse intervals. The TMS strength was steadily increased after each interval, from 10% to full intensity, which can be seen by the increasing level of noise.

In order to eliminate this noise the TMS coil has to be electrically isolated from the capacitor bank while it recharges. To accomplish this we connected two industrial contactors (Tyco Electronics KILOVAC LEV200 Contactors, www.tycoelectronics.com)in series with the TMS coil (Fig. 7). Contactors function like relays, but have arc suppression systems to prevent pitting or fusing of their contacts from potentials in excess of a kilovolt. This is necessary as the TMS system puts out seven kilovolts when set to maximum intensity. The contactors are controlled by pin 10 of the TMS console. This pin outputs a high signal when the TMS is armed, closing the contactors and

allowing a pulse to be delivered. When it is disarmed the contactors open, breaking the connection between the TMS unit and the coil. By arming the TMS right before delivering a pulse, and then disarming it before the next image acquisition, we were able to eliminate the noise seen in figure 6. In figure 8 we again scanned a phantom while delivering TMS pulses of increasing strength in between each image acquisition; however this time we used the modified coil control box and disconnected the TMS coil during image acquisitions. As you can see from the time series, the noise is effectively eliminated.

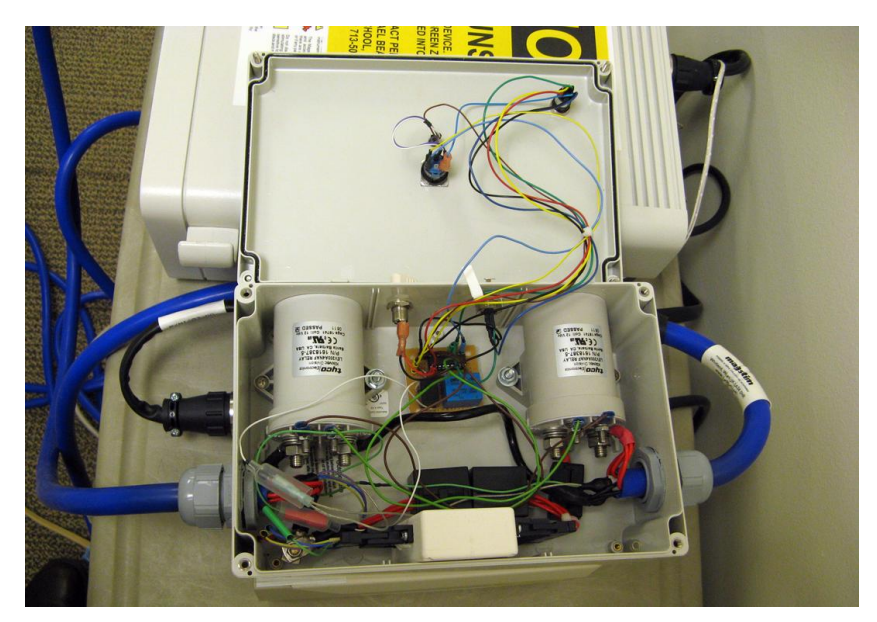


Figure 7 The coil control box opened to show the industrial contactors. The contactors act as a switch, connecting or disconnecting the TMS coil from the rest of the system at both the positive and negative leads.

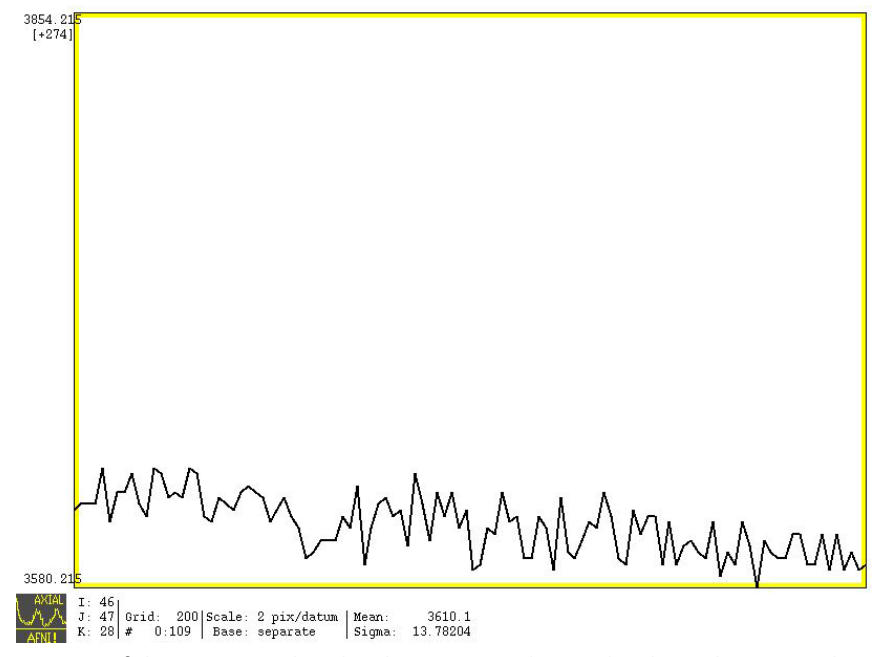


Figure 8 Time series of the same voxel under the same conditions, but here the new coil control box is being used. Since the coil is now physically disconnected from the TMS when it is not being triggered, there is now no induced current caused by the charging snubbing capacitors.

To test whether the system is now usable in an fMRI scanner we performed a simple experiment in which we had a subject alternate between tapping her for ten trials and keeping them still for another ten. In every trial that she tapped her fingers we delivered a TMS pulse. Figure 9 shows a time series of a voxel in primary motor cortex, the vertical lines separate each block of 20 trials. As you can see we were able to record a strong signal in response to her motor activity. The scale is this figure is the same as figures 6 and 8. Notice that the signal is significantly smaller than the noise shown in figure 6; this signal would be completely obscured if the capacitor charging noise was still present. Figure 10 shows an axial cross section of her brain with activation overlaid.

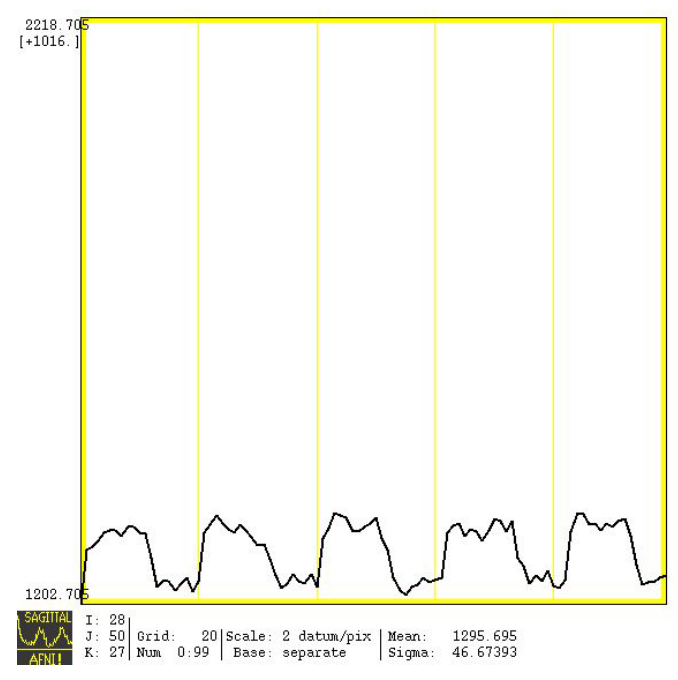


Figure 9 Time series of a voxel in primary motor cortex showing activation in response to finger taps; the subject is tapping her fingers for ten trials then keeping them still for ten trials. The TMS is triggered in every trial that she taps her fingers. The vertical lines separate each block of twenty trials.

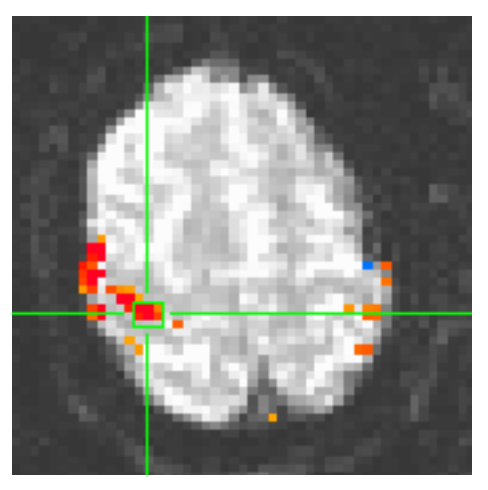


Figure 10 Activation map showing responses to finger tapping. The crosshairs show the location of the voxel whose time series is shown in figure 9.

Further Refinement, the TMS Coil Acting as an Antenna and Noise from the TMS Console

Although the majority of noise has been removed, a small amount remains due to the now open TMS coil acting as an antenna. Any noise picked by the leads of the coil

is taken into the bore of the scanner, and the TMS console itself generates a small amount of noise. The left column of Figure 11 shows what normal images of the phantom should look like while the right column show images collected with the TMS system present and active. While the majority of the area within the scanner is undistorted, the superior-most region does show a significant amount of noise (bottom right image). If this area happened to correspond with a region of interest, the quality of data would be greatly diminished.

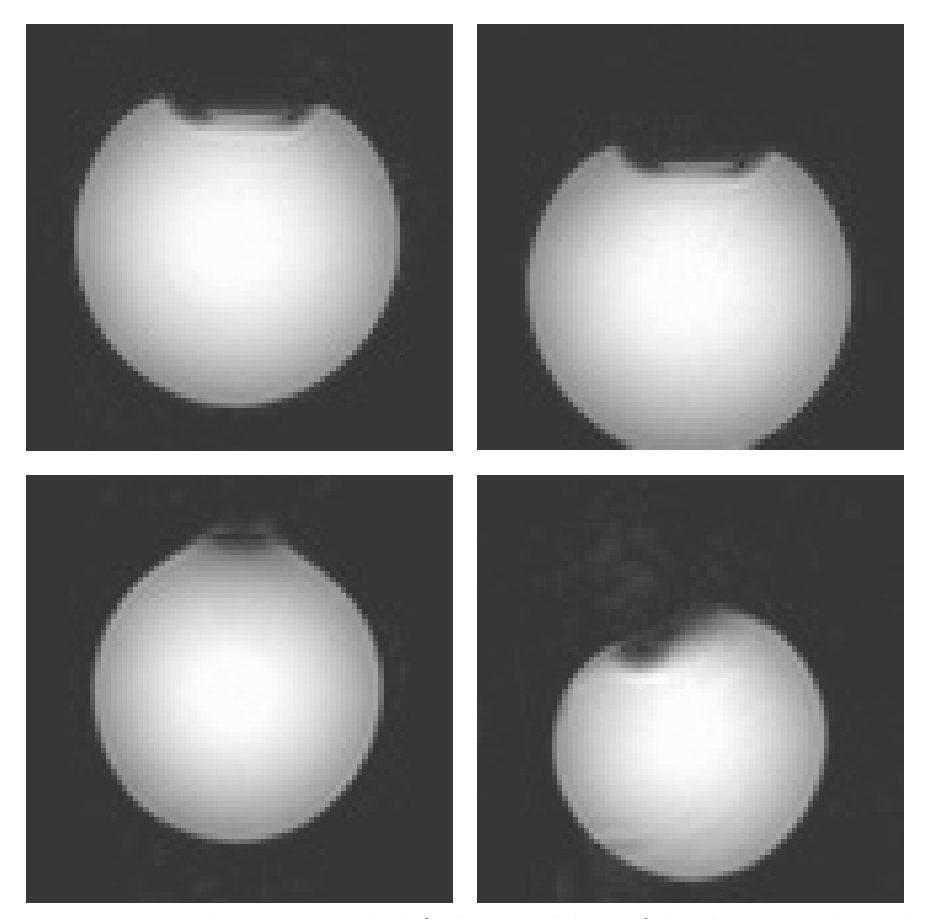


Figure 11 Remaining noise. The images on the left show axial slices of the phantom without the TMS system present, and the one images on the right show slices with the TMS system present and active. The top images are through the midline whereas the bottom images are more superior. Notice the distortion in the bottom right image.

To remove this noise the TMS console will be moved out of the scanner room, and the penetration panel of the scanner room will have to be rebuilt to include the Souriau circular connectors that the TMS coil uses, so that a connection for the coil can be provided without comprising the noise shielding of the scanner room. Additionally filters will have to be connected in series with the leads of the TMS coil to prevent noise from outside the scanner room, including the noise generated by the TMS consol, from being piped in to the room by the coil. Unfortunately filters capable of withstanding the high currents of the TMS pulse (up to two kiloamps) are extremely large, heavy, and expensive. Fortunately noise is not an issue while the TMS pulse is being delivered, since image acquisition is not being performed at that time. As a result we could use relays to disconnect the filters while the pulse is being delivered, and reconnect them at all other times. The currents generated in the coil by noise are on the order of hundreds of milliamps, therefore small and inexpensive filters can be used.

Chapter 7: Industrial Internship: Simultaneous Intracranial or Intracortical Recording and Stimulation

Introduction

Researchers have used both cortical recording and stimulation for decades in order to investigate brain anatomy and physiology. Researchers will often record from areas of interest while delivering stimuli (Hubel and Wiesel 1962), or having the subject perform a task (Georgopoulos, et al. 1986), so that they can understand how neurons or brain areas process information. Stimulating brain areas provides a uniquely direct way to understand the functionality of a brain area, as stimulating a specific area can often produce a behavior (Milad, et al. 2004) or percept (Murphey, et al. 2008) in the subject. Additionally even stronger stimulation can be used to disrupt processing in an area (Murasugi, et al. 1993) so that the importance of that brain area for a specific function can be evaluated.

It would be highly desirable to be able to record and stimulate at the same time; for example recording in surrounding tissue while stimulating would allow a researcher to quantify the extent of cortical area that the stimulation is affecting. Likewise, by stimulation in one area while recording in a distal region connectivity could be established if resulting activity were recorded, and the number of intermediate connections could be deduced from the latency. Unfortunately there are considerable engineering challenges to overcome in order to be able to record while stimulating; this is largely because while neuron potentials are on the scale of microvolts, stimulation generally has to be on the order of millivolts or even volts in order to get an appreciable effect.

This chapter describes a project completed during an industrial internship at Blackrock Microimplantible Systems. The project consisted of testing and debugging a system for concurrent microstimulation and recording, which at the time was called the Stim Project. The system was designed to be connected to the Cerebus system, which is Blackrock's 128 channel data acquisition system. The Cerebus system consists of a Neural Signal Processing (NSP) unit, and a Neural Signal Amplifier (NSA) that has four banks of 32-channel inputs. The NSA receives the analog signals from the microelectrode(s) and amplifies them as well as providing some analog filtering before passing them onto the NSP. The NSP converts the signals into digital form, and can perform a number of processing functions on the data (such as spike counting, spike sorting, adjustable digital filtering, etc.) before passing the data to a computer for viewing by the user. A single Stim Project unit was intended to allow concurrent stimulation and recording on 32 channels, and would plug into one bank of the NSA. The system was designed to be controlled through a serial port. The same computer could be used to both receive data from the Cerebus system and control the Stim Project.

Before the Stim Project could be a viable product, several challenges inherent to simultaneous stimulation and recording had to be addressed. First the system must be sensitive enough to be able to record the action potential of a single neuron with a high level of resolution, yet be fairly immune to cross-talk and outside electromagnetic interference that would drown out or obscure the signal. Secondly during stimulation currents that are orders of magnitude larger than neural signals are used. These signals

must not be allowed to drive the sensitive NSA into saturation during stimulation since it can take several seconds for it to recover, which is almost an eternity when recording neural signals. Additionally if there are any capacitances in the system these large currents can leave residual charges that can likewise saturate the NSA or obscure the neural signal. The following describes how I explored and addressed these issues.

Cross-Talk and EMI Susceptibility

The switching board appears to be well shielded on the side that the signal cable connects to, providing a high degree of immunity from channel-to-channel crosstalk when the board is connected to a load. Although the channel-to-channel cross-talk could reach over 5% on a neighboring channel when floating (a maximum 257mV_{pk} was recorded with a 5V_{pk} input stimulus), when the board was connected to a microarray suspended in saline the signal on neighboring channels was not measurably higher than that created by purely channel-to-channel conduction through the saline medium. Likewise, this shielding also provides a high level of protection from EMI in the stimulus cable. As shown in figure 1A, an electrode carrying a 5V_{pk} signal brought close to the stimulus cable did not provide a measurable amount of interference. Figure 1B shows that bringing the electrode close to the board on the side of the cable also does not produce a recordable amount of EMI. However, when that same electrode is brought to the opposite side of the board it creates a signal of over $5mV_{pk}$ (fig. 1C). This can cause a problem if the cable comes into close proximity with the switching board as shown in figure 1D. As a result any user will have to take care that the switching board is used in

an environment that is relatively free of EMI, which is usually a requirement of any electrophysiological study; and the user will have to take care when setting up the apparatus that the cable does not double-back or wrap around the PCB board.

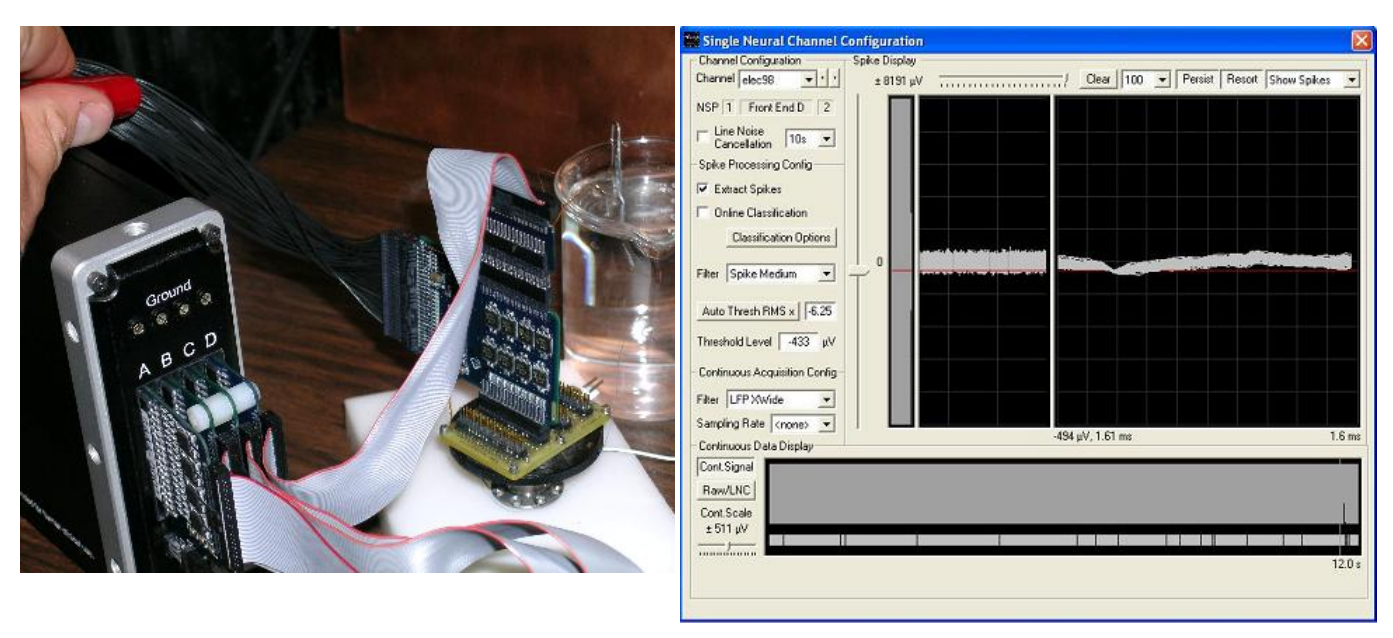


Fig. 1A The switching board shows high immunity from EMI at the cable.

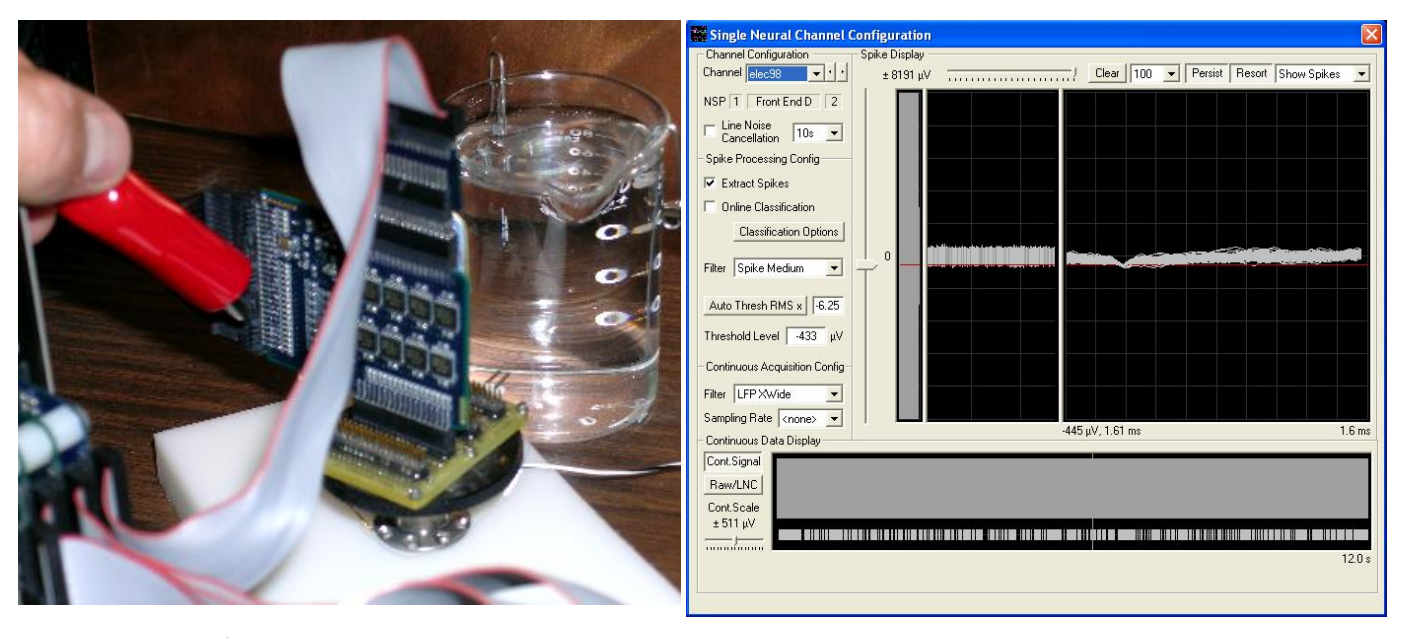


Fig. 1B The side of the board that connects to the stimulus cable also shows high immunity.

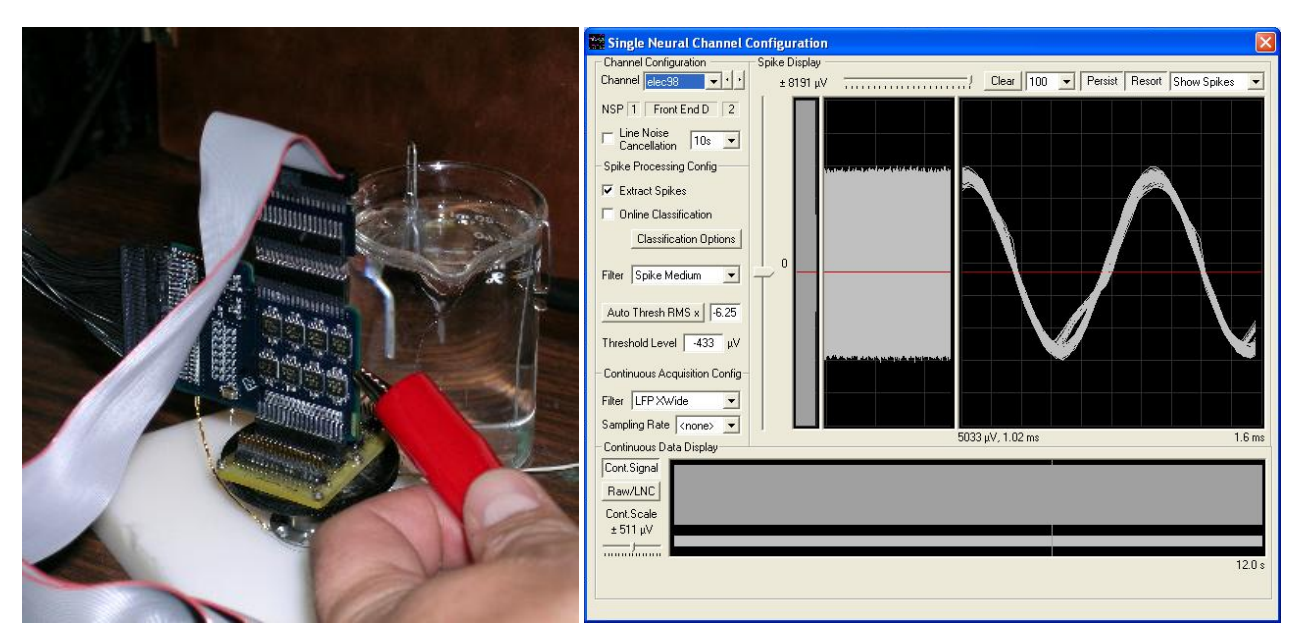


Fig. 1C The side opposite the stimulus cable shows high susceptibility to EMI.

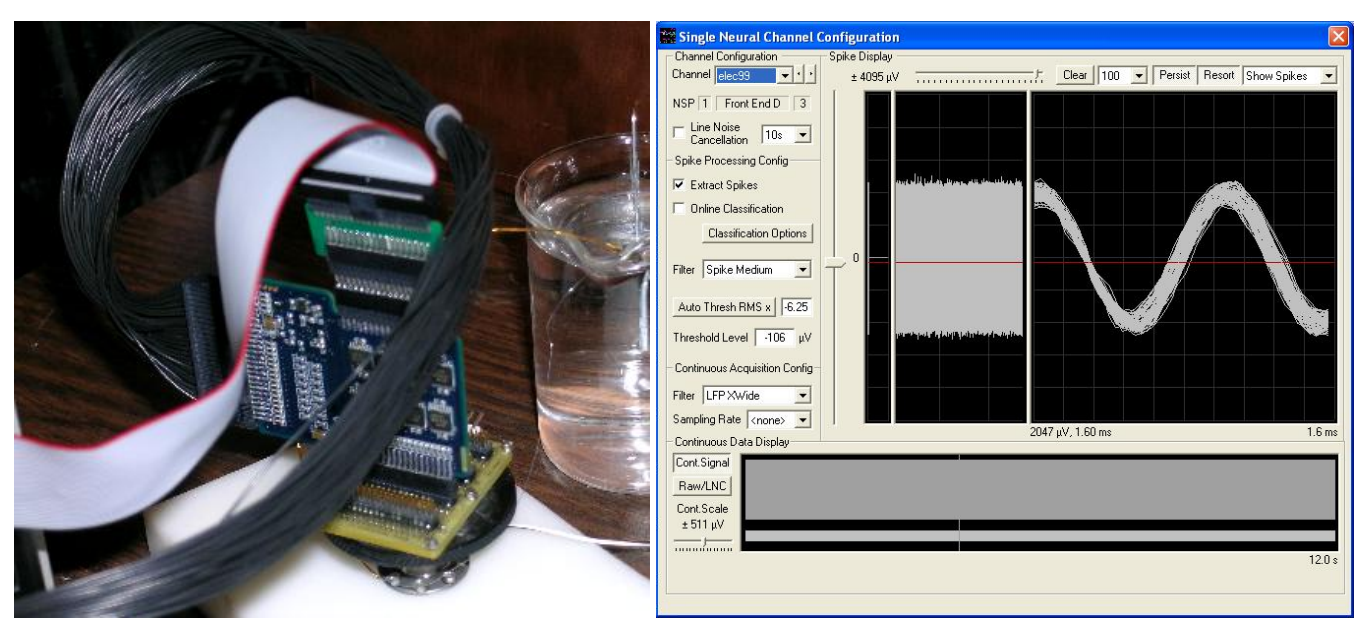


Fig. 1D The cable should not come near the opposite side of the board due to its high EMI susceptibility.

Stimulus Signal Leakage

When the switching board is set to record, the stimulus waveform of that channel shows up on the coinciding channel of the Cerebus system as if it were being recorded from the electrode. The amount of signal that "leaks" through varies from channel to channel, with channels 17, 19, and 24 being particularly problematic. Table 1 below shows the level that a 1kHz 5V_{pk} sinusoidal input "leaks" onto each recording channel.

Although this "leakage" shows up on other channels with varying amounts of attenuation (except on channels 17, 19, and 24, where a leaked signal can show up more strongly than on the channels the stimulus is actually applied), the pattern seems to be based on the channel layout on the stimulus PCB rather than the microelectrode layout. Also the signal does not show up on neighboring channels that aren't connected to the Stim Project, and non-sinusoidal waveforms such as square waves are heavily distorted. This indicates that the problem is not caused by current leaking across the switches and into the electrode, but is instead a byproduct of the cross-talk issue discussed in the previous section. However, the Stim Project has an output status signal (labeled STAT on the mainboard) that signals whether the stimulus board is in stimulus or recording mode; and since virtually all cortical stimulators have a trigger function this signal can easily be used to gate the input waveform and eliminate the problem.

Channel #	Leakage Voltage (μV)	Channel #	Leakage Voltage (μV)
1	548	17	1442
2	449	18	252
3	119	19	1726
4	512	20	404
5	560	21	375
6	252	22	249
7	378	23	155
8	321	24	1973
9	110	25	156
10	126	26	578
11	290	27	186
12	259	28	284
13	172	29	267
14	335	30	184
15	388	31	445
16	300	32	683

 $\textbf{Table 1} \ \text{Amount of leakage of each channel}. \ \ \text{The stimulus waveform was a 1kHz 5V}_{pk} \ \text{sinusoid}.$

Capacitance Issues

With any microstimulus/microrecording system there is always the issue that after stimulation lingering voltages due to capacitance in the system will obscure the

miniscule neural voltages that the system is trying to record. This is especially true with any system to be used with Cerebus system; the very fine resolution of the NSA restricts it to a window of ±8mV. Any voltage larger than ±8mV will drive the amp into saturation. To test how quickly the system could recover from a stimulus cycle, a second function generator was added to the experimental setup which was connected to two electrodes submerged on opposite sides of the saline beaker which contained the microelectrode array. The Status output of the mainboard (labeled STAT on the main board, it gives a high TTL signal when the Stim Project is set to stimulate and a low signal when set to record) was used to trigger the function generators, this way the first function generator activated and provided a stimulus signal to the stimulus inputs of the Stim Project when it was set to stimulate, and when the Stim Project was switched to record the first function generator turned off and the second function generator activated, providing a waveform to the saline. By using two distinct waveforms for stimulation and for the saline, this made it very easy to distinguish the source of all signals recorded by the Cerebus. A serial port controller program was then used to cycle the Stim Project through several periods of two seconds of stimulating, followed by four seconds of recording. Recordings were from the 32 channels connected through the Stim Project as well as the neighboring 32 channels connected through a headstage bypass adaptor to make differentiating between capacitance of the microelectrode array and capacitance and voltage fluctuation of the Stim Project possible.

Figure 2 shows the result of this using a 1kHz, $2.5V_{pk}$ sinusoid as the stimulating waveform, and a 1kHz, $10mV_{pk}$ square wave with a 25% duty cycle as the waveform

across the saline medium (NeuroExplorer 4 was used for these and the following illustrations). As shown in figure 2A the Stim Project is set to stimulate and a stimulus waveform is triggered at t=0.745s, which is immediately picked up by the electrodes not connected to the Stim Project. The channels connected to the Stim Project show a fluctuation at the time of switching. At time t=2.745 the Stim Project is switched to record (fig. 2B) and the saline waveform triggers (after a programmed 5ms delay so that the transition can be easily discerned). As can be seen in the figure the Stim Project channel is not able to immediately record the saline waveform, but the neighboring channels can (in another recording not illustrated here the 5ms delay was turned off to verify that the neighboring channels are capable of recording in less than a millisecond). As shown in figure 2C, the Stim Project channel is not capable of recording the saline waveform until after a delay of nearly 3 seconds. It takes another 40ms for the recording to reach maximum amplitude (fig. 2D).

This experiment was repeated with a variety of different stimulus waveforms (monopolar and bipolar square waves, sinusoids, sawtooths, and triangle waves) with a variety of amplitudes (0.1-5V_{pk}) and a variety of frequencies (500-10,000Hz). In each case the Stim Project channels were unable to record until after a delay of 3 seconds ±50ms. The neighboring channels were always able to record without a measurable delay. The experiment was repeated again without a stimulus waveform (fig. 3) and again the channels connected to the Stim Project had a delay of almost 3 seconds before being able to record while the neighboring channels had no discernable delay. This demonstrates that electrode capacitance is not an issue in the recovery time, and

that instead that capacitances of the Stim Project switching board coupled with large voltage fluctuations at the time of switching are the cause (the voltage fluctuations are more clearly illustrated in figure 5 of the next subsection, with the inclusion of unfiltered recordings).

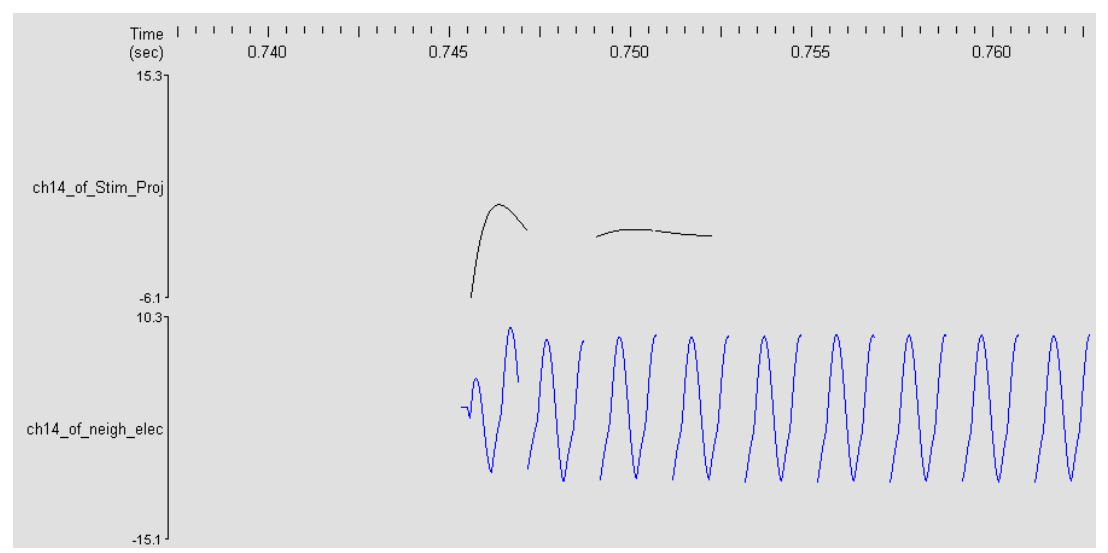


Fig. 2A At t=0.745s the stimulus is turned on, and is recorded by the neighboring electrodes not connected throught the Stim Project.

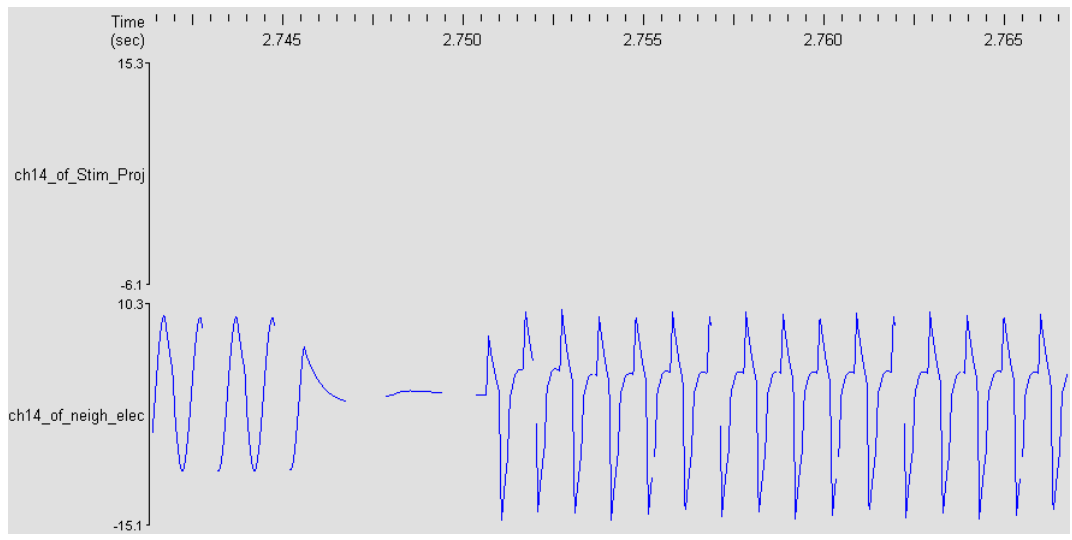


Fig. 2B Two seconds later the Stim Project is set to record and the stimulus waveform is turned off. 5ms later a 1kHz bipolar square wave with a 50% duty cycle is applied to the saline medium. The Stim Project does not immediately register the waveform.

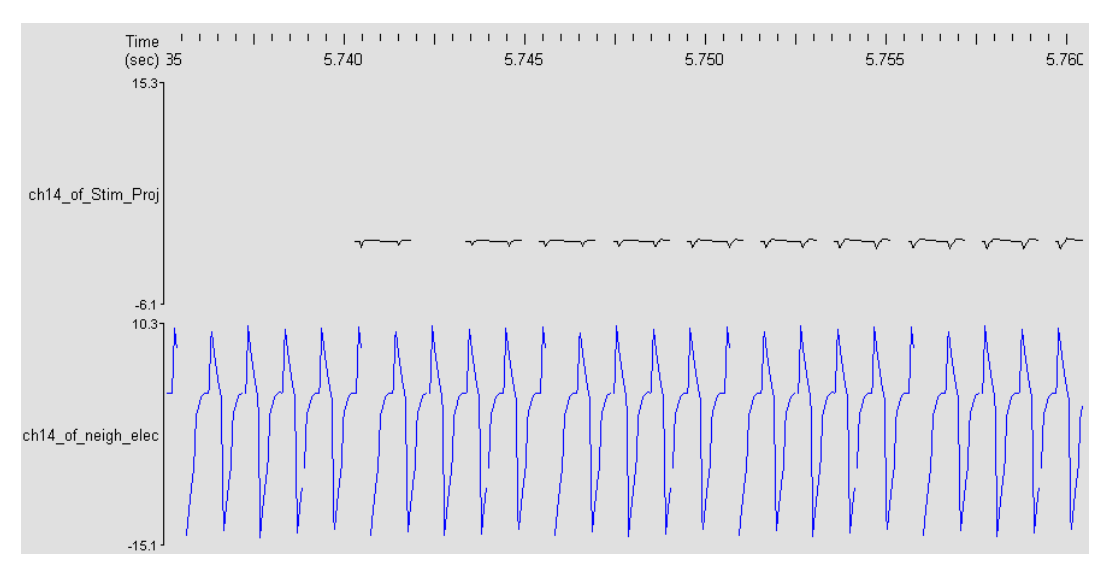


Fig. 2C At t= 5.740, 2,995ms after the Stim Project was set to record, the stimulus begins to appear.

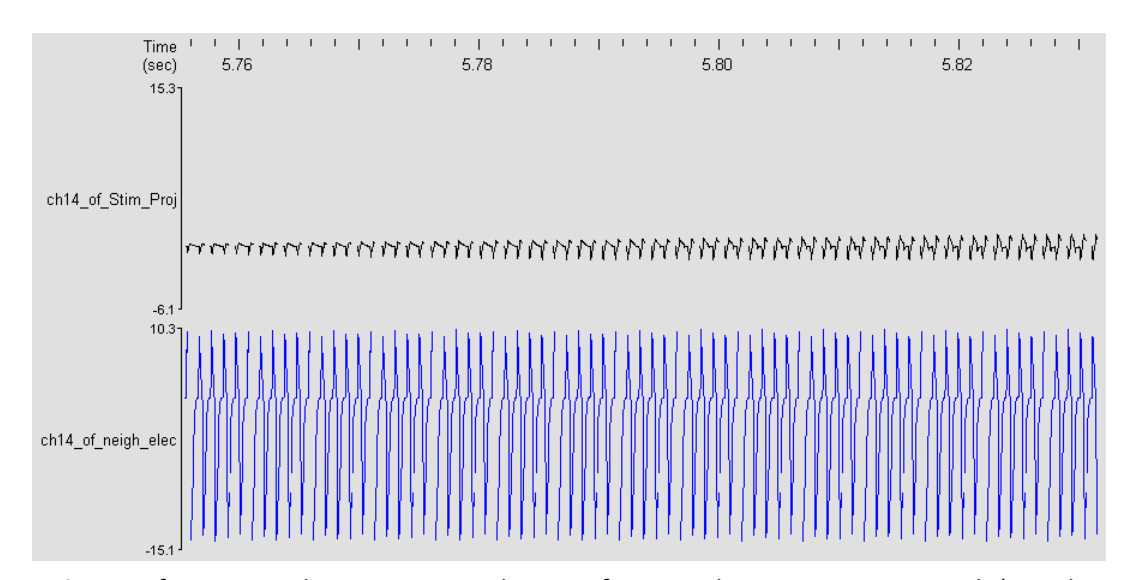


Fig. 2D After ~40ms the Stim Project the waveform reaches maximum strength (signal recorded through the Stim project are always attenuated compared to direct recording.)

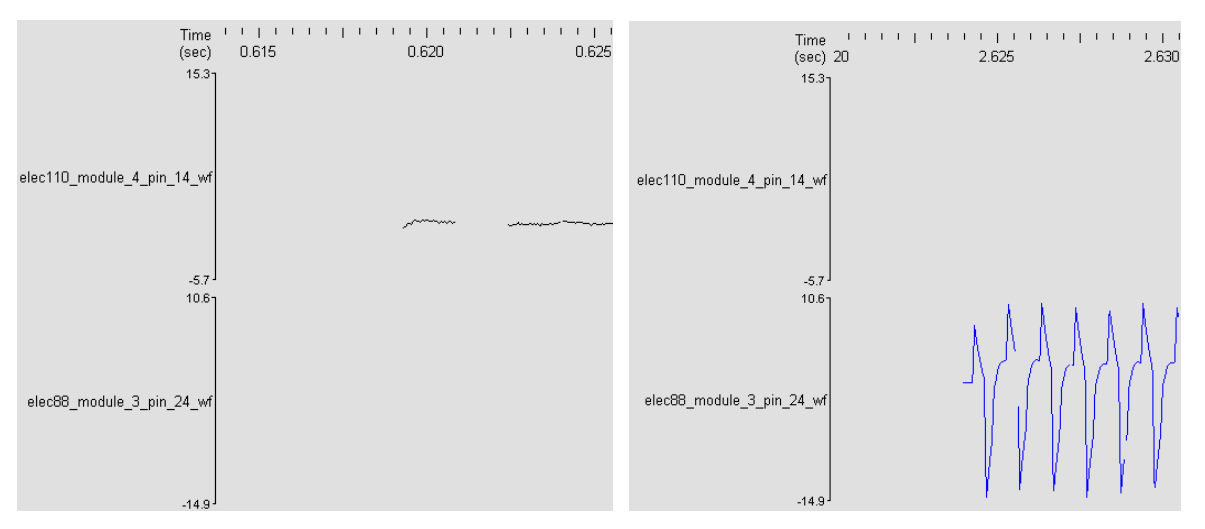


Fig. 3A&B Here the Stim Project was set to stimulate at t=0.619s, however no stimulus waveform was delivered. At t=2.619s the Stim Project was set to record, and again after a 5ms delay a 1kHz bipolar square wave with a 50% duty cycle was applied to the saline medium.

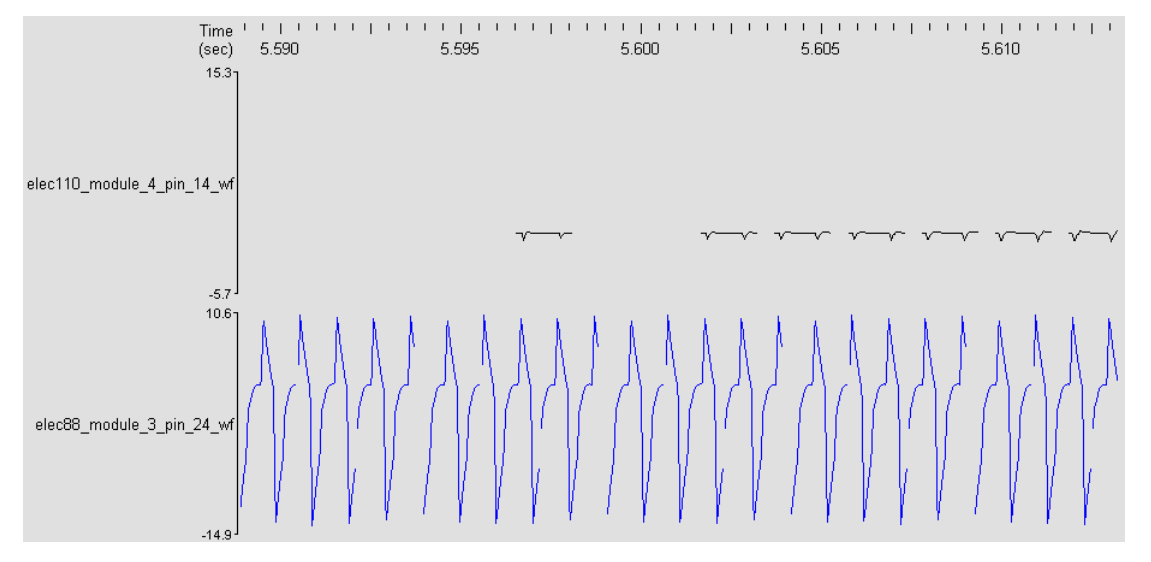


Fig. 3C Even without a stimulus waveform, the Stim Project could not record until t=5.596, a nearly 3 second delay.

Grounding Resistors

One possible solution to the capacitance issue is the inclusion of grounding resistors to give the capacitive charge an avenue to drain to ground. To test this, wires with connected SIPP sockets were soldered to the electrode inputs and amplifier

outputs of two of the channels of the Stim Project switching board (fig. 4). This allowed resistors of different values to be connected to determine the optimal value of resistance to use. The experiment described in the preceding subsection was again repeated with varying resistances; values significantly above $1M\Omega$ had no discernable effect, with values approaching 0.5MΩ making a significant improvement. Requiring such small values is unfortunate however; since many customers will be using electrodes with resistances approaching or surpassing $1M\Omega$, such small grounding resistors will result in a large signal loss. Figure 5 illustrates the effect that $540k\Omega$ grounding resistors have on reducing latency. Here we see that the addition of a grounding resistor to the electrode input of channel 16 (second waveform from the top) reduces the latency by almost a second when compared to channel 18 (third waveform from the top), which does not have a grounding resistor attached. Attaching a grounding resistor to the amplifier output of channel 14 (first waveform from the top) reduces the latency by over two seconds. Figure 5 also includes the waveforms of channels 14, 16 and 18 prior to filtering (the fifth through eighth waveforms from the top), which shows the level of voltage shift created by switching states (note the change in scale), and how that voltage has to return to relatively close to baseline before recording can begin.

Despite the large improvement gained by the addition of grounding resistors the latency is still approximately a second, which is still orders of magnitude above a desirable level so another solution must be applied. Simply reducing the resistance of grounding resistors will too greatly reduce signal strength to be considered.

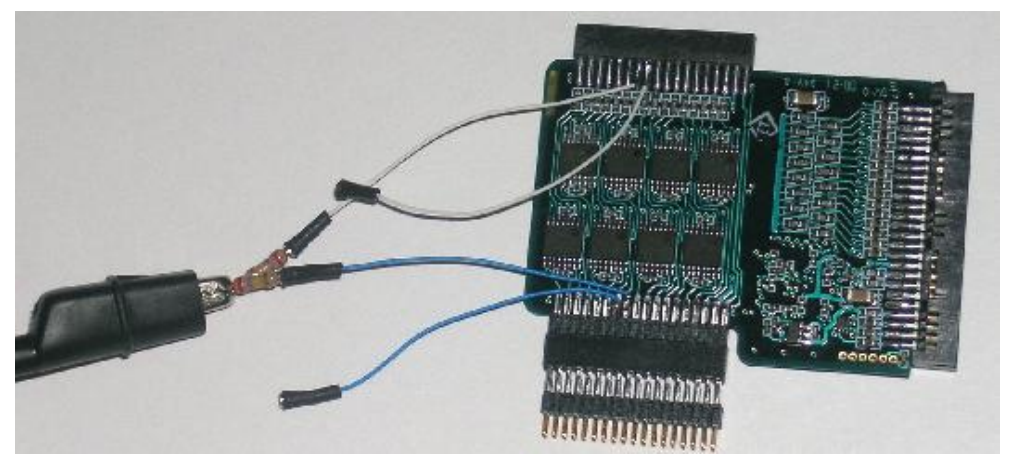


Fig. 4 Wires were soldered the electrode inputs (white) and amplifier outputs (blue) of channels 14 and 16 to allow the connection of grounding resistors.

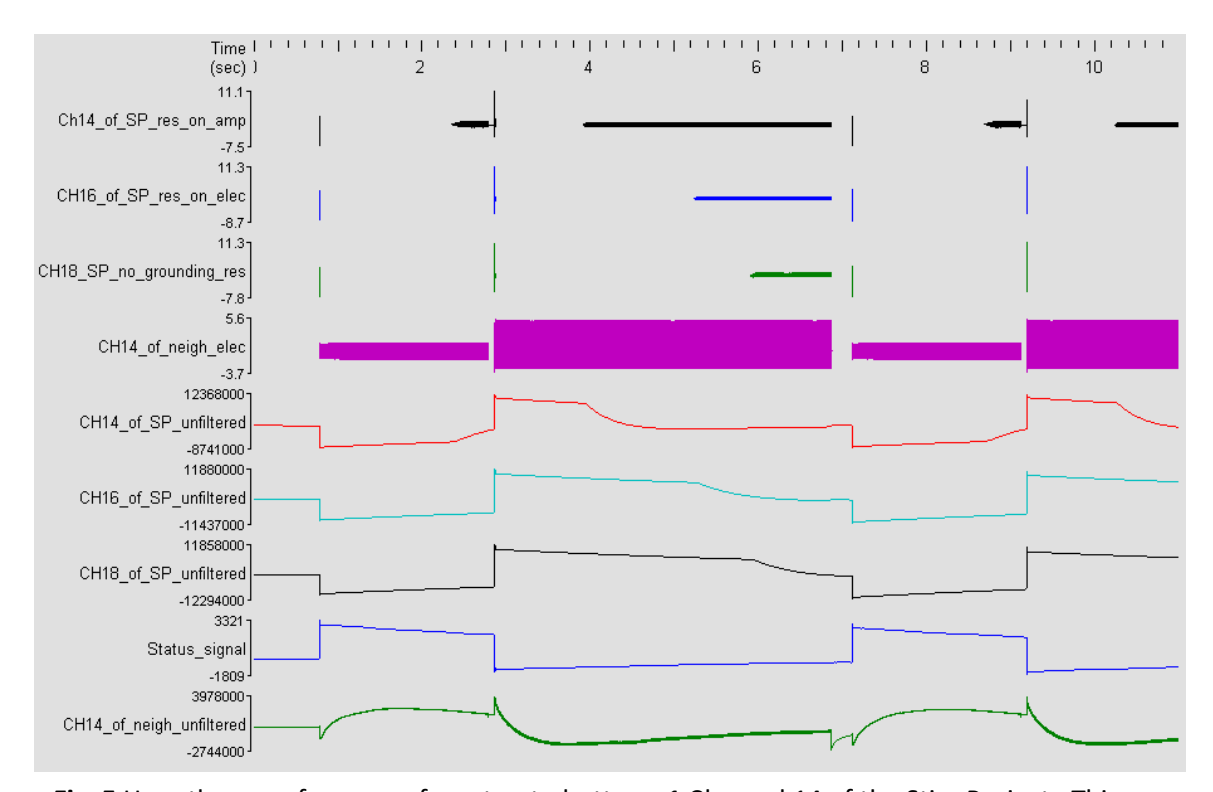


Fig. 5 Here the waveforms are from top to bottom: **1** Channel 14 of the Stim Project. This channel has a 540kΩ grounding resistor connected in parallel with the amplifier output of the switching board. **2** Channel 16 of the Stim Project. This channel has a 540kΩ grounding resistor connected in parallel with the electrode input of the switching board. **3** Channel 18 of the Stim Project. This channel has no grounding resistors attached. **4** A channel not connected through the Stim Project recording from the saline medium. **5-7** Unfiltered outputs of channels 14, 16, and 18 showing the large voltages that are the result fluctuations during switching (note the change in scale, and the correlation between when the voltage begins to return to baseline and when recording is possible). **8** The status signal, high indicates the Stim Project is set to stimulate, low indicates recording is selected. **9** Unfiltered output of the channel not connected to the Stim Project.

Fast Settle Feature of the NSA

Fortunately when the NSA was designed, the responsible engineer (Shane Guillory) predicted that at some point a device for concurrent stimulation and recording would be implemented. As a result he included a fast settling switch that when activated bypasses an RC loop that is used for filtering, providing a shunt for a capacitive charge. This switch can potentially be controlled by software, but since this feature has never been used before that software has not yet been written. To test if the fast settle switch can be used to reduce the recording latency I disconnected the input from the FPGA that controls it on one of the WERM boards of an NSA, and soldered it to a wire that extended outside of the NSA case. The fast settle feature could then be turned on and off by applying 5V or grounding the wire.

The result is shown in figure 6A below. As can be seen in the figure the latency has been virtually eliminated. Figure 6B shows the recording at maximum temporal resolution which reveals the latency to be ~3.5ms. This was repeated with different waveforms and the latency was consistently 3.5ms. However, as can also be seen in figure 6A the stimulus waveform is now being recorded when the Stim Project is set to stimulate. This could be the result of one of two things: it could be another instance the cross-talk issue that we saw previously; or it could be that the switches are not switching properly, or are leaky when open, which would be a severe problem. To test this all switches were tested using a multimeter under the same conditions of the

aforementioned experiment. All switches showed a resistance of 110-150Ω while closed and showed an open circuit while open, so all were switching properly and no leakage was detected. To test whether capacitive coupling was the cause, a constant signal was applied to the saline solution and the Stim Project was repeatedly switched from stimulate to record. As shown in figure 7A, a sinusoidal signal recorded from the saline becomes larger when the Stim Project is set to record. If a leaky switch were present, the opposite would occur since a leaky open switch would have a higher impedance than a closed switch; but in case of capacitive coupling the amplifier side is floating when the switch is open, acting like an antenna, hence the larger signal. Likewise when a square wave is applied as shown in figure 7B, it became heavily distorted when the Stim Project is set to stimulate, likewise negating the possibility of a leaky or malfunctioning switch and indicating cross-talk. In general practice the user would engage the fast settle feature a few milliseconds prior to recording and it would be disengaged prior to stimulation, in which case this cross-talk will not be visible.

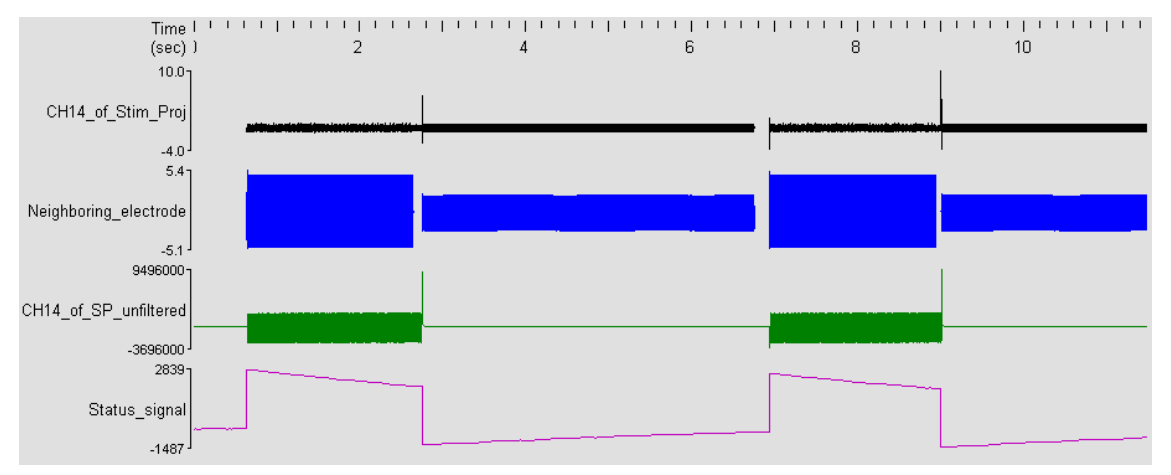


Fig. 6A The result of using the fast-settle feature of the NSA. Notice that the Stim Project can now record immediately after switching, and that the unfiltered waveform no longer has a capacitive voltage that remains after switching. Also notice that cross-talk can now be seen while the Stim Project is stimulating.

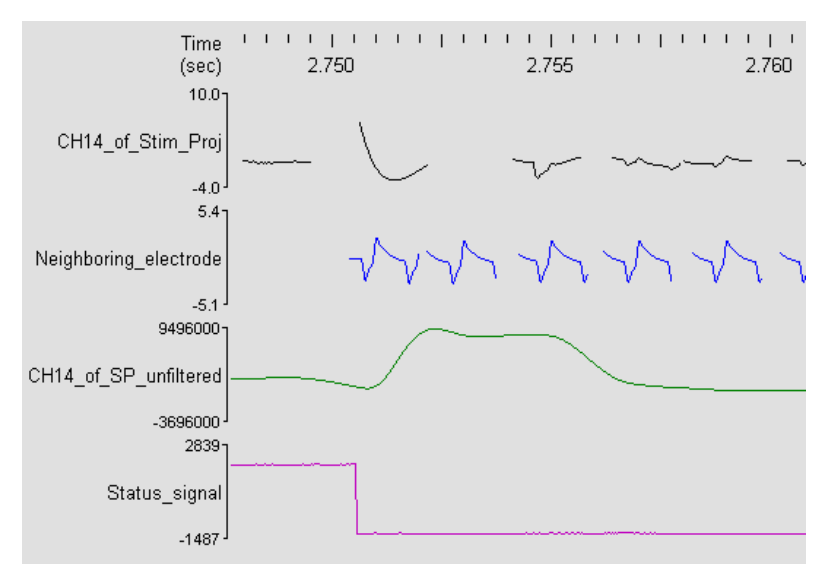


Fig. 6B Zooming in reveals the latency to be ~3.5ms.

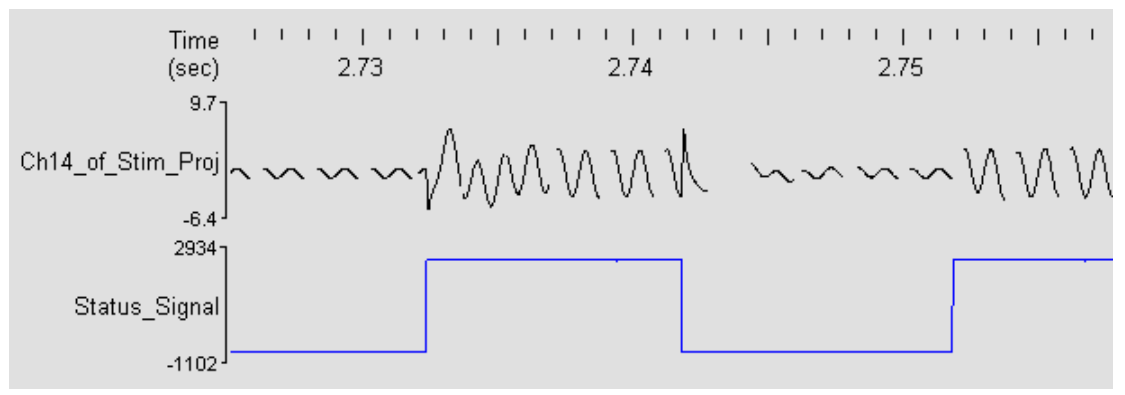


Fig. 7A A constant 1kHz sinusoid is applied to the saline medium. When the Stim Project is set to stimulate the signal gets stronger.

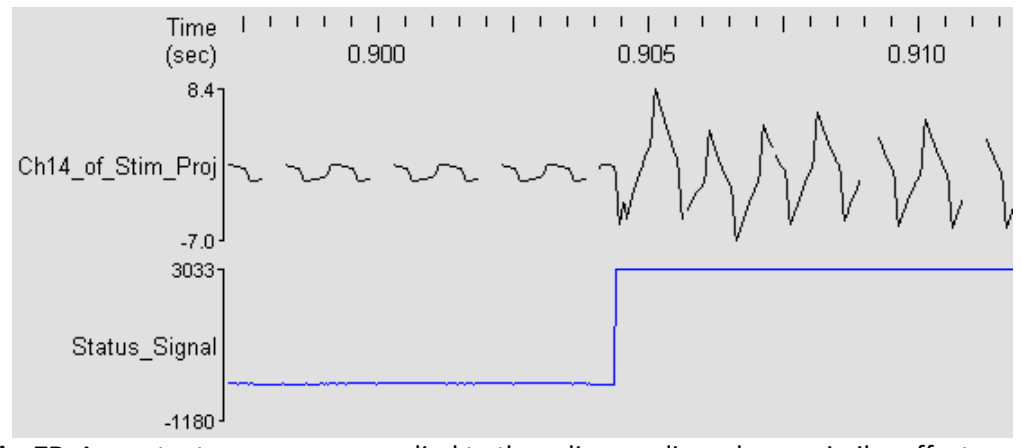


Fig. 7B A constant square wave applied to the saline medium show a similar effect, as well as distortion of the waveform. This demonstrates that the signal is the result of capacitive coupling rather than resistive leakage.

Summary and Suggested Solutions

The Stim Project performed mostly favorably; however before the Stim Project can be a viable product the fast settle feature of the NSA must be made accessible. This could be done either by introduction of new software or altering the current software of the Cerebus system to allow software control (however it appears that this would also involve reprogramming the FPGAs of the NSA's WERM boards, as they are currently programmed to hold the fast settle switch permanently open); or by modifying the NSA so that it included a port for hardware control. Additionally, if the cross-talk could be reduced in some way, possibly by using a grounded metallic casing for the switching board to provide shielding, or by adding a ground plane to the PCB, it would make for a more robust and user-friendly system. One last suggestion not discussed previously in this document would be to reconsider using a serial port to control the system; the delays inherent with serial port transmission could very easily make the fine temporal control that some types of electrophysiological experiments require very frustrating to implement.

Summary

We explored many aspects of multisensory interactions between audition, vision, and somatosensation. Before we could study somatosensation using fMRI, we had to build a tactile stimulator that was compatible with the MRI environment. Chapter one describes the system that was built based on commercially available piezoelectric bending actuators. This system proved to be able to deliver robust, computer-controlled tactile stimulation to several parts of the body simultaneously.

In chapter two we used these piezoelectric stimulators to find responses to tactile stimuli in a visual area responsible for processing motion, area MST. Why would a visual motion area respond to tactile stimulation? One possible answer is that this multimodal integration aids in hand-eye coordination. This contradicts the classical model of dedicated sensory cortices, and supports a model that includes strongly interconnected areas of sensory cortex that includes at least some parallel processing between them.

In chapter three, we used the piezoelectric stimulators to investigate the superior temporal sulcus multisensory area, an area that had previously been shown to be involved in integrating auditory and visual information. STSms overlaps with Wernicke's area, an area that has long been known to be critical for understanding both spoken and written language. Since we demonstrated that STSms also responds to tactile stimulation, could this area be the neural substrate for touch replacement that allows the use of Braille? If so, our finding suggest that touch replacement could also be used to help deaf people understand spoken language by using a device that translates

auditory information into vibrations in the range perceivable by human somatosensation.

In the fourth chapter we used both small and large piezoelectric stimulators to stimulate individual fingers, the hip and the foot of subjects in the MR scanner. We were able to correctly decode touches to individual fingers 68 percent of the time using fMRI multivoxel pattern analysis; this accuracy could approach 100% using a higher resolution method such as intracortical recordings. It would then be possible to provide high-resolution artificial somatosensory percepts, which could be built into a prosthetic hand to provide tactile feedback similar to a biological hand.

In chapter five we conducted psychophysical experiments using the piezoelectric stimulators to investigate the impact of auditory stimuli on the detection and perception of tactile stimuli. We found that auditory stimuli aid in the detection of near-threshold tactile stimuli, and the auditory tones influence the perception of vibrotactile frequency.

Chapter six described how we adapted a commercially available TMS system for use in an MRI scanner. We demonstrated that our system works well enough to detect the hemodynamic response in human subjects while simultaneously delivering TMS pulses. In future experiments, we will disrupt somatosensory cortex with TMS and study how this affects responses to somatosensory stimuli delivered with the piezoelectric stimulators.

The final chapter covered improvements of a system for concurrent microrecording and microstimulation during an industrial internship at Blackrock

Microimplantible Systems. The original system had a delay of recording after stimulating of over two seconds, which made the device effectively unusable as responses to electrical stimulation occur on the order of tens of milliseconds. By introducing a shunt to ground, the delay was reduced to 3.5 milliseconds, providing the temporal resolution needed for studying brain function in human patients and non-human primates.

.

References

- Adolphs R. (2003): Cognitive neuroscience of human social behaviour. Nat Rev Neurosci 4(3):165-78.
- Allison T, Puce A, McCarthy G. (2000): Social perception from visual cues: role of the STS region. Trends Cogn Sci 4(7):267-278.
- Allman BL, Meredith MA. (2007): Multisensory processing in "unimodal" neurons: cross-modal subthreshold auditory effects in cat extrastriate visual cortex. J Neurophysiol 98(1):545-9.
- Amedi A, Jacobson G, Hendler T, Malach R, Zohary E. (2002): Convergence of visual and tactile shape processing in the human lateral occipital complex. Cereb Cortex 12(11):1202-12.
- Amedi A, Malach R, Hendler T, Peled S, Zohary E. (2001): Visuo-haptic object-related activation in the ventral visual pathway. Nat Neurosci 4(3):324-30.
- Argall BD, Saad ZS, Beauchamp MS. (2006): Simplified intersubject averaging on the cortical surface using SUMA. Hum Brain Mapp 27(1):14-27.
- Aristotle. 350 B.C.E. On Sense and the Sensible.: The Internet Classics Archive, translated by J. I. Beare.
- Arthurs OJ, Williams EJ, Carpenter TA, Pickard JD, Boniface SJ. (2000): Linear coupling between functional magnetic resonance imaging and evoked potential amplitude in human somatosensory cortex. Neuroscience 101(4):803-6.
- Backes WH, Mess WH, van Kranen-Mastenbroek V, Reulen JP. (2000): Somatosensory cortex responses to median nerve stimulation: fMRI effects of current amplitude and selective attention. Clin Neurophysiol 111(10):1738-44.
- Barker AT, Jalinous R, Freeston IL. (1985): Non-invasive magnetic stimulation of human motor cortex. Lancet 1(8437):1106-7.
- Baylis GC, Rolls ET, Leonard CM. (1987): Functional subdivisions of the temporal lobe neocortex. J Neurosci 7(2):330-42.
- Beauchamp MS. (2005a): See me, hear me, touch me: multisensory integration in lateral occipital-temporal cortex. Curr Opin Neurobiol 15(2):145-53.
- Beauchamp MS. (2005b): Statistical criteria in FMRI studies of multisensory integration. Neuroinformatics 3(2):93-113.
- Beauchamp MS, Argall BD, Bodurka J, Duyn JH, Martin A. (2004a): Unraveling multisensory integration: patchy organization within human STS multisensory cortex. Nat Neurosci 7(11):1190-2.

- Beauchamp MS, Cox RW, DeYoe EA. (1997): Graded effects of spatial and featural attention on human area MT and associated motion processing areas. J Neurophysiol 78(1):516-20.
- Beauchamp MS, Lee KE, Argall BD, Martin A. (2004b): Integration of auditory and visual information about objects in superior temporal sulcus. Neuron 41(5):809-23.
- Beauchamp MS, Lee KE, Haxby JV, Martin A. (2002): Parallel visual motion processing streams for manipulable objects and human movements. Neuron 34(1):149-59.
- Beauchamp MS, Lee KE, Haxby JV, Martin A. (2003): FMRI responses to video and point-light displays of moving humans and manipulable objects. J Cogn Neurosci 15(7):991-1001.
- Beauchamp MS, Petit L, Ellmore TM, Ingeholm J, Haxby JV. (2001): A parametric fMRI study of overt and covert shifts of visuospatial attention. Neuroimage 14(2):310-21.
- Beauchamp MS, Ro T. (2008): Neural substrates of sound—touch synesthesia after a thalamic lesion. Journal of Neuroscience 28:13696—13702.
- Beauchamp MS, Yasar NE, Frye RE, Ro T. (2008): Touch, sound and vision in human superior temporal sulcus. Neuroimage 41(3):1011-20.
- Beauchamp MS, Yasar NE, Kishan N, Ro T. (2007): Human MST but not MT responds to tactile stimulation. J Neurosci 27(31):8261-7.
- Bertelson P. 1999. Ventriloquism: A case of crossmodal perceptual grouping. In: Gisa Aschersleben E, Talis Bachmann E, et al., editors. Cognitive contributions to the perception of spatial and temporal events.: North-Holland/Elsevier Science Publishers. p xiii, 460.
- Bertelson P, Aschersleben G. (1998): Automatic visual bias of perceived auditory location. Psychonomic Bulletin & Review 5:482-489.
- Bizley JK, Nodal FR, Bajo VM, Nelken I, King AJ. (2007): Physiological and anatomical evidence for multisensory interactions in auditory cortex. Cereb Cortex 17(9):2172-89.
- Blake R, Sobel KV, James TW. (2004): Neural synergy between kinetic vision and touch. Psychol Sci 15(6):397-402.
- Bove M, Diverio M, Pozzo T, Schieppati M. (2001): Neck muscle vibration disrupts steering of locomotion. J Appl Physiol 91(2):581-8.
- Bremmer F, Schlack A, Shah NJ, Zafiris O, Kubischik M, Hoffmann K, Zilles K, Fink GR. (2001):
 Polymodal motion processing in posterior parietal and premotor cortex: a human fMRI study strongly implies equivalencies between humans and monkeys. Neuron 29(1):287-96.
- Brett M, Johnsrude IS, Owen AM. (2002): The problem of functional localization in the human brain. Nat Rev Neurosci 3(3):243-9.

- Briggs RW, Dy-Liacco I, Malcolm MP, Lee H, Peck KK, Gopinath KS, Himes NC, Soltysik DA, Browne P, Tran-Son-Tay R. (2004): A pneumatic vibrotactile stimulation device for fMRI. Magn Reson Med 51(3):640-3.
- Brisben AJ, Hsiao SS, Johnson KO. (1999): Detection of vibration transmitted through an object grasped in the hand. J Neurophysiol 81(4):1548-58.
- Bruce C, Desimone R, Gross CG. (1981): Visual properties of neurons in a polysensory area in superior temporal sulcus of the macaque. J Neurophysiol 46(2):369-84.
- Burton H, McLaren DG, Sinclair RJ. (2006): Reading embossed capital letters: an fMRI study in blind and sighted individuals. Hum Brain Mapp 27(4):325-39.
- Burton H, Sinclair RJ, McLaren DG. (2004): Cortical activity to vibrotactile stimulation: an fMRI study in blind and sighted individuals. Hum Brain Mapp 23(4):210-28.
- Callan DE, Jones JA, Munhall K, Kroos C, Callan AM, Vatikiotis-Bateson E. (2004): Multisensory integration sites identified by perception of spatial wavelet filtered visual speech gesture information. J Cogn Neurosci 16(5):805-16.
- Calvert GA. (2001): Crossmodal processing in the human brain: insights from functional neuroimaging studies. Cereb Cortex 11(12):1110-23.
- Calvert GA, Campbell R, Brammer MJ. (2000): Evidence from functional magnetic resonance imaging of crossmodal binding in the human heteromodal cortex. Curr Biol 10(11):649-57.
- Celebrini S, Newsome WT. (1995): Microstimulation of extrastriate area MST influences performance on a direction discrimination task. J Neurophysiol 73(2):437-48.
- Chang C-C, Lin C-J. (2001): LIBSVM: a library for support vector machines.
- Clavagnier S, Falchier A, Kennedy H. (2004): Long-distance feedback projections to area V1: implications for multisensory integration, spatial awareness, and visual consciousness. Cogn Affect Behav Neurosci 4(2):117-26.
- Clemo HR, Allman BL, Donlan MA, Meredith MA. (2007): Sensory and multisensory representations within the cat rostral suprasylvian cortex. J Comp Neurol 503(1):110-27.
- Corbetta M, Akbudak E, Conturo TE, Snyder AZ, Ollinger JM, Drury HA, Linenweber MR, Petersen SE, Raichle ME, Van Essen DC and others. (1998): A common network of functional areas for attention and eye movements. Neuron 21(4):761-73.
- Cox DD, Savoy RL. (2003): Functional magnetic resonance imaging (fMRI) "brain reading": detecting and classifying distributed patterns of fMRI activity in human visual cortex. Neuroimage 19(2 Pt 1):261-70.

- Cox RW. (1996): AFNI: software for analysis and visualization of functional magnetic resonance neuroimages. Comput Biomed Res 29(3):162-73.
- d'Avossa G, Tosetti M, Crespi S, Biagi L, Burr DC, Morrone MC. (2007): Spatiotopic selectivity of BOLD responses to visual motion in human area MT. Nat Neurosci 10(2):249-55.
- Dahl CD, Logothetis N, Kayser C. Functional Organization of Responses in the Polysensory Temporal Region (STP) in the Macaque Monkey; 2007. p 713-714.
- Dale AM. (1999): Optimal experimental design for event-related fMRI. Hum Brain Mapp 8(2-3):109-14.
- Deuchert M, Ruben J, Schwiemann J, Meyer R, Thees S, Krause T, Blankenburg F, Villringer K, Kurth R, Curio G and others. (2002): Event-related fMRI of the somatosensory system using electrical finger stimulation. Neuroreport 13(3):365-9.
- Dickson J, Drury H, Van Essen DC. (2001): 'The surface management system' (SuMS) database: a surface-based database to aid cortical surface reconstruction, visualization and analysis. Philos Trans R Soc Lond B Biol Sci 356(1412):1277-92.
- Disbrow E, Roberts T, Krubitzer L. (2000): Somatotopic organization of cortical fields in the lateral sulcus of Homo sapiens: evidence for SII and PV. J Comp Neurol 418(1):1-21.
- Disbrow E, Roberts T, Poeppel D, Krubitzer L. (2001): Evidence for interhemispheric processing of inputs from the hands in human S2 and PV. J Neurophysiol 85(5):2236-44.
- Downar J, Crawley AP, Mikulis DJ, Davis KD. (2000): A multimodal cortical network for the detection of changes in the sensory environment. Nat Neurosci 3(3):277-83.
- Driver J, Noesselt T. (2008): Multisensory interplay reveals crossmodal influences on 'sensory-specific' brain regions, neural responses, and judgments. Neuron 57(1):11-23.
- Driver J, Spence C. (1998a): Attention and the crossmodal construction of space. Trends in Cognitive Sciences 2(7):254-262.
- Driver J, Spence C. (1998b): Crossmodal attention. Current Opinion in Neurobiology 8:245-253.
- Dumoulin SO, Bittar RG, Kabani NJ, Baker CL, Jr., Le Goualher G, Bruce Pike G, Evans AC. (2000): A new anatomical landmark for reliable identification of human area V5/MT: a quantitative analysis of sulcal patterning. Cereb Cortex 10(5):454-63.
- Eickhoff SB, Amunts K, Mohlberg H, Zilles K. (2006a): The human parietal operculum. II. Stereotaxic maps and correlation with functional imaging results. Cereb Cortex 16(2):268-79.
- Eickhoff SB, Grefkes C, Zilles K, Fink GR. (2007): The somatotopic organization of cytoarchitectonic areas on the human parietal operculum. Cereb Cortex 17(8):1800-11.

- Eickhoff SB, Schleicher A, Zilles K, Amunts K. (2006b): The human parietal operculum. I. Cytoarchitectonic mapping of subdivisions. Cereb Cortex 16(2):254-67.
- Eickhoff SB, Stephan KE, Mohlberg H, Grefkes C, Fink GR, Amunts K, Zilles K. (2005): A new SPM toolbox for combining probabilistic cytoarchitectonic maps and functional imaging data. Neuroimage 25(4):1325-35.
- Ernst MO, Banks MS, Bulthoff HH. (2000): Touch can change visual slant perception. Nat Neurosci 3(1):69-73.
- Falchier A, Clavagnier S, Barone P, Kennedy H. (2002): Anatomical evidence of multimodal integration in primate striate cortex. J Neurosci 22(13):5749-59.
- Farne A, Ladavas E. (2002): Auditory peripersonal space in humans. Journal of Cognitive Neuroscience 14(7):1030-1043.
- Felleman DJ, Van Essen DC. (1991): Distributed hierarchical processing in the primate cerebral cortex. Cereb Cortex 1(1):1-47.
- Fischl B, Sereno MI, Dale AM. (1999): Cortical surface-based analysis. II: Inflation, flattening, and a surface-based coordinate system. Neuroimage 9(2):195-207.
- Fischl B, van der Kouwe A, Destrieux C, Halgren E, Segonne F, Salat DH, Busa E, Seidman LJ, Goldstein J, Kennedy D and others. (2004): Automatically parcellating the human cerebral cortex. Cereb Cortex 14(1):11-22.
- Foxe JJ, Wylie GR, Martinez A, Schroeder CE, Javitt DC, Guilfoyle D, Ritter W, Murray MM. (2002): Auditory-somatosensory multisensory processing in auditory association cortex: an fMRI study. J Neurophysiol 88(1):540-3.
- Georgopoulos AP, Schwartz AB, Kettner RE. (1986): Neuronal population coding of movement direction. Science 233(4771):1416-9.
- Gescheider GA, Barton WG, Bruce MR, Goldberg JH, Greenspan MJ. (1969): Effects of simultaneous auditory stimulation on the detection of tactile stimuli. J Exp Psychol 81(1):120-5.
- Geyer S, Schleicher A, Zilles K. (1999): Areas 3a, 3b, and 1 of human primary somatosensory cortex. Neuroimage 10(1):63-83.
- Ghazanfar AA, Schroeder CE. (2006): Is neocortex essentially multisensory? Trends Cogn Sci 10(6):278-85.
- Gillmeister H, Eimer M. (2007): Tactile enhancement of auditory detection and perceived loudness. Brain Res 1160:58-68.

- Gizewski ER, Koeze O, Uffmann K, de Greiff A, Ladd ME, Forsting M. (2005): Cerebral activation using a MR-compatible piezoelectric actuator with adjustable vibration frequencies and in vivo wave propagation control. Neuroimage 24(3):723-30.
- Glover GH. (1999): Deconvolution of impulse response in event-related BOLD fMRI. Neuroimage 9(4):416-29.
- Goebel R, Khorram-Sefat D, Muckli L, Hacker H, Singer W. (1998): The constructive nature of vision: direct evidence from functional magnetic resonance imaging studies of apparent motion and motion imagery. Eur J Neurosci 10(5):1563-73.
- Golaszewski SM, Siedentopf CM, Baldauf E, Koppelstaetter F, Eisner W, Unterrainer J, Guendisch GM, Mottaghy FM, Felber SR. (2002): Functional magnetic resonance imaging of the human sensorimotor cortex using a novel vibrotactile stimulator. Neuroimage 17(1):421-30.
- Graham SJ, Staines WR, Nelson A, Plewes DB, McIlroy WE. (2001): New devices to deliver somatosensory stimuli during functional MRI. Magn Reson Med 46(3):436-42.
- Grefkes C, Fink GR. (2005): The functional organization of the intraparietal sulcus in humans and monkeys. J Anat 207(1):3-17.
- Grefkes C, Geyer S, Schormann T, Roland P, Zilles K. (2001): Human somatosensory area 2: observer-independent cytoarchitectonic mapping, interindividual variability, and population map. Neuroimage 14(3):617-31.
- Grill-Spector K, Kourtzi Z, Kanwisher N. (2001): The lateral occipital complex and its role in object recognition. Vision Res 41(10-11):1409-22.
- Grill-Spector K, Malach R. (2004): The human visual cortex. Annu Rev Neurosci 27:649-77.
- Grossman ED, Blake R. (2002): Brain Areas Active during Visual Perception of Biological Motion. Neuron 35(6):1167-75.
- Guest S, Catmur C, Lloyd D, Spence C. (2002): Audiotactile interactions in roughness perception. Exp Brain Res 146(2):161-71.
- Hackett TA, De La Mothe LA, Ulbert I, Karmos G, Smiley J, Schroeder CE. (2007): Multisensory convergence in auditory cortex, II. Thalamocortical connections of the caudal superior temporal plane. J Comp Neurol 502(6):924-52.
- Hagen MC, Franzen O, McGlone F, Essick G, Dancer C, Pardo JV. (2002): Tactile motion activates the human middle temporal/V5 (MT/V5) complex. Eur J Neurosci 16(5):957-64.
- Halpern DL, Blake R, Hillenbrand J. (1986): Psychoacoustics of a chilling sound. Percept Psychophys 39(2):77-80.

- Harrington GS, Wright CT, Downs JH, 3rd. (2000): A new vibrotactile stimulator for functional MRI. Hum Brain Mapp 10(3):140-5.
- Hauser MD, Konishi M. 1999. The Design of Animal Communication. Cambridge, MA: MIT Press.
- Haxby JV, Gobbini MI, Furey ML, Ishai A, Schouten JL, Pietrini P. (2001): Distributed and overlapping representations of faces and objects in ventral temporal cortex. Science 293(5539):2425-30.
- Haynes JD, Rees G. (2005a): Predicting the orientation of invisible stimuli from activity in human primary visual cortex. Nat Neurosci 8(5):686-91.
- Haynes JD, Rees G. (2005b): Predicting the stream of consciousness from activity in human visual cortex. Curr Biol 15(14):1301-7.
- Haynes JD, Rees G. (2006): Decoding mental states from brain activity in humans. Nat Rev Neurosci 7(7):523-34.
- Heeger DJ, Ress D. (2002): What does fMRI tell us about neuronal activity? Nat Rev Neurosci 3(2):142-51.
- Hein G, Doehrmann O, Muller NG, Kaiser J, Muckli L, Naumer MJ. (2007): Object familiarity and semantic congruency modulate responses in cortical audiovisual integration areas. J Neurosci 27(30):7881-7.
- Hikosaka K, Iwai E, Saito H, Tanaka K. (1988): Polysensory properties of neurons in the anterior bank of the caudal superior temporal sulcus of the macaque monkey. J Neurophysiol 60(5):1615-37.
- Hotting K, Roder B. (2004): Hearing cheats touch, but less in congenitally blind than in sighted individuals. Psychol Sci 15(1):60-4.
- Hubel DH, Wiesel TN. (1962): Receptive fields, binocular interaction and functional architecture in the cat's visual cortex. J Physiol 160:106-54.
- Huk AC, Dougherty RF, Heeger DJ. (2002): Retinotopy and functional subdivision of human areas MT and MST. J Neurosci 22(16):7195-205.
- Iguchi Y, Hoshi Y, Nemoto M, Taira M, Hashimoto I. (2007): Co-activation of the secondary somatosensory and auditory cortices facilitates frequency discrimination of vibrotactile stimuli. Neuroscience 148(2):461-72.
- Ilg UJ, Schumann S. (2007): Primate area MST-l is involved in the generation of goal-directed eye and hand movements. J Neurophysiol 97(1):761-71.
- Ingeholm JE, Dold GR, Pfeffer LE, Ide D, Goldstein SR, Johnson KO, Van Boven RW. (2006): The Helix: A multi-modal tactile stimulator for human functional neuroimaging. J Neurosci Methods 155(2):217-23.

- Ishai A, Ungerleider LG, Haxby JV. (2000): Distributed neural systems for the generation of visual images. Neuron 28(3):979-90.
- Joachims T. 1999. Making large-scale SVM learning practical. In: Scholkopf B, Burges C, Smola A, editors. Advances in kernel methods--support vector learning. Cambridge, MA: MIT Press.
- Johnson RM, Burton PC, Ro T. (2006): Visually induced feelings of touch. Brain Research 1073-1074:398-406.
- Jousmaki V, Hari R. (1998): Parchment-skin illusion: sound-biased touch. Curr Biol 8(6):R190.
- Kaas JH, Nelson RJ, Sur M, Lin CS, Merzenich MM. (1979): Multiple representations of the body within the primary somatosensory cortex of primates. Science 204(4392):521-3.
- Kamitani Y, Tong F. (2005): Decoding the visual and subjective contents of the human brain. Nat Neurosci 8(5):679-85.
- Kamitani Y, Tong F. (2006): Decoding seen and attended motion directions from activity in the human visual cortex. Curr Biol 16(11):1096-102.
- Kanwisher N, McDermott J, Chun MM. (1997): The fusiform face area: a module in human extrastriate cortex specialized for face perception. J Neurosci 17(11):4302-11.
- Karnath HO, Sievering D, Fetter M. (1994): The interactive contribution of neck muscle proprioception and vestibular stimulation to subjective "straight ahead" orientation in man. Exp Brain Res 101(1):140-6.
- Kay KN, Naselaris T, Prenger RJ, Gallant JL. (2008): Identifying natural images from human brain activity. Nature 452(7185):352-5.
- Kayser C, Petkov CI, Augath M, Logothetis NK. (2005): Integration of touch and sound in auditory cortex. Neuron 48(2):373-84.
- Kell CA, von Kriegstein K, Rosler A, Kleinschmidt A, Laufs H. (2005): The sensory cortical representation of the human penis: revisiting somatotopy in the male homunculus. J Neurosci 25(25):5984-7.
- Kennett S, Taylor-Clarke M, Haggard P. (2001): Noninformative vision improves the spatial resolution of touch in humans. Current Biology 11(15):1188-1191.
- Komatsu H, Wurtz RH. (1988): Relation of cortical areas MT and MST to pursuit eye movements.

 I. Localization and visual properties of neurons. J Neurophysiol 60(2):580-603.
- Kourtzi Z, Bulthoff HH, Erb M, Grodd W. (2002): Object-selective responses in the human motion area MT/MST. Nat Neurosci 5(1):17-8.

- Kriegeskorte N, Bandettini P. (2007): Combining the tools: activation- and information-based fMRI analysis. Neuroimage 38(4):666-8.
- Kriegeskorte N, Goebel R, Bandettini P. (2006): Information-based functional brain mapping. Proc Natl Acad Sci U S A 103(10):3863-8.
- Kurth R, Villringer K, Mackert BM, Schwiemann J, Braun J, Curio G, Villringer A, Wolf KJ. (1998): fMRI assessment of somatotopy in human Brodmann area 3b by electrical finger stimulation. Neuroreport 9(2):207-12.
- LaConte S, Strother S, Cherkassky V, Anderson J, Hu X. (2005): Support vector machines for temporal classification of block design fMRI data. Neuroimage 26(2):317-29.
- LaConte SM, Peltier SJ, Hu XP. (2007): Real-time fMRI using brain-state classification. Hum Brain Mapp 28(10):1033-44.
- Lakatos P, Chen CM, O'Connell MN, Mills A, Schroeder CE. (2007): Neuronal oscillations and multisensory interaction in primary auditory cortex. Neuron 53(2):279-92.
- Laurienti PJ, Perrault TJ, Stanford TR, Wallace MT, Stein BE. (2005): On the use of superadditivity as a metric for characterizing multisensory integration in functional neuroimaging studies. Exp Brain Res 166(3-4):289-97.
- Leung YY, Bensmaia SJ, Hsiao SS, Johnson KO. (2005): Time-course of vibratory adaptation and recovery in cutaneous mechanoreceptive afferents. J Neurophysiol 94(5):3037-45.
- Lewis JW, Van Essen DC. (2000a): Corticocortical connections of visual, sensorimotor, and multimodal processing areas in the parietal lobe of the macaque monkey. J Comp Neurol 428(1):112-37.
- Lewis JW, Van Essen DC. (2000b): Mapping of architectonic subdivisions in the macaque monkey, with emphasis on parieto-occipital cortex. J Comp Neurol 428(1):79-111.
- Lim SH, Dinner DS, Pillay PK, Luders H, Morris HH, Klem G, Wyllie E, Awad IA. (1994): Functional anatomy of the human supplementary sensorimotor area: results of extraoperative electrical stimulation. Electroencephalogr Clin Neurophysiol 91(3):179-93.
- Logothetis NK, Pauls J, Augath M, Trinath T, Oeltermann A. (2001): Neurophysiological investigation of the basis of the fMRI signal. Nature 412(6843):150-7.
- Macaluso E, Driver J. (2005): Multisensory spatial interactions: a window onto functional integration in the human brain. Trends Neurosci 28(5):264-71.
- Macaluso E, George N, Dolan R, Spence C, Driver J. (2004): Spatial and temporal factors during processing of audiovisual speech: a PET study. Neuroimage 21(2):725-32.

- Malach R, Reppas JB, Benson RR, Kwong KK, Jiang H, Kennedy WA, Ledden PJ, Brady TJ, Rosen BR, Tootell RB. (1995): Object-related activity revealed by functional magnetic resonance imaging in human occipital cortex. Proc Natl Acad Sci U S A 92(18):8135-9.
- Marconi B, Genovesio A, Battaglia-Mayer A, Ferraina S, Squatrito S, Molinari M, Lacquaniti F, Caminiti R. (2001): Eye-hand coordination during reaching. I. Anatomical relationships between parietal and frontal cortex. Cereb Cortex 11(6):513-27.
- Milad MR, Vidal-Gonzalez I, Quirk GJ. (2004): Electrical stimulation of medial prefrontal cortex reduces conditioned fear in a temporally specific manner. Behav Neurosci 118(2):389-94.
- Miller LM, D'Esposito M. (2005): Perceptual fusion and stimulus coincidence in the cross-modal integration of speech. J Neurosci 25(25):5884-93.
- Mitchel T, Hutchinson R, Niculescu R, Pereira F, Wang X. (2004): Learning to Decode Cognitive States from Brain Images. Machine Learning(57):145-175.
- Murasugi CM, Salzman CD, Newsome WT. (1993): Microstimulation in visual area MT: effects of varying pulse amplitude and frequency. J Neurosci 13(4):1719-29.
- Murphey DK, Yoshor D, Beauchamp MS. (2008): Perception matches selectivity in the human anterior color center. Curr Biol 18(3):216-20.
- Murray MM, Molholm S, Michel CM, Heslenfeld DJ, Ritter W, Javitt DC, Schroeder CE, Foxe JJ. (2005): Grabbing your ear: rapid auditory-somatosensory multisensory interactions in low-level sensory cortices are not constrained by stimulus alignment. Cereb Cortex 15(7):963-74.
- Navarra J, Soto-Faraco S, Spence C. (2007): Adaptation to audiotactile asynchrony. Neurosci Lett 413(1):72-6.
- Nelissen K, Vanduffel W, Orban GA. (2006): Charting the lower superior temporal region, a new motion-sensitive region in monkey superior temporal sulcus. J Neurosci 26(22):5929-47.
- Nelson RJ, Sur M, Felleman DJ, Kaas JH. (1980): Representations of the body surface in postcentral parietal cortex of Macaca fascicularis. J Comp Neurol 192(4):611-43.
- Nichols T, Brett M, Andersson J, Wager T, Poline JB. (2005): Valid conjunction inference with the minimum statistic. Neuroimage 25(3):653-60.
- Noesselt T, Rieger JW, Schoenfeld MA, Kanowski M, Hinrichs H, Heinze HJ, Driver J. (2007): Audiovisual temporal correspondence modulates human multisensory superior temporal sulcus plus primary sensory cortices. J Neurosci 27(42):11431-41.
- Norman KA, Polyn SM, Detre GJ, Haxby JV. (2006): Beyond mind-reading: multi-voxel pattern analysis of fMRI data. Trends Cogn Sci 10(9):424-30.

- O'Craven KM, Kanwisher N. (2000): Mental imagery of faces and places activates corresponding stiimulus-specific brain regions. J Cogn Neurosci 12(6):1013-23.
- O'Craven KM, Rosen BR, Kwong KK, Treisman A, Savoy RL. (1997): Voluntary attention modulates fMRI activity in human MT-MST. Neuron 18(4):591-8.
- Occelli V, Spence C, Zampini M. (2008): The effect of sound intensity on the audiotactile crossmodal dynamic capture effect. Exp Brain Res.
- Ogawa S, Lee TM. (1990): Magnetic resonance imaging of blood vessels at high fields: in vivo and in vitro measurements and image simulation. Magn Reson Med 16(1):9-18.
- Ogawa S, Lee TM, Kay AR, Tank DW. (1990): Brain magnetic resonance imaging with contrast dependent on blood oxygenation. Proc Natl Acad Sci U S A 87(24):9868-72.
- Ogawa S, Menon RS, Kim SG, Ugurbil K. (1998): On the characteristics of functional magnetic resonance imaging of the brain. Annu Rev Biophys Biomol Struct 27:447-74.
- Ozcan M, Baumgartner U, Vucurevic G, Stoeter P, Treede RD. (2005): Spatial resolution of fMRI in the human parasylvian cortex: comparison of somatosensory and auditory activation. Neuroimage 25(3):877-87.
- Padberg J, Seltzer B, Cusick CG. (2003): Architectonics and cortical connections of the upper bank of the superior temporal sulcus in the rhesus monkey: an analysis in the tangential plane. J Comp Neurol 467(3):418-34.
- Pauling L, Coryell CD. (1936): The Magnetic Properties and Structure of Hemoglobin, Oxyhemoglobin and Carbonmonoxyhemoglobin. Proc Natl Acad Sci U S A 22(4):210-6.
- Pavani F, Spence C, Driver J. (2000): Visual capture of touch: out-of-the-body experiences with rubber gloves. Psychol Sci 11(5):353-9.
- Peelen MV, Wiggett AJ, Downing PE. (2006): Patterns of fMRI activity dissociate overlapping functional brain areas that respond to biological motion. Neuron 49(6):815-22.
- Peltier S, Stilla R, Mariola E, LaConte S, Hu X, Sathian K. (2007): Activity and effective connectivity of parietal and occipital cortical regions during haptic shape perception. Neuropsychologia 45(3):476-83.
- Perrault TJ, Jr., Vaughan JW, Stein BE, Wallace MT. (2005): Superior colliculus neurons use distinct operational modes in the integration of multisensory stimuli. J Neurophysiol 93(5):2575-86.
- Petit L, Beauchamp MS. (2003): Neural basis of visually guided head movements studied with fMRI. J Neurophysiol 89(5):2516-27.

- Platt J, Cristiani N, Shawe-Taylor J. 2000. Large margin DAGs for multiclass classification. In: Solla S, Leen T, Muller K-R, editors. Advances in neural information processing. Cambridge, MA: MIT Press. p 547-553.
- Posner MI. (1980): Orienting of attention. Quarterly Journal of Experimental Psychology 32:3-25.
- Price CJ. (2000): The anatomy of language: contributions from functional neuroimaging. J Anat 197 Pt 3:335-59.
- Raichle ME, MacLeod AM, Snyder AZ, Powers WJ, Gusnard DA, Shulman GL. (2001): A default mode of brain function. Proc Natl Acad Sci U S A 98(2):676-82.
- Raij T, Uutela K, Hari R. (2000): Audiovisual integration of letters in the human brain. Neuron 28(2):617-25.
- Recanzone GH. (1998): Rapidly induced auditory plasticity: the ventriloquism aftereffect. Proc Natl Acad Sci U S A 95(3):869-75.
- Ricciardi E, Vanello N, Sani L, Gentili C, Scilingo EP, Landini L, Guazzelli M, Bicchi A, Haxby JV, Pietrini P. (2007): The effect of visual experience on the development of functional architecture in hMT+. Cereb Cortex 17(12):2933-9.
- Ro T, Farne A, Johnson RM, Wedeen V, Chu Z, Wang ZJ, Hunter JV, Beauchamp MS. (2007): Feeling sounds after a thalamic lesion. Annals of Neurology 62:433-441.
- Ro T, Wallace R, Hagedorn J, Farnè A, Pienkos E. (2004): Visual enhancing of tactile perception in posterior parietal cortex. Journal of Cognitive Neuroscience 16:24-30.
- Rock I, Mack A, Adams L, Hill AL. (1965): Adaptation to contradictory information from vision and touch. Psychonomic Science 3(10):435-436.
- Rock I, Victor J. (1964): Vision and touch: An experimentally created conflict between the two senses. Science 143:594-596.
- Rockland KS, Ojima H. (2003): Multisensory convergence in calcarine visual areas in macaque monkey. Int J Psychophysiol 50(1-2):19-26.
- Roy CS, Sherrington CS. (1890): On the Regulation of the Blood-supply of the Brain. J Physiol 11(1-2):85-158 17.
- Ruben J, Schwiemann J, Deuchert M, Meyer R, Krause T, Curio G, Villringer K, Kurth R, Villringer A. (2001): Somatotopic organization of human secondary somatosensory cortex. Cereb Cortex 11(5):463-73.
- Rushworth MF, Behrens TE, Johansen-Berg H. (2006): Connection patterns distinguish 3 regions of human parietal cortex. Cereb Cortex 16(10):1418-30.

- Saito DN, Yoshimura K, Kochiyama T, Okada T, Honda M, Sadato N. (2005): Cross-modal binding and activated attentional networks during audio-visual speech integration: a functional MRI study. Cereb Cortex 15(11):1750-60.
- Sathian K, Zangaladze A, Hoffman JM, Grafton ST. (1997): Feeling with the mind's eye. Neuroreport 8(18):3877-81.
- Saxe R, Brett M, Kanwisher N. (2006): Divide and conquer: a defense of functional localizers. Neuroimage 30(4):1088-96; discussion 1097-9.
- Schroeder CE, Foxe J. (2005): Multisensory contributions to low-level, 'unisensory' processing. Curr Opin Neurobiol 15(4):454-8.
- Schroeder CE, Lakatos P, Kajikawa Y, Partan S, Puce A. (2008): Neuronal oscillations and visual amplification of speech. Trends Cogn Sci 12(3):106-13.
- Schroeder CE, Lindsley RW, Specht C, Marcovici A, Smiley JF, Javitt DC. (2001): Somatosensory input to auditory association cortex in the macaque monkey. J Neurophysiol 85(3):1322-7.
- Schurmann M, Caetano G, Hlushchuk Y, Jousmaki V, Hari R. (2006): Touch activates human auditory cortex. Neuroimage 30(4):1325-31.
- Sekiyama K, Kanno I, Miura S, Sugita Y. (2003): Auditory-visual speech perception examined by fMRI and PET. Neurosci Res 47(3):277-87.
- Seltzer B, Cola MG, Gutierrez C, Massee M, Weldon C, Cusick CG. (1996): Overlapping and nonoverlapping cortical projections to cortex of the superior temporal sulcus in the rhesus monkey: double anterograde tracer studies. J Comp Neurol 370(2):173-90.
- Sereno MI, Huang RS. (2006): A human parietal face area contains aligned head-centered visual and tactile maps. Nat Neurosci 9(10):1337-43.
- Serino A, Bassolino M, Farne A, Ladavas E. (2007): Extended multisensory space in blind cane users. Psychol Sci 18(7):642-8.
- Sherrick CE. 1976. The antagonisms of hearing and touch. In: Hirsh SK, Eldredge, D.H., Hirsh, I.J., Silverman, S.R., editor. Hearing and Davis: Essays honoring Hallowell Davis. St. Louis, MO: Washington University Press. p 149-158.
- Simmons WK, Bellgowan PS, Martin A. (2007): Measuring selectivity in fMRI data. Nat Neurosci 10(1):4-5.
- Smiley JF, Hackett TA, Ulbert I, Karmas G, Lakatos P, Javitt DC, Schroeder CE. (2007):

 Multisensory convergence in auditory cortex, I. Cortical connections of the caudal superior temporal plane in macaque monkeys. J Comp Neurol 502(6):894-923.

- Spence C, Driver J. (1997): Audiovisual links in exogenous covert spatial orienting. Percept Psychophys 59(1):1-22.
- Spence C, Nicholls MER, Gillespie N, Driver J. (1998): Cross-modal links in exogenous covert spatial orienting between touch, audition, and vision. Perception & Psychophysics 60:544-557.
- Stein BE, Meredith MA. 1993. The Merging of the Senses: MIT Press.
- Stippich C, Hofmann R, Kapfer D, Hempel E, Heiland S, Jansen O, Sartor K. (1999): Somatotopic mapping of the human primary somatosensory cortex by fully automated tactile stimulation using functional magnetic resonance imaging. Neurosci Lett 277(1):25-8.
- Tipper SP, Lloyd D, Shorland B, Dancer C, Howard LA, McGlone F. (1998): Vision influences tactile perception without proprioceptive orienting. Neuroreport: An International Journal for the Rapid Communication of Research in Neuroscience 9(8):1741-1744.
- Tipper SP, Phillips N, Dancer C, Lloyd D, Howard LA, McGlone F. (2001): Vision influences tactile perception at body sites that cannot be viewed directly. Exp Brain Res 139(2):160-7.
- Tommerdahl M, Hester KD, Felix ER, Hollins M, Favorov OV, Quibrera PM, Whitsel BL. (2005): Human vibrotactile frequency discriminative capacity after adaptation to 25 Hz or 200 Hz stimulation. Brain Res 1057(1-2):1-9.
- Tootell RB, Reppas JB, Kwong KK, Malach R, Born RT, Brady TJ, Rosen BR, Belliveau JW. (1995): Functional analysis of human MT and related visual cortical areas using magnetic resonance imaging. J Neurosci 15(4):3215-30.
- Treue S, Maunsell JH. (1996): Attentional modulation of visual motion processing in cortical areas MT and MST. Nature 382(6591):539-41.
- van Atteveldt N, Formisano E, Goebel R, Blomert L. (2004): Integration of letters and speech sounds in the human brain. Neuron 43(2):271-82.
- van Atteveldt NM, Formisano E, Blomert L, Goebel R. (2007): The effect of temporal asynchrony on the multisensory integration of letters and speech sounds. Cereb Cortex 17(4):962-74.
- Van Essen DC. (2004): Surface-based approaches to spatial localization and registration in primate cerebral cortex. Neuroimage 23 Suppl 1:S97-107.
- Vroomen J, Gelder Bd. (2000): Sound enhances visual perception: Cross-modal effects of auditory organization on vision. Journal of Experimental Psychology: Human Perception & Performance 26(5):1583-1590.
- Wagner AD, Schacter DL, Rotte M, Koutstaal W, Maril A, Dale AM, Rosen BR, Buckner RL. (1998): Building memories: remembering and forgetting of verbal experiences as predicted by brain activity. Science 281(5380):1188-91.

- Weisser V, Stilla R, Peltier S, Hu X, Sathian K. (2005): Short-term visual deprivation alters neural processing of tactile form. Exp Brain Res 166(3-4):572-82.
- Whitney D, Ellison A, Rice NJ, Arnold D, Goodale M, Walsh V, Milner D. (2007): Visually guided reaching depends on motion area MT+. Cereb Cortex 17(11):2644-9.
- Wright TM, Pelphrey KA, Allison T, McKeown MJ, McCarthy G. (2003): Polysensory interactions along lateral temporal regions evoked by audiovisual speech. Cereb Cortex 13(10):1034-43.
- Xiong JH, Gao JH, Lancaster JL, Fox PT. (1995): Clustered pixels analysis for functional MRI activation studies of the human brain. Human Brain Mapping 3:287-301.
- Yasar NE, Beauchamp MS. (2006): A variable-amplitude multichannel vibrotactile somatosensory stimulator for fMRI. Soc for Neurosci Abstr 32:804.25.
- Young JP, Herath P, Eickhoff S, Choi J, Grefkes C, Zilles K, Roland PE. (2004): Somatotopy and attentional modulation of the human parietal and opercular regions. J Neurosci 24(23):5391-9.
- Yousry TA, Schmid UD, Alkadhi H, Schmidt D, Peraud A, Buettner A, Winkler P. (1997): Localization of the motor hand area to a knob on the precentral gyrus. A new landmark. Brain 120 (Pt 1):141-57.
- Zampini M, Torresan D, Spence C, Murray MM. (2007): Auditory-somatosensory multisensory interactions in front and rear space. Neuropsychologia 45(8):1869-77.
- Zhang M, Mariola E, Stilla R, Stoesz M, Mao H, Hu X, Sathian K. (2005): Tactile discrimination of grating orientation: fMRI activation patterns. Hum Brain Mapp 25(4):370-7.